Title
Effects of Diet on Copper Metabolism

Author
Harder, Nathaniel

Publication Date
2023

Peer reviewed|Thesis/dissertation

Effects of Diet on Copper Metabolism

By

NATHANIEL HARDER

THESIS

Submitted in partial satisfaction of the requirements for the degree of

Doctor of Philosophy

in

Chemistry

in the

OFFICE OF GRADUATE STUDIES

of the

UNIVERSITY OF CALIFORNIA

DAVIS

Approved:

Marie Heffern

Sheila David

Patricia Oteiza

Committee in Charge

2023

Contents

Acknowledgments

How do you start to thank and acknowledge everyone that has helped you along the way that built you up to a Ph.D. and through it? There is no way that I will be able to thank everyone in the way they all deserve but here is my attempt to thank the people that directly shaped my Ph.D. journey.

To Marie, I want to thank you for taking a chance on a biologist that is trying to find a way to do chemistry. You pushed me in ways that helped me become a much more confident and much better scientist and person. I am eternally grateful for the opportunities that you have given me to grow and learn. I cannot thank you enough for the space you have allowed me to develop. Thank you for putting up with my crazy ideas, my need for an automatic pipette, and my Horrible Capitalization and grammar.

To my friends that supported me throughout this journey, before, during, and as I move forwards, I am incredibly thankful for the joy and help you all have given me throughout this incredibly difficult time. I would like to highlight members of the Heffern lab that have been there for each other. We have seen each other in our best and worst times and have become more than coworkers. So, thank you, Vanessa, JJ, Sam, and Jess. I would have never made it through without you all. Michael, you have always been a pillar of excellence and mentorship and it cannot be understated how much you helped me. To all the undergrads in the Heffern lab, thank you for helping make it an amazing time. Specifically, to Hannah, Valerie, and Sonia, thank you for all the incredible help and conversations that we had over the years. You all were instrumental in helping me through grad school. Everyone in the Heffern lab has been amazing, so thank you all!

Thank you, Sarah, for keeping me sane as I struggled through times in grad school. You were incredibly important in allowing me to balance work and life and that can't be undervalued throughout this process. Tora, you have been with me through some of the hardest times at work and despite your constant meowing in the mirror, have always been able to cheer me up. Alexis, you too have been an amazing joy despite your very aggressive nose.

Thank you to the collaborators that helped so much along the way. The Oteiza lab, Dr. Oteiza and Dr. Eleonora specifically, you both helped get me started down the right path and helped with the palmitate project. The Medici lab, Dr. Medici, Noreene, and Dr. Gaurav, thank you for the help and mentorship, and amazingly fruitful collaborations. I very much appreciate everything you have taught me. Thank you to the staff members at UC Davis for keeping things running from vivarium staff to chemistry staff, and custodian staff. Alvin, sorry for the floors. Brad, thank you for being there for everyone all the time, you are the best of us. Thank you Gunrock pub for the discounts and for providing a great place to work and write most of a paper and my entire thesis.

Lastly thank you to my family. You have provided me with so much strength and support over the years and you are the reason I have been able to get here. Mom and Dad, thank you for all the help and for putting up with very nerdy children. Joseph, thank you for being an inspiration as a person and scientist. You helped get me into science and have helped me along the way so much. Finally thank you to my grandparents who are no longer with us. Thank you, Grandpapa, Grandmama, Guta, and Saba, for showing strength, kindness, and persistence in face of incredible struggles. You all have been inspirational and are greatly missed.

Abstract

In the thesis presented here, we investigate the effects of dietary changes on copper metabolism. With increases in incidences of metabolic diseases like non-alcoholic fatty liver disease (NAFLD) and diabetes, there is a need to understand the mechanisms that drive metabolic changes to disease pathogenesis. To this end, in the past 10 years, researchers have investigated the roles of diet on changes to metal micronutrient misregulation. The research presented in this thesis builds upon past findings, and focuses on the relationship between diet, copper regulation, and the progression of metabolic diseases.

Chapter one offers insight into the state of research on copper metabolism and the interconnectivity of macronutrients, like fats and sugars, to copper biology. The chapter provides background information key to the comprehension of the thesis. Chapter two investigates the effects of a two-week sugar intervention on human serum. We note changes in metal micronutrient markers related to iron, copper, and zinc that point to a connection between the caloric intake of healthy individuals and metal micronutrient metabolism. Focusing on copper, we did not observe significant changes in the concentration of ceruloplasmin, the main serum copper chaperone, but did note changes in copper dependent ceruloplasmin activity pointing to a change in copper loading of the protein. The activity was positively correlated to changes in total serum copper, while the concentration was not. This observation challenges the current methods of clinical copper quantification that are traditionally measured through the concentration of ceruloplasmin. Chapter three builds on the observations in Chapter two, as a structural investigation of the effects of glucose on ceruloplasmin. We probed the effects of glucose-mediated cleavage on ceruloplasmin's copper status and cleavage sites. Preliminary data shows notable changes resulting in a fragmentation of the protein and loss of copper that may be related to observed changes in copper metabolism in chapter 2. Chapter four focuses on the mechanisms related to decreases in copper concentrations in the livers of mice with fatty livers. We established a cell model to probe the mechanisms that lead to this copper dyshomeostasis. We propose a mechanism for metal misregulation in liver cells

through the release of copper from the mitochondria into the cytosol, which leads to activation of export and sequestration mechanisms that help to explain the observed intracellular state of copper deficiency.

Chapter 1: Introduction to copper biology and metabolism

1.1 Introduction to copper in health and disease

Copper is an essential micronutrient that plays a wide variety of roles in biology, from cell signaling and radical scavenging to structural integrity and energy production (Figure 1.1).[1–5] Metal micronutrients are derived from the diet in foods such as legumes, shellfish, and beans.[6,7] Copper, as with other micronutrients, is supplemented by vitamin intake however it is estimated that 25% of the population of the United States may not reach the guidelines delineated by the recommended dietary allowance.[4,8] In addition to the amount of copper consumed, human regulation of copper can be influenced by other factors, such as diseases and diet.[9–12]

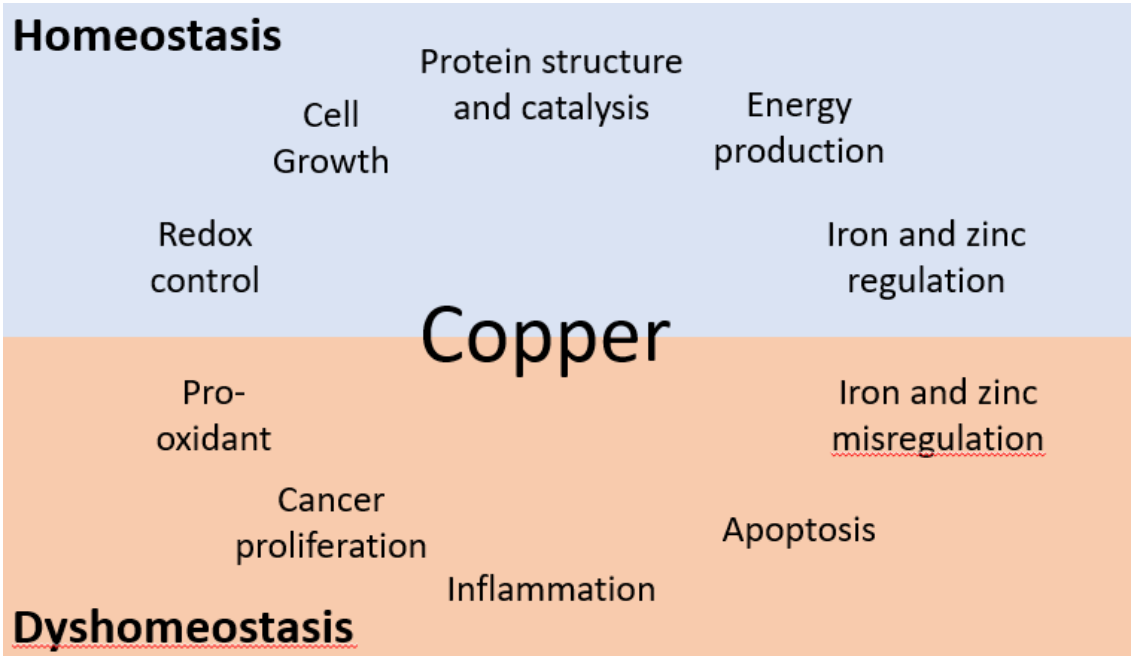

Figure 1.1 Roles of copper in health and disease. Presented here are the several roles of copper in both homeo- and dyshomeostasis, demonstrating the need for copper in health as well as the need for proper regulation of the metal.

Copper in the body can be characterized as a Janus-faced nutrient wherein it is essential, yet when misregulated can lead to incredibly deleterious diseases, including cancer, fatty liver disease, and Alzheimer's disease.[13–15] Misregulation of the metal is multifaceted and can be characterized by an overload, a deficiency, or both depending on the organ and disease in question. Copper overload can be found in many types of cancers as copper facilitates the increased metabolic load required for cell

growth.[13,16] Non-alcoholic fatty liver disease induces a state of hepatic copper deficiency, conversely, human subjects considered obese, but critically without hepatic steatosis (liver inflammation), demonstrate a copper overload in the liver and fat stores.[10,17] Studies on a key copper transporter highlight this effect in mouse models, wherein copper supplementation increased the transporter in certain organs, like the liver and heart, while decreasing it in the intestines.[18] All told, these pathologies and mechanisms hint at a complex and dynamic pathway that requires additional research and tools to uncover the location and status of copper.

While copper is posited to play a role in these diseases, recent studies highlight a connection between diet and metal homeostasis. This is especially evident concerning the influence of macronutrients like fats and sugars on copper metabolism in the body with implications for human health and wellness. It is suggested that the connections between diet and metals are through bioavailability, absorption, and processing but whether these interactions are directly related to nutrient-metal binding, disruption of protein-metal binding, or through intracellular pathways, remains unclear.[9,19–23] The work presented in this thesis, aims to highlight the role of nutrients like fats and sugars on copper metabolism and their implications for health and diet through studies on cell models, protein biochemistry, and human studies. To introduce this work, it is important to understand how copper is regulated within the human body.

1.2 Introduction to copper metabolism

In the past 10 to 20 years, research in the field of copper biology has significantly increased with studies providing key insights into the mechanisms of action of copper transporters and copper homeostasis throughout prokaryotes, eukaryotes, and the human body.[1,24–26] Work by Dr. Svetlana Lutsenko and others has driven the field forward with understanding and discovering the roles of proteins in the copper import, export, and intracellular mobilization pathways in humans. Despite the blossoming of discoveries in the field, many copper pathways are still not understood, critically the methods of copper storage in the

mitochondria as well as key pathways that regulate copper internalization and mobilization throughout the interior of the cell.[27–29]

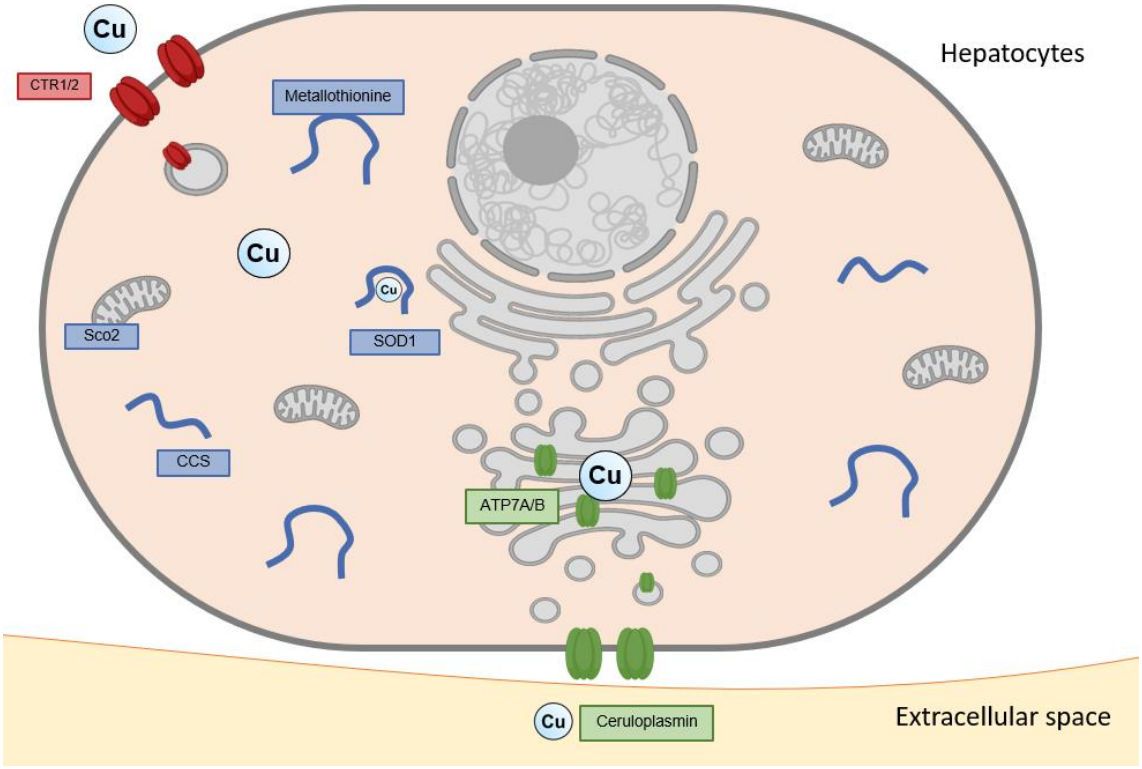

Figure 1.2 Basic schematic of copper metabolism. Selected proteins and pathways associated with copper metabolism highlighting importers (in red), chaperones and cytosolic proteins (in blue), and transporters and serum chaperones (in green).

To understand the movement of copper within the cell, it is important to highlight key proteins that play a role in the function of copper in biology (Figure 1.2). As the work in this dissertation focuses on the interactions of copper in the liver and the circulatory system, the pathways presented here are specific for these systems and may be shifted or altered in different organs. This introduction is by no means a comprehensive review of copper metabolism and pathways and serves only to introduce important proteins and pathways involved to comprehend the subject broached in the following chapters of this dissertation. For more thorough explanations of copper metabolism, I recommend articles from Ruiz et al.[30], Lutsenko[1,24], and Linder[31] for more detailed and in-depth reviews.

1.2.1 Intracellular copper pathways

The majority of copper is imported through the membrane by CTR1, a multimer membrane protein, that can act at the membrane or in lysosomes in instances of copper acquisition by endocytosis.[32–35] CTR1 favors the import of cuprous ions, Cu(I), and may be associated with a copper reductase for import.[36] The importer will hold copper at the cytosolic membrane for protein chaperones to bind the metal for further transport within the cell.[37,38] Additional copper transporters are present including CTR2, however, the distinct roles of these proteins have yet to be established.[39] Intracellular chaperones transport the copper atoms to their respective locations and proteins for loading into proteins or they are passaged to other chaperones and transporters. These chaperones include CCS, a protein for loading copper into the antioxidant protein SOD1, ATOX1, and COMMD1, proteins involved in copper transport to exporter proteins, COX17, a chaperone hypothesized to shuttle copper within the mitochondria and glutathione, a polypeptide responsible for maintenance of the reducing environment of the cytosol with metal binding properties.[2,40–44] Each chaperone has a posited unique role that may not fully encapsulate the complexity of the chaperone's role in copper biology.

1.2.2 Copper in the mitochondria

The main location for copper within the cell is the mitochondria, the powerhouse of the cell, as copper is critical for the electron transport chain (ETC) and thus energy metabolism and ATP generation.[44,45] On top of its critical use for energy production, the organelle can also influence intracellular redox states, endoplasmic reticulum stress, and apoptosis.[46–48] Metals like copper and iron are key in these processes of the organelle. The mitochondria are proposed to store and use a significant amount of copper that may play a role in the function of the mitochondria or may be functionalized for use in the ETC when necessary.[30,47] Thus, proper metal homeostasis is of utmost importance.[30,49,50] Copper is exchanged from COX17 to a variety of chaperones and proteins like SCO1 and SCO2, which play a role in loading copper into cytochrome c oxidase, an integral protein in the ETC.[28,44,51] Cytochrome c oxidase contains two copper sites

that are both catalytically active for the electron transfer from cytochrome c in the ETC.[52] However, much of the nature of copper import and localization towards the mitochondria has yet to be elucidated.[53] The species of a copper-binding and potential storage protein is not understood and is often referred to as CuL, a copper ligand that has yet to be identified.[30,47] With such essential control of energy production, the organelle is a key player in the effects observed in nutrient overload and deficient diseases and may hold information on the intersection of metals and diet.

1.2.3 Cellular copper export

As important as copper import and distribution is within the cell, the pathways for export are equally critical given the double-edged sword of copper, which can lead to cell death by generating reactive oxygen species (ROS).[54] As mentioned above, the chaperones ATOX1 and COMMD1 play roles in the movement of copper towards export and sequestering mechanisms. These chaperones shuttle copper to ATP7A and ATP7B, copper transporter intermembrane proteins found in the Golgi apparatus and the extracellular membrane.[31,55–57] The location of these proteins is contingent on the status of copper within the cells with studies showing mobilization of liver ATP7B towards the extracellular membrane in states of copper overload and the Golgi apparatus when in a state of copper deficiency.[57] It is thought that the status of copper within the cell influences phosphorylation (through an unknown pathway) of the transporters that may play a role in the subcellular localization, and may be related to the movement of copper into proteins or towards the direct excretion of copper.[53,58] While different roles of ATP7A and ATP7B are not fully differentiated, it is hypothesized that ATP7B is primarily in the liver while ATP7A is primarily thought to be in the intestinal cells. Both serve to load copper into the extracellular proteins ceruloplasmin and hephaestin or for alternative extracellular copper mobilization, like secretion into the bile.[18,19,31,59] Recent research has highlighted copper sequestering proteins like SLC46A3 which is implicated in loading copper into lysosomes and intracellular sequestering mechanisms.[60] Despite the identification of a wide variety of proteins responsible for copper metabolism and distribution in the cell, more may yet be identified and

characterized. To this end, even proteins that have long been identified (like ATP7A and ATP7B) have roles that have not yet been fully established, muddling pathway analysis of copper trafficking.

1.2.4 Considerations on copper in the serum

The dearth of knowledge is not limited to copper regulation within the cell, but outside as well. While the concentration of serum copper is similar to that of other metals like iron and zinc (~10 μM), the speciation of the metal is not well characterized.[61–64] Ceruloplasmin contains 4 to 8 copper atoms per protein and is responsible for the oxidation of Fe(II) to Fe(III), enabling the binding of iron to transferrin.[59,61,65] The protein is implicated in copper transport in the serum for movement of copper from the liver to other organs, as well as oxidant properties, and tyrosinase activity.[66,67] There is a consensus of research that the majority of copper is bound to ceruloplasmin, however, the percent of copper bound to ceruloplasmin varies depending on the study, from 50 to 95% of serum copper bound to the ferroxidase.[9,31,59,61,63] This host of activities has led to its characterization as a "moonlighting" protein.[67] Recent data has highlighted that the trafficking of copper from serum to organs is complex and not fully characterized.[34,68]

The remaining serum-derived copper is thought to be bound to serum albumin, other less prevalent copper proteins, and a small percentage is found in a labile form.[69] This labile form is not "free copper" but bound to protein, peptide, and small molecule motifs with lower affinities for copper than albumin, which can result in changes in the biological activity of the molecule.[70–72] The characterization of copper species in the blood has remained unclear, with the concentrations of labile copper proving equally elusive. Proposed calculations based on overall copper concentration and ceruloplasmin concentration in the serum may provide pertinent information on the amounts of non-ceruloplasmin bound copper. These calculations, however, make assumptions on the amount of copper loaded into ceruloplasmin and the state of ceruloplasmin that require additional validation as they can lead to negative values of labile copper.[64,73]

1.3 Scope of thesis

Variations of protein levels and gene expression of the copper proteins demonstrate the dynamic nature of homeostasis within the cell and allow researchers to track biological changes in copper metabolism in response to stimuli. In this thesis, we aim to build on understanding the interplay between macronutrients and metal micronutrients as well as their implications on biology and human health. By studying changes in intracellular and extracellular copper proteins, we work adds pieces to the puzzle of copper metabolism. The research presented in this work focuses on: firstly, a study on the effects of sugar consumption on serum metal status, secondly the mechanistic effects of glucose on ceruloplasmin function and biological activity, and finally the mechanisms underlying hepatic copper misregulation in a state of fatty acid overload.

The second chapter highlights the effects of sugar diets on serum metal metabolism and biomarkers. With collaborations with Dr. Valentina Medici (UC Davis Medical Center) and Dr. Kimber Stanhope (UC Davis School of Veterinary Medicine). In a study run by Drs. Medici and Stanhope, young healthy adults consumed beverages sweetened with glucose, fructose, high fructose corn syrup (HFCS), or aspartame for two weeks and demonstrated that consumption of both fructose- and HFCS-sweetened beverages increased cardiovascular disease risk factors.[74–76] Baseline and intervention serum samples from 107 participants of this study were measured for copper metabolism (copper, ceruloplasmin ferroxidase activity, ceruloplasmin protein), zinc, and iron metabolism (iron, ferritin, and transferrin) parameters. Fructose and/or glucose consumption were associated with decreased ceruloplasmin ferroxidase activity and serum copper and zinc concentrations. Ceruloplasmin protein levels did not change in response to intervention. The changes in copper concentrations were correlated with zinc, but not with iron. The decreases in copper, ceruloplasmin ferroxidase activity, ferritin, and transferrin were inversely associated with the increases in metabolic risk factors associated with sugar consumption, specifically, apolipoprotein CIII, triglycerides, or post-meal glucose, insulin, and lactate responses. These findings are the first evidence

that consumption of sugar-sweetened beverages can alter clinical parameters of transition metal metabolism in healthy subjects.

To uncover the mechanism behind the sugar-induced copper changes in chapter two, investigated how glucose can alter ceruloplasmin's activity and structure. Previous literature had found that glucose can result in a change in ceruloplasmin by non-enzymatic cleavage, which may account for the changes in activity but not concentration that we found the preceding study. Incubation of ceruloplasmin for 30 minutes at 37˚C with glucose demonstrated a surprising trend with an apparent glucose control over the activity of ceruloplasmin. Fasting levels of glucose (1 and 5 mM) decrease ceruloplasmin activity, conversely, post-prandial levels (10 and 15 mM), increase activity. Currently, we are investigating the effects of glucose on the copper centers of ceruloplasmin on the activity of the protein. Long exposures, 10 days, of ceruloplasmin with glucose demonstrate increases in protein fragmentation along with a decrease in copper-dependent activity. Ceruloplasmin has large sequence homology to coagulation Factor V, and as such, fragments may have pro-coagulation activities. Preliminary assays demonstrate an increase in plasma coagulation of glucose incubated ceruloplasmin and may point to disease pathogenesis. Future work will aim to identify ceruloplasmin fragment sequences as well as probe glucose alterations in serum.

My final chapter examines the changes in the copper trafficking mechanisms of liver cells exposed to excess fatty acids. Fatty acid uptake was induced in liver hepatocarcinoma cells, HepG2, by treatment with the saturated fatty acid, palmitic acid. Changes in chaperones, transporters, and chelators demonstrate an initial state of copper overload in the cell that, over time, shifts to a state of copper deficiency. This deficiency is due to the sequestration of copper both into the membrane-bound copper protein, hephaestin, as well as lysosomal units. These changes are independent of changes in copper concentration, supporting perturbations in copper localization at the subcellular level. We hypothesize that fat accumulation triggers an initial copper miscompartmentalization within the cell, due to disruptions in mitochondrial copper balance, which induces a homeostatic response to cytosolic copper overload. This

leads the cell to activate copper export and sequestering mechanisms that in turn induces a condition of cytosolic copper deficiency. Taken together, this work provides molecular insight underlying previously observed phenotypes in clinical and rodent models linking copper-deficient states to obesity-associated disorders.

The connection between copper metabolism and macronutrients has become more established with studies highlighting the intersection between copper, sugars, and fats.[10,77–79] While the mechanisms behind these connections are still tenuous the diverging effects of diet on copper add a complexity that deserves future investigations.[70,77] Together, these chapters highlight the interactions between copper and metabolism to add to the growing body of work on the intersection of macro- and micronutrients.

1.4 References

(1) Lutsenko, S. Human Copper Homeostasis: A Network of Interconnected Pathways. *Curr. Opin. Chem. Biol.* 2010, *14* (2), 211–217.

(2) Culotta, V. C.; Klomp, L. W.; Strain, J.; Casareno, R. L.; Krems, B.; Gitlin, J. D. The Copper Chaperone for Superoxide Dismutase. *J. Biol. Chem.* 1997, *272* (38), 23469–23472.

(3) Festa, R. A.; Thiele, D. J. Copper: An Essential Metal in Biology. *Current Biology*. Cell Press November 8, 2011, p R877.

(4) Burkhead, J. L.; Collins, J. F. Nutrition Information Brief—Copper. *Adv. Nutr.* 2022, *13* (2), 681.

(5) Bost, M.; Houdart, S.; Oberli, M.; Kalonji, E.; Huneau, J.-F.; Margaritis, I. Dietary Copper and Human Health: Current Evidence and Unresolved Issues. *J. Trace Elem. Med. Biol.* 2016, *35*, 107–115.

(6) Ma, J.; Betts, N. M. Zinc and Copper Intakes and Their Major Food Sources for Older Adults in the 1994–96 Continuing Survey of Food Intakes by Individuals (CSFII). *J. Nutr.* 2000, *130* (11), 2838–2843.

(7) Olmedo, P.; Hernández, A. F.; Pla, A.; Femia, P.; Navas-Acien, A.; Gil, F. Determination of Essential Elements (Copper, Manganese, Selenium and Zinc) in Fish and Shellfish Samples. Risk and Nutritional Assessment and Mercury-Selenium Balance. *Food Chem. Toxicol.* 2013, *62*, 299–307.

(8) Klevay, L. M. Is the Western Diet Adequate in Copper? *Journal of Trace Elements in Medicine and Biology*. J Trace Elem Med Biol December 2011, pp 204–212.

(9) Harder, N. H. O.; Hieronimus, B.; Stanhope, K. L.; Shibata, N. M.; Lee, V.; Nunez, M. V.; Keim, N. L.;

Bremer, A.; Havel, P. J.; Heffern, M. C.; et al. Effects of Dietary Glucose and Fructose on Copper, Iron, and Zinc Metabolism Parameters in Humans. *Nutrients* 2020, *12* (9), 1–14.

(10) Heffern, M. C.; Park, H. M.; Au-Yeung, H. Y.; Van de Bittner, G. C.; Ackerman, C. M.; Stahl, A.; Chang, C. J. In Vivo Bioluminescence Imaging Reveals Copper Deficiency in a Murine Model of Nonalcoholic Fatty Liver Disease. *Proc. Natl. Acad. Sci. U. S. A.* 2016, *113* (50), 14219–14224.

(11) Aigner, E.; Strasser, M.; Haufe, H.; Sonnweber, T.; Hohla, F.; Stadlmayr, A.; Solioz, M.; Tilg, H.; Patsch, W.; Weiss, G.; et al. A Role for Low Hepatic Copper Concentrations in Nonalcoholic Fatty Liver Disease. *Am. J. Gastroenterol.* 2010, *105* (9), 1978–1985.

(12) Song, M.; Vos, M.; McClain, C. Copper-Fructose Interactions: A Novel Mechanism in the Pathogenesis of NAFLD. *Nutrients* 2018, *10* (11), 1815.

(13) Brady, D. C.; Crowe, M. S.; Turski, M. L.; Hobbs, G. A.; Yao, X.; Chaikuad, A.; Knapp, S.; Xiao, K.; Campbell, S. L.; Thiele, D. J.; et al. Copper Is Required for Oncogenic BRAF Signalling and Tumorigenesis. *Nature* 2014, *509* (7501), 492–496.

(14) Antonucci, L.; Porcu, C.; Iannucci, G.; Balsano, C.; Barbaro, B. Non-Alcoholic Fatty Liver Disease and Nutritional Implications: Special Focus on Copper. *Nutrients* 2017, *9* (10).

(15) Navarro, J. A.; Schneuwly, S. Copper and Zinc Homeostasis: Lessons from Drosophila Melanogaster. *Frontiers in Genetics*. Frontiers Media S.A. December 21, 2017, p 223.

(16) Porcu, C.; Antonucci, L.; Barbaro, B.; Illi, B.; Nasi, S.; Martini, M.; Licata, A.; Miele, L.; Grieco, A.; Balsano, C. Copper/MYC/CTR1 Interplay: A Dangerous Relationship in Hepatocellular Carcinoma. *Oncotarget* 2018, *9* (10), 9325–9343.

(17) Yang, H.; Liu, C. N.; Wolf, R. M.; Ralle, M.; Dev, S.; Pierson, H.; Askin, F.; Steele, K. E.; Magnuson, T. H.; Schweitzer, M. A.; et al. Obesity Is Associated with Copper Elevation in Serum and Tissues. *Metallomics* 2019, *11* (8), 1363–1371.

(18) Chun, H.; Catterton, T.; Kim, H.; Lee, J.; Kim, B. E. Organ-Specific Regulation of ATP7A Abundance Is Coordinated with Systemic Copper Homeostasis. *Sci. Reports 2017 71* 2017, *7* (1), 1–13.

(19) Harder, N. H. O.; Lee, H. P.; Flood, V. J.; Juan, J. A. S.; Gillette, S. K.; Heffern, M. C. Fatty Acid Uptake in Liver Hepatocytes Induces Relocalization and Sequestration of Intracellular Copper. *Front. Mol. Biosci.* 2022, *9*.

(20) Morrell, A.; Tallino, S.; Yu, L.; Burkhead, J. L. The Role of Insufficient Copper in Lipid Synthesis and Fatty-Liver Disease. *IUBMB Life* 2017, *69* (4), 263–270.

(21) Christides, T.; Sharp, P. Sugars Increase Non-Heme Iron Bioavailability in Human Epithelial Intestinal and Liver Cells. *PLoS One* 2013, *8* (12), 83031.

(22) Song, M.; Schuschke, D. A.; Zhou, Z.; Chen, T.; Pierce, W. M.; Wang, R.; Johnson, W. T.; McClain, C. J. High Fructose Feeding Induces Copper Deficiency in Sprague-Dawley Rats: A Novel Mechanism for Obesity Related Fatty Liver. *J. Hepatol.* 2012, *56* (2), 433–440.

(23) POLLACK, S.; KAUFMAN, R. M.; CROSBY, W. H. Iron Absoption: Effects of Sugars and Reducing Agents. *Blood* 1964, *24* (5), 577–581.

(24) Lutsenko, S. Copper Trafficking to the Secretory Pathway. *Metallomics* 2016, *8* (9), 840–852.

(25) Członkowska, A.; Litwin, T.; Dusek, P.; Ferenci, P.; Lutsenko, S.; Medici, V.; Rybakowski, J. K.; Weiss, K. H.; Schilsky, M. L. Wilson Disease. *Nature Reviews Disease Primers*. Nature Publishing Group December 1, 2018.

(26) Chandrangsu, P.; Rensing, C.; Helmann, J. D. Metal Homeostasis and Resistance in Bacteria. *Nat. Rev. Microbiol.* 2017, *15* (6), 338.

(27) Nevitt, T.; Ohrvik, H.; Thiele, D. J. Charting the Travels of Copper in Eukaryotes from Yeast to Mammals. *Biochim. Biophys. Acta* 2012, *1823* (9), 1580–1593.

(28) Leary, S. C.; Cobine, P. A.; Kaufman, B. A.; Guercin, G. H.; Mattman, A.; Palaty, J.; Lockitch, G.; Winge, D. R.; Rustin, P.; Horvath, R.; et al. The Human Cytochrome c Oxidase Assembly Factors SCO1 and SCO2 Have Regulatory Roles in the Maintenance of Cellular Copper Homeostasis. *Cell Metab.* 2007, *5* (1), 9–20.

(29) Zischka, H.; Einer, C. Mitochondrial Copper Homeostasis and Its Derailment in Wilson Disease. *Int. J. Biochem. Cell Biol.* 2018, *102*, 71–75.

(30) Ruiz, L. M.; Libedinsky, A.; Elorza, A. A. Role of Copper on Mitochondrial Function and Metabolism . *Frontiers in Molecular Biosciences* . 2021.

(31) Linder, M. C. Copper Homeostasis in Mammals, with Emphasis on Secretion and Excretion. A Review. *Int. J. Mol. Sci.* 2020, *21* (14), 1–22.

(32) Kim, H.; Son, H.-Y.; Bailey, S. M.; Lee, J. Deletion of Hepatic Ctr1 Reveals Its Function in Copper Acquisition and Compensatory Mechanisms for Copper Homeostasis. *AJP Gastrointest. Liver Physiol.* 2008, *296* (2), G356–G364.

(33) Kahra, D.; Kovermann, M.; Wittung-Stafshede, P. The C-Terminus of Human Copper Importer Ctr1 Acts as a Binding Site and Transfers Copper to Atox1. *Biophys. J.* 2016, *110* (1), 95.

(34) Kidane, T. Z.; Farhad, R.; Lee, K. J.; Santos, A.; Russo, E.; Linder, M. C. Uptake of Copper from Plasma Proteins in Cells Where Expression of CTR1 Has Been Modulated. *BioMetals* 2012, *25* (4), 697–709.

(35) Lee, J.; Prohaska, J. R.; Thiele, D. J. Essential Role for Mammalian Copper Transporter Ctr1 in Copper Homeostasis and Embryonic Development. *Proc. Natl. Acad. Sci. U. S. A.* 2001, *98* (12), 6842–6847.

(36) Stefaniak, E.; Płonka, D.; Drew, S. C.; Bossak-Ahmad, K.; Haas, K. L.; Pushie, M. J.; Faller, P.; Wezynfeld, N. E.; Bal, W. The N-Terminal 14-Mer Model Peptide of Human Ctr1 Can Collect Cu(Ii) from Albumin. Implications for Copper Uptake by Ctr1. *Metallomics* 2018, *10* (12), 1723–1727.

(37) Maryon, E. B.; Molloy, S. A.; Kaplan, J. H. Cellular Glutathione Plays a Key Role in Copper Uptake Mediated by Human Copper Transporter 1. *Am. J. Physiol. - Cell Physiol.* 2013, *304* (8), C768.

(38) Levy, A. R.; Nissim, M.; Mendelman, N.; Chill, J.; Ruthstein, S. Ctr1 Intracellular Loop Is Involved in the Copper Transfer Mechanism to the Atox1 Metallochaperone. *J. Phys. Chem. B* 2016, *120* (48), 12334–12345.

(39) Öhrvik, H.; Thiele, D. J. The Role of Ctr1 and Ctr2 in Mammalian Copper Homeostasis and Platinum-Based Chemotherapy. *J. Trace Elem. Med. Biol.* 2015, *31*, 178.

(40) Zaccak, M.; Qasem, Z.; Gevorkyan-Airapetov, L.; Ruthstein, S. An EPR Study on the Interaction

between the Cu(I) Metal Binding Domains of ATP7B and the Atox1 Metallochaperone. *Int. J. Mol. Sci.* 2020, *21* (15), 1–13.

(41) Bertinato, J.; Iskandar, M.; L'Abbé, M. R. Copper Deficiency Induces the Upregulation of the Copper Chaperone for Cu/Zn Superoxide Dismutase in Weanling Male Rats. *J. Nutr.* 2003, *133* (1), 28–31.

(42) Stewart, D. J.; Short, K. K.; Maniaci, B. N.; Burkhead, J. L. COMMD1 and PtdIns(4,5)P2 Interaction Maintain ATP7B Copper Transporter Trafficking Fidelity in HepG2 Cells. *J. Cell Sci.* 2019, *132* (19).

(43) De Bie, P.; Van De Sluis, B.; Klomp, L.; Wijmenga, C. The Many Faces of the Copper Metabolism Protein MURR1/COMMD1. *Journal of Heredity*. Oxford Academic November 1, 2005, pp 803–811.

(44) Cobine, P. A.; Pierrel, F.; Winge, D. R. Copper Trafficking to the Mitochondrion and Assembly of Copper Metalloenzymes. *Biochimica et Biophysica Acta - Molecular Cell Research*. Elsevier July 1, 2006, pp 759–772.

(45) Van Der Bliek, A. M.; Sedensky, M. M.; Morgan, P. G. Cell Biology of the Mitochondrion. *Genetics* 2017, *207* (3), 843–871.

(46) Yi, H.; Wang, K.; Du, B.; He, L.; Hiuting, H. O.; Qiu, M.; Zou, Y.; Li, Q.; Jin, J.; Zhan, Y.; et al. Aleuritolic Acid Impaired Autophagic Flux and Induced Apoptosis in Hepatocellular Carcinoma HepG2 Cells. *Molecules* 2018, *23* (6).

(47) Leary, S. C.; Winge, D. R.; Cobine, P. A. "Pulling the Plug" on Cellular Copper: The Role of Mitochondria in Copper Export. *Biochim. Biophys. Acta - Mol. Cell Res.* 2009, *1793* (1), 146–153.

(48) Martinvalet, D. The Role of the Mitochondria and the Endoplasmic Reticulum Contact Sites in the Development of the Immune Responses. *Cell Death Dis. 2018 93* 2018, *9* (3), 1–15.

(49) Cobine, P. A.; Moore, S. A.; Leary, S. C. Getting out What You Put in: Copper in Mitochondria and Its Impacts on Human Disease. *Biochim. Biophys. Acta - Mol. Cell Res.* 2021, *1868* (1), 118867.

(50) Prohaska, J. R. Changes in Cu,Zn-Superoxide Dismutase, Cytochrome c Oxidase, Glutathione Peroxidase and Glutathione Transferase Activities in Copper-Deficient Mice and Rats. *J. Nutr.* 1991, *121* (3), 355–363.

(51) Hill, S.; Deepa, S. S.; Sataranatarajan, K.; Premkumar, P.; Pulliam, D.; Liu, Y.; Soto, V. Y.; Fischer, K. E.; Van Remmen, H. Sco2 Deficient Mice Develop Increased Adiposity and Insulin Resistance. *Mol. Cell. Endocrinol.* 2017, *455*, 103–114.

(52) Horn, D.; Barrientos, A. Mitochondrial Copper Metabolism and Delivery to Cytochrome c Oxidase. *IUBMB Life* 2008, *60* (7), 421–429.

(53) Lutsenko, S. Dynamic and Cell-Specific Transport Networks for Intracellular Copper Ions. *J. Cell Sci.* 2021, *134* (21).

(54) Jomova, K.; Valko, M. Advances in Metal-Induced Oxidative Stress and Human Disease. *Toxicology* 2011, *283* (2), 65–87.

(55) Lowe, J.; Taveira-da-Silva, R.; Hilário-Souza, E. Dissecting Copper Homeostasis in Diabetes Mellitus. *IUBMB Life* 2017, *69* (4), 255–262.

(56) Mak, C. M.; Lam, C.-W. Diagnosis of Wilson's Disease: A Comprehensive Review. *Crit. Rev. Clin.*

Lab. Sci. 2008, *45* (3), 263–290.

(57) Barnes, N.; Bartee, M. Y.; Braiterman, L.; Gupta, A.; Ustiyan, V.; Zuzel, V.; Kaplan, J. H.; Hubbard, A. L.; Lutsenko, S. Cell-Specific Trafficking Suggests a New Role for Renal ATP7B in the Intracellular Copper Storage. *Traffic* 2009, *10* (6), 767–779.

(58) Bartee, M. Y.; Ralle, M.; Lutsenko, S. The Loop Connecting Metal-Binding Domains 3 and 4 of ATP7B Is a Target of a Kinase-Mediated Phosphorylation. *Biochemistry* 2009, *48* (24), 5573.

(59) Vashchenko, G.; MacGillivray, R. T. A. Multi-Copper Oxidases and Human Iron Metabolism. *Nutrients* . 2013.

(60) Kim, J. H.; Matsubara, T.; Lee, J.; Fenollar-Ferrer, C.; Han, K.; Kim, D.; Jia, S.; Chang, C. J.; Yang, H.; Nagano, T.; et al. Lysosomal SLC46A3 Modulates Hepatic Cytosolic Copper Homeostasis. *Nat. Commun.* 2021, *12* (1).

(61) Hellman, N. E.; Gitlin, J. D. Ceruloplasmin Metabolism and Function. *Annu. Rev. Nutr.* 2002, *22* (1), 439–458.

(62) Kelly, D.; Crotty, G.; O'Mullane, J.; Stapleton, M.; Sweeney, B.; O'Sullivan, S. S. The Clinical Utility of a Low Serum Ceruloplasmin Measurement in the Diagnosis of Wilson Disease. *Ir. Med. J.* 2016, *109* (1), 341–343.

(63) Członkowska, A.; Rodo, M.; Wierzchowska-Ciok, A.; Smolinski, L.; Litwin, T. Accuracy of the Radioactive Copper Incorporation Test in the Diagnosis of Wilson Disease. *Liver Int.* 2018, *38* (10), 1860–1866.

(64) Woimant, F.; Djebrani-Oussedik, N.; Poujois, A. New Tools for Wilson's Disease Diagnosis: Exchangeable Copper Fraction. *Ann. Transl. Med.* 2019, *7* (S2), S70–S70.

(65) Jiang, B.; Liu, G.; Zheng, J.; Chen, M.; Maimaitiming, Z.; Chen, M.; Liu, S.; Jiang, R.; Fuqua, B. K.; Dunaief, J. L.; et al. Hephaestin and Ceruloplasmin Facilitate Iron Metabolism in the Mouse Kidney. *Sci. Rep.* 2016, *6* (1), 1–11.

(66) Mukhopadhyay, C. K.; Fox, P. L. Ceruloplasmin Copper Induces Oxidant Damage by a Redox Process Utilizing Cell-Derived Superoxide as Reductant. *Biochemistry* 1998, *37* (40), 14222–14229.

(67) Bielli, P.; Calabrese, L. Structure to Function Relationships in Ceruloplasmin: A "moonlighting" Protein. *Cell. Mol. Life Sci. C. 2002 599* 2002, *59* (9), 1413–1427.

(68) Ramos, D.; Mar, D.; Ishida, M.; Vargas, R.; Gaite, M.; Montgomery, A.; Linder, M. C. Mechanism of Copper Uptake from Blood Plasma Ceruloplasmin by Mammalian Cells. *PLoS One* 2016, *11* (3), e0149516.

(69) Linder, M. C. Ceruloplasmin and Other Copper Binding Components of Blood Plasma and Their Functions: An Update. *Metallomics* 2016, *8* (9), 887–905.

(70) Lee, V. J.; Heffern, M. C. Structure-Activity Assessment of Flavonoids as Modulators of Copper Transport. *Front. Chem.* 2022, *0*, 930.

(71) Stevenson, M. J.; Farran, I. C.; Uyeda, K. S.; San Juan, J. A.; Heffern, M. C. Analysis of Metal Effects on C-Peptide Structure and Internalization. *ChemBioChem* 2019, *20* (19), 2447–2453.

(72) Stevenson, M. J.; Uyeda, K. S.; Harder, N. H. O.; Heffern, M. C. Metal-Dependent Hormone

Function: The Emerging Interdisciplinary Field of Metalloendocrinology. *Metallomics* 2018.

(73) Twomey, P. J.; Viljoen, A.; House, I. M.; Reynolds, T. M.; Wierzbicki, A. S. Adjusting Copper Concentrations for Caeruloplasmin Levels in Routine Clinical Practice. *J. Clin. Pathol.* 2006, *59* (8), 867.

(74) Stanhope, K. L.; Medici, V.; Bremer, A. A.; Lee, V.; Lam, H. D.; Nunez, M. V.; Chen, G. X.; Keim, N. L.; Havel, P. J. A Dose-Response Study of Consuming High-Fructose Corn Syrup-Sweetened Beverages on Lipid/Lipoprotein Risk Factors for Cardiovascular Disease in Young Adults. *Am. J. Clin. Nutr.* 2015, *101* (6), 1144–1154.

(75) Stanhope, K. L.; Bremer, A. A.; Medici, V.; Nakajima, K.; Ito, Y.; Nakano, T.; Chen, G.; Fong, T. H.; Lee, V.; Menorca, R. I.; et al. Consumption of Fructose and High Fructose Corn Syrup Increase Postprandial Triglycerides, LDL-Cholesterol, and Apolipoprotein-B in Young Men and Women. *J. Clin. Endocrinol. Metab.* 2011, *96* (10), E1596.

(76) Hieronimus, B.; Griffen, S. C.; Keim, N. L.; Bremer, A. A.; Berglund, L.; Nakajima, K.; Havel, P. J.; Stanhope, K. L. Effects of Fructose or Glucose on Circulating ApoCIII and Triglyceride and Cholesterol Content of Lipoprotein Subfractions in Humans. *J. Clin. Med.* 2019, *8* (7), 913.

(77) Song, M.; Vos, M. B.; McClain, C. J. Copper-Fructose Interactions: A Novel Mechanism in the Pathogenesis of NAFLD. *Nutrients*. MDPI AG November 1, 2018.

(78) Song, M.; Li, X.; Zhang, X.; Shi, H.; Vos, M. B.; Wei, X.; Wang, Y.; Gao, H.; Rouchka, E. C.; Yin, X.; et al. Dietary Copper-Fructose Interactions Alter Gut Microbial Activity in Male Rats. *Am. J. Physiol. - Gastrointest. Liver Physiol.* 2018, *314* (1), G119–G130.

(79) Morrell, A.; Tripet, B. P.; Eilers, B. J.; Tegman, M.; Thompson, D.; Copié, V.; Burkhead, J. L. Copper Modulates Sex-Specific Fructose Hepatoxicity in Nonalcoholic Fatty Liver Disease (NALFD) Wistar Rat Models. *J. Nutr. Biochem.* 2020, *78*, 108316.

Chapter 2: Effects of Dietary Glucose and Fructose on Copper, Iron, and Zinc Metabolism Parameters in Humans

Adapted with Permission from:

Nathaniel H. O. Harder, Bettina Hieronimus, Kimber L. Stanhope, Noreene M. Shibata, Vivien Lee, Marinelle V. Nunez, Nancy L. Keim, Andrew Bremer, Peter J. Havel, Marie C. Heffern and Valentina Medici.

2.1 Introduction

Copper, iron, and zinc are essential transition metals, participating as cofactors in the activity of numerous enzymes. They can contribute to crucial metabolic processes, including energy and lipid metabolism, one-carbon metabolism, electron transport chain, neuromodulation, and antioxidant mechanisms.[1–3] Given the fine limits existing between the physiological concentrations at which these metals are essential and their toxic pro-oxidant activities when present in excess, interconnected transporters and chaperones tightly regulate absorption and metabolism.

Copper is absorbed throughout the small intestine via copper transporter 1 (CTR1).[4] In the portal circulation, a significant portion of copper is loosely bound to albumin and delivered to hepatocytes where specialized chaperones carry copper to its specific metabolic sites. In particular, copper is delivered to the transporter ATPase copper transporting beta (ATP7B) which is responsible for the excretion of copper via ceruloplasmin.[5] Ceruloplasmin is the main plasma copper carrier, believed to carry 40–70% of copper in plasma of healthy people. Its copper-bound form, known as holoceruloplasmin, carries an average of six copper atoms, but it can also circulate as its copper-free form, apoceruloplasmin.[6] Ceruloplasmin is essential to iron transport and metabolism through its ferroxidase activity, which catalyzes the conversion of Fe^{2+} to Fe^{3+}. Ceruloplasmin plasma levels are of clinical relevance, mainly in the diagnosis of Wilson disease, a genetic condition caused by *ATP7B* pathogenic variants.[7-9] Changes in plasma copper levels and parameters of copper metabolism are connected to metabolic conditions, including obesity and fatty liver, and dietary factors.[2,10] However, the significance of copper excess or deficiency in metabolism and the methods to measure them are subjects of ongoing debate. Epidemiological data over the past few decades show declining mineral and trace element contents in the Western diet.[11,12] In obese patients, plasma copper levels are positively correlated with body mass index (BMI).[13] Obesity is accompanied by increased plasma ceruloplasmin levels and increased copper concentration in visceral fat.[14] Conversely, patients with fatty liver present lower hepatic and plasma copper and lower plasma ceruloplasmin levels compared to

healthy people and patients with other liver diseases.[15] In addition, hepatic copper concentration is inversely correlated with the severity of hepatic steatosis and features of metabolic syndrome.[15] The provision of a high fructose diet in rats caused worsening of fatty liver, particularly when associated with marginal copper deficiency.[16]

However, copper is not the only transition metal playing a role in metabolism and the antioxidant response. Both iron and zinc have equally complex and important regulatory roles in the body, playing essential functions as co-factors in energy production and homeostasis. Misregulation of these metals has been linked to numerous diseases, from metabolic to neurodegenerative diseases. [17-19] Iron, similarly to copper, can undergo redox active chemistry, having disastrous effects on cells and the body if not properly regulated.[20-22] Ferritin (an iron storage protein) and transferrin (an iron chaperone) are traditionally used alongside iron concentrations as biomarkers for serum iron status. [23,24] Zinc, on the other hand, is not redox active yet imparts significant function to a large number of proteins in both structural and enzyme active sites.[25] These metals have been shown to play significant roles in lipid metabolism. For instance, PPARγ, which regulates lipid metabolism, utilizes zinc fingers for DNA binding and is downregulated in zinc deficient conditions, while intracellular catalytic iron is believed to facilitate lipid peroxidation.[26-28] As such, understanding how these metals and their markers are affected by environmental factors, such as dietary sugar intake, is likely to prove important in the diagnosis or treatment of metabolic diseases.

Human and in vivo data in the metal micronutrient field are lacking. Clinical parameters assessing systemic metal status and metabolism and flow between organs are limited, likely due to discrepancies in the available data and the difficulties in their interpretation. In the case of copper, most clinical laboratories provide plasma ceruloplasmin protein levels assessed by immunologic assay; however, this parameter does not differentiate between apoceruloplasmin and holoceruloplasmin.[29-31] Ceruloplasmin (enzymatic) ferroxidase activity could aid in the direct quantification and speciation of copper in plasma, but it is not normally provided in clinical practice. Other parameters, including radioactive copper incorporation and

exchangeable copper, appear promising and could potentially enable a better assessment of copper status, but remain unvalidated.[32,33] To study the effects of dietary components such as sugar consumption on transition metal levels and the resulting metabolic changes, improved clinical parameters for assessing these metal levels are necessary.

In the current study, we analyzed serum copper, iron, and zinc metabolism parameters and their relation to lipid metabolism in healthy, younger (18–40 years) male and female subjects who consumed beverages sweetened with glucose, fructose, high fructose corn syrup (HFCS), or aspartame for two weeks. We provide evidence that intake of sugar-sweetened beverages results in changes of copper, iron, and zinc status and metabolism in association with markers of lipid metabolism.

2.2 Materials and Methods

2.2.1 Human Subjects and Study Design

Subjects in this study are a subgroup from a NIH-funded, parallel-arm, double-blinded diet-intervention study. Subject characteristics and detailed study design were previously reported.[34,35] In brief, the study occurred in three phases: (I) 3.5-day inpatient baseline; (II) 12-day outpatient intervention; and (III) 3.5-day inpatient intervention. Subjects resided at the UC Davis Clinical and Translational Science Center Clinical Research Center (CCRC) during inpatient periods. Each experimental group was matched according to sex, BMI, fasting triglyceride (TG), cholesterol, high-density lipoprotein (HDL), and insulin. This study reports results from 107 of the 187 original participants consuming beverages containing aspartame (n = 23), glucose (n = 28), fructose (n = 28), and HFCS composed of 45% glucose and 55% fructose (n = 28). For 5 weeks prior to the study, subjects were asked to restrict daily intake of sugar-containing beverages to one 8-oz serving of fruit juice and stop consuming all vitamin and mineral dietary or herbal supplements.

Informed written consent was obtained from each subject and the study protocol conformed to the ethical guidelines of the 1975 Declaration of Helsinki as reflected in a priori approval by the Institutional

Review Board at the University of California, Davis; IRB #214709 (19 August 2018) and #1332484 (5 December 2018).

2.2.2 Diet

During the 12-day outpatient phase, subjects were provided with and instructed to drink three servings of sweetened beverage per day (one per meal), consume their normal diet, and abstain from other sugar-containing beverages, including fruit juice. The sugar-sweetened beverages contained glucose (STALEYDEX® crystalline dextrose, Tate and Lyle, Hoffman Estates, IL, USA), fructose (KRYSTAR® crystalline fructose, Tate and Lyle, Hoffman Estates, IL, USA), or HFCS (ISOSWEET® 5500, Tate and Lyle, Hoffman Estates, IL, USA). These beverages were formulated as 15% sugar in water (weight/weight) and flavored with unsweetened Kool-Aid® drink mix (Kraft Foods, Northfield, IL, USA). The three daily servings of sugar-sweetened beverage in total provided 25% of daily energy requirement, equivalent to approximately 4.5 12-ounce cans of a standard soft drink per day. Daily energy requirements were calculated by the Mifflin equation with adjustments of 1.3 for activity on the inpatient 24-h serial blood collection days and 1.5 for the other days.[36] The control beverages were sweetened with aspartame (Market Pantry™ sugar-free drink mix, Target Brands Inc., Minneapolis, MN, USA) and were provided as 3 daily servings comparable in quantity to the sugar-sweetened beverages. Riboflavin was added as a compliance biomarker to the sweetened beverages and measured by fluorimetry in urine collected from the subjects during both the inpatient and outpatient phases.[37] Urinary riboflavin levels did not differ between groups, and levels during the outpatient phase were not different than levels during the inpatient phase when consumption was monitored.[34,35] Subjects were instructed to abstain from alcohol the day before check-in to the CCRC.

2.2.3 Serum Metals and Ceruloplasmin Ferroxidase Activity

Fasting serum (30-min clotting time) was collected between 07:00 and 08:00 following subject check-in during both the baseline and intervention inpatient phase. Serum and sweetened beverage aliquots were digested in 1N Ultrex II nitric acid (Avantor JT Baker, Radnor Township, PA, USA) at 4 °C for 24 h then

centrifuged at 3000 rpm/4 °C for 12 min in a Sorvall Legend X1R centrifuge (Thermo Fisher Scientific, Waltham, MA, USA) and supernatant collected. Iron, copper, and zinc levels were measured by inductively coupled plasma mass spectrometry at the UC Davis Interdisciplinary Center for Plasma Mass Spectrometry. Sweetened beverage samples were analyzed separately to determine if metal content in the Kool-aid drink mixes were significantly different from one another; no significant differences were found (Figure 2.S1). Ceruloplasmin ferroxidase activity was measured with a colorimetric assay (EIACPLC, Invitrogen, Carlsbad, CA, USA). According to the manufacturer's protocols, samples were diluted 1:50 in the commercial assay buffer and a colorimetric ceruloplasmin substrate was added. Plates were incubated at 30 °C for 60 min and absorbances were read at 560 nm using a Synergy H1 microplate reader (Bio Tek, Winooski, VT, USA).

2.2.4 Serum Protein Levels

Serum protein levels were measured using commercially available ELISAs according to the manufacturers' protocols. Samples were diluted 1:400,000 for ceruloplasmin (EC4201-1, Assaypro, St. Charles, MO, USA); 1:250,000 for transferrin (ab187391, Abcam, Cambridge, MA, USA); and 1:10 for ferritin (ab200018, Abcam, Cambridge, MA, USA). Samples and standards were run in duplicate and their absorbance was measured using a Synergy H1 microplate reader (Bio Tek, Winooski, VT, USA).

2.2.5 Plasma Lipid and Glucose Parameters

As previously reported[34,35], 24-h serial plasma samples were collected every 30 or 60 min starting at 08:00 during the third day of each inpatient phase and analyzed for TG, lipoproteins, insulin, and glucose. In the current study these data were utilized for the purpose of novel correlation analyses with metal and metal biomarker parameters. Plasma TG concentrations were measured at all time points and calculated for mean 24-h concentration and for total 24-h area under the curve (AUC) by the trapezoidal method. TG, apolipoprotein CIII (apoCIII), and lactate concentrations were measured with a Polychem Chemistry Analyzer (PolyMedCo Inc., Cortland Manor, New York, USA) with reagents from MedTest DX (Canton, MI, USA). Glucose was measured with an automated glucose analyzer (YSI, Inc., Yellow Springs, OH, USA) and

insulin by radioimmunoassay (Millipore, St. Charles, MO). Changes in glucose and insulin amplitude were calculated as post-meal zenith minus pre-meal nadir concentration for each meal and averaged for the 3 meals.

2.2.6 Statistical Analyses

Metal concentrations in the sweetened beverages and baseline variables were analyzed by one-way ANOVA.

Each metal outcome was analyzed for the effect of beverage group in a MIXED procedure repeated measures (time) analysis of covariance (ANCOVA) using SAS 9.4 (Cary, NC, USA). The model included adjustments for sex, BMI, time, and beverage x time, with Tukey's post-test for beverage x time. Identical repeated measures ANCOVAs that included adjustment for the change in BMI were also conducted. The percentage change of each outcome was analyzed by the general linear model ANCOVA; the beverage interventions were included as its proportional contents of monosaccharides (fructose and glucose) as separate variables. Therefore, fructose was input as 1 for fructose and 0 for glucose, glucose as 0 for fructose and 1 for glucose, HFCS as 0.55 for fructose and 0.45 for glucose, and aspartame as 0 for both fructose and glucose. The model was adjusted for outcome at baseline, BMI, and sex. Covariates that decreased the sensitivity of the model were removed. Outcomes significantly affected by BMI were further assessed by two-tailed unpaired *t*-test (Microsoft Excel; Microsoft, Redmond, WA, USA) with subjects separated into two cohorts by BMI< or ≥25 kg/m^2.

Partial Pearson correlations adjusted for BMI and sex (SAS 9.4) were used to assess the relationships between: (1) metal markers at baseline; (2) changes in metal markers; and (3) changes in metal markers and metabolic markers. Significant relationships between changes in metal markers and metabolic markers were further tested by partial Pearson correlations adjusted for fructose, glucose, BMI, and sex.

p-values < 0.05 were considered significant.

2.3 Results

2.3.1 Baseline Measures

There were no significant differences in baseline characteristics between the four intervention groups (Table 2.1) or in the copper, iron, and zinc content of the study beverages (Figure 2.S1).

Table 2.1 Description of subjects at baseline by sugar consumed. Means ± SEMs are shown. BMI, body mass index; HFCS, high fructose corn syrup.

	Glucose *n* = 28	Fructose *n* = 28	HFCS *n* = 28	Aspartame *n* = 23	Total *n* = 107
BMI	25.4 ± 0.7	25.8 ± 0.7	24.9 ± 0.8	24.8 ± 0.7	25.3 ± 0.4
Age	26.8 ± 1.2	26.0 ± 1.1	26.8 ± 1.2	25.4 ± 1.3	26.3 ± 1.6
Sex	15 M/13 F	15 M/13 F	15 M/13 F	11 M/12 F	56 M/51 F
% M/F	53.6/46.4	53.6/46.4	53.6/46.4	47.9/53.1	52.3/47.7

2.3.2 Effects of Glucose, Fructose, HFCS, and Aspartame on Metals and Metal Metabolism Markers

Table 2.2 shows the absolute values of the seven metal-associated outcomes (three metals and four metal metabolism markers) at baseline and after intervention. Ceruloplasmin concentration was not affected by the consumption of the sweetened beverages. The serum concentrations of all other metal-associated outcomes decreased over time; however, there were no significant effects of beverage group or beverage x time (Table 2.3). Subjects consuming HFCS and glucose exhibited the most marked decreases in copper concentrations (HFCS: −83.9 ± 25.3, 2 weeks vs. 0 weeks, Tukey's post-test adjusted *p*-value: 0.0019; glucose: −77.6 ± 13.8 ppb; adjusted *p*-value = 0.0069). Ceruloplasmin ferroxidase activity was also decreased following HFCS or glucose consumption; however, when adjusted for multiple comparisons, the decreases were not significant (HFCS: −2.0 ± 0.53 U/mL, unadjusted *p*-value: 0.0049; adjusted *p* = 0.089; glucose: −2.1 ± 0.9 U/mL, unadjusted *p*-value: 0.0029, adjusted *p*-value: 0.056). Subjects consuming HFCS or glucose also exhibited decreased zinc concentrations (HFCS: −93.3 ± 29.3 ppb; Tukey's post-test unadjusted *p*-value: 0.0006; adjusted *p*-value: 0.014; glucose: −80.0 ± 25.2 ppb; Tukey's post-test unadjusted *p*-value: 0.0032; adjusted *p*-value: 0.060, 2 weeks versus 0 weeks). Adjustment of the repeated measures ANCOVAs for the change in BMI tended to strengthen rather than attenuate these results and did not reveal any additional effect of the beverage interventions.

Table 2.2 Serum metals and metal metabolism markers during consumption of aspartame, glucose, fructose, or HFCS-sweetened beverages at week 0 and week 2. Means ± SEMs are shown. Cp, ceruloplasmin; Cp-ferrox, ceruloplasmin ferroxidase activity.

	Aspartame		Glucose		Fructose		HFCS	
	Week 0	Week 2	Week 0	Week 2	Week 0	Week 2	Week 0	Week 2
Cp (µg/mL)	773 ± 125	1095 ± 287	920 ± 157	815 ± 125	1098 ± 258	805 ± 198	885 ± 146	984 ± 156
Cp-ferrox (U/mL)	26.8 ± 2.5	26.8 ±2.3	28.2 ± 2.2	26.1 ± 1.8	28.8 ± 1.5	27.7 ± 1.5	29.5 ± 2.3	27.5 ± 2.1
Transferrin (mg/dL)	93.6 ± 6.6	84.87 ± 6.5	104.2 ± 4.4	104.4 ± 6.2	101.2 ± 5.1	94.0 ± 5.8	109.2 ± 5.7	94.0 ± 5.4
Ferritin (ng/mL)	37.7 ± 10.2	28.9 ± 7.54	48.7 ± 7.9	36.8 ± 7.1	45.6 ± 8.4	28.7 ± 5.7	41.9 ± 6.0	31.1 ± 5.3
Copper (ppb)	912 ± 49	881 ± 41	976 ± 55	869 ± 43	953 ± 34	898 ± 32	1019 ± 55	935 ± 49
Iron (ppb)	1029 ± 77	726 ± 68	920 ± 82	825 ± 78	1037 ± 87	796 ± 53	1007 ± 74	750 ± 59
Zinc (ppb)	975 ± 37	957 ± 30	1012 ± 24	932 ± 33	983 ± 24	969 ± 24	991 ± 33	897 ± 22

Sex was a significant factor in the model (Table 2.3). However, the differences between male and female in copper, ceruloplasmin ferroxidase activity, zinc, iron, and ferritin levels were specific to baseline and not due to an effect of intervention.

Table 2.3 *p*-values for the MIXED procedure repeated measures (time) ANCOVA testing each outcome for the effects of beverage, sex, BMI, time, and beverage x time. Significant values are in bold.

	Beverage *p*-value	Sex *p*-value	BMI *p*-value	Time *p*-value	Beverage x time *p*-value
Cp	0.972	0.615	0.289	0.945	0.087
Cp-ferrox	0.873	**0.005**	0.255	**<0.001**	0.161
Copper	0.203	**<0.001**	**<0.001**	**<0.001**	0.331
Zinc	0.737	**<0.001**	0.558	**<0.001**	0.084
Iron	0.916	**0.001**	**0.039**	**<0.001**	0.442
Ferritin	0.878	**<0.001**	0.177	**<0.001**	0.284
Transferrin	0.104	0.355	0.590	**0.003**	0.209

There were significant relationships between BMI and both iron and copper (Table 2.3). To further investigate these relationships, subjects were stratified by BMI (BMI < 25 and BMI ≥ 25), and iron and copper concentrations were compared at both baseline and intervention (Table 2.4). Serum copper concentrations tended to be higher and iron concentrations lower at baseline in subjects with BMI ≥ 25 compared to those with BMI < 25. After intervention, copper was significantly higher in subjects with BMI ≥ 25, but a BMI-influenced difference in iron was no longer apparent.

Table 2.4 Copper and iron concentrations in subjects divided by BMI into normal weight (<25 kg/m^2) or overweight and obese (≥25 kg/m^2) groups. An unpaired, two-tailed *t*-test was used to analyze significance between BMI groups. Mean ± SEM are shown.

		BMI < 25 (*n* = 51)	BMI ≥ 25 (*n* = 56)	*p*-value
Copper	Baseline	918 ± 33	995 ± 30	0.08
	Intervention	847 ± 29	936 ± 29	**0.03**
Iron	Baseline	1107 ± 64	899 ± 47	**0.008**
	Intervention	779 ± 53	776 ± 40	0.97

To further investigate the changes over time, we analyzed each outcome in a model that assessed the specific effects of glucose and fructose. Copper and ceruloplasmin ferroxidase activity were significantly influenced by the effects of fructose and/or glucose (Figure 2.1). Glucose, consumed at 25% of energy requirement, accounted for −7.06% ± 3.26% of the change in copper (p = 0.033) and −9.23% ± 3.46% of the change in ceruloplasmin ferroxidase activity (p = 0.009). Fructose, consumed at 25% of energy requirement, accounted for −7.26% ± 3.4% of the change in ceruloplasmin ferroxidase activity (p = 0.035). Glucose consumption also contributed to the decrease in serum zinc concentrations (−8.41% ± 4.1%, p = 0.045) (Figure 2.1). Neither glucose nor fructose consumption contributed to the significant decreases in iron status markers observed during the two-week intervention (data not shown).

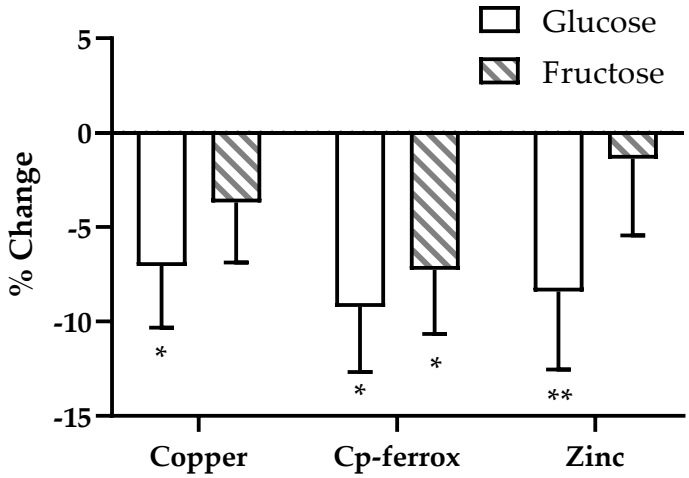

Figure 2.1 Estimates of the effects of fructose and glucose on the percentage changes of serum copper, Cp-ferrox, and zinc in subjects consuming beverages containing fructose, glucose, HFCS, or aspartame for 2 weeks. General linear model ANCOVA with beverage interventions described as the proportional

contents of fructose and glucose as separate variables. Model included adjustments for BMI and sex. * $p < 0.05$, ** $p < 0.01$, effect of glucose or fructose.

2.3.3. Correlations of Baseline Serum Metal Concentrations with Baseline Metal Metabolic Markers

Partial Pearson correlations of baseline metals and their metabolism markers were adjusted for BMI and sex (Table 2.5). This analysis of baseline metal markers presents some interesting correlations, with copper positively correlated to ceruloplasmin ferroxidase activity (r = 0.520, $p < 0.001$), but not ceruloplasmin concentration (r = 0.125, $p = 0.204$). In addition to this lack of significance with copper, ceruloplasmin concentration is negatively correlated to its ferroxidase activity (r = −0.452, $p < 0.001$). Zinc was also found to be negatively correlated with ceruloplasmin concentration (r = −0.208, $p = 0.033$). Iron concentrations were positively correlated to both transferrin (r = 0.350, $p < 0.001$) and ferritin (r = 0.241, $p = 0.014$).

Table 2.5 Partial correlation between baseline metal and metal metabolism markers adjusted for BMI and sex. $p < 0.05$ are shown in bold with positive associations (r > 0) shown in blue, and negative associations (r < 0) shown in red.

		Copper	Iron	Zinc	Cp-ferrox	Cp	Transferrin	Ferritin
Copper	r		−0.131	−0.082	0.520	0.125	0.014	−0.237
	p		0.184	0.411	**<0.001**	0.204	0.890	0.016
Iron	r	−0.131		0.048	−0.098	0.016	0.350	0.241
	p	0.184		0.628	0.321	0.872	**<0.001**	**0.014**
Zinc	r	−0.0815	0.048		0.132	−0.208	0.169	−0.088
	p	0.411	0.628		0.178	**0.033**	0.087	0.376
Cp-ferrox	r	0.520	−0.098	0.132		−0.452	0.028	−0.153
	p	**<0.001**	0.321	0.178		**<0.001**	0.778	0.119
Cp	r	0.125	0.016	−0.208	−0.452		−0.032	−0.014
	p	0.204	0.872	**0.033**	**<0.001**		0.746	0.889
Transferrin	r	0.014	0.350	0.169	0.028	−0.032		0.103
	p	0.890	**<0.001**	0.087	0.778	0.746		0.295
Ferritin	r	−0.237	0.241	−0.088	−0.153	−0.014	0.103	
	p	0.016	**0.014**	0.376	0.119	0.889	0.295	

2.3.4 Correlations of Changes in Serum Metal Concentrations with Changes in Metal Metabolism Markers

Correlations of the changes from week 0 to week 2, adjusted for BMI and sex, highlighted different interactions between metal markers than observed with baseline correlations (Table 2.6). ΔCopper was strongly positively correlated with Δzinc (r = 0.359, $p < 0.001$) and Δceruloplasmin ferroxidase activity (r = 0.572, $p < 0.001$) along with a weaker positive correlation with Δceruloplasmin concentration (r = 0.235, $p = 0.016$). ΔIron concentrations were strongly correlated with only Δtransferrin (r = 0.445, $p < 0.001$). These significant relationships were not attenuated in additional partial correlation analyses that included adjustment for fructose, glucose, BMI, and sex (data not shown).

Table 2.6 Partial correlation between changes from week 0 to week 2 in metal and metal metabolism markers adjusted for BMI and sex. $p < 0.05$ are shown in bold with positive associations (r > 0) shown in blue.

		Copper	Iron	Zinc	Cp-ferrox	Cp	Transferrin	Ferritin
Copper	r		0.114	0.358	0.572	0.235	−0.046	0.069
	p		0.251	**<0.001**	**<0.001**	**0.016**	0.642	0.492
Iron	r	0.114		0.204	0.040	−0.032	0.445	0.049
	p	0.251		0.036	0.687	0.745	**<0.001**	0.624
Zinc	r	0.358	0.204		0.309	0.173	0.191	−0.091
	p	**<0.001**	0.036		0.687	0.078	0.052	0.360
Cp-ferrox	r	0.572	0.040	0.309		0.187	0.093	0.041
	p	**<0.001**	0.687	0.687		0.056	0.346	0.676
Cp	r	0.235	−0.032	0.173	0.187		0.017	0.143
	p	**0.016**	0.745	0.078	0.056		0.864	0.147
Transferrin	r	−0.046	0.445	0.191	0.093	0.017		0.045
	p	0.642	**<0.001**	0.052	0.346	0.864		0.648
Ferritin	r	0.069	0.049	−0.091	0.041	0.143	0.045	
	p	0.492	0.624	0.360	0.676	0.147	0.648	

2.3.5 Correlations of Changes in Serum Metal Concentrations with Changes in Metabolism Markers

Partial correlations, with adjustments for BMI and sex, between changes from week 0 to week 2 of metal markers, and changes in selected metabolic markers showed negative correlations (Table 2.7). ΔCopper was negatively correlated with Δfasting levels of apoCIII (r = −0.25, $p = 0.011$). ΔCeruloplasmin ferroxidase activity was negatively correlated with the Δamplitude of glucose (r = −0.260, $p = 0.007$), insulin (r = −0.270, $p = 0.007$), and lactate (r = −0.300, $p = 0.003$). ΔIron metabolism was also related to changes in

metabolic markers. ΔTransferrin concentration was negatively correlated with Δpostprandial apoCIII (r = −0.200, p = 0.046) and Δferritin was negatively correlated with Δpostprandial TG levels (r = −0.220, p = 0.025), ΔTG AUC (r = −0.230, p = 0.021), Δfasting apoCIII (r = −0.290, p = 0.003), Δpostprandial apoCIII (r = −0.290, p = 0.003), and Δlactate amplitude (r = −0.21, p = 0.039). These significant inverse relationships were not attenuated in additional partial correlation analyses that included adjustment for fructose, glucose, BMI, and sex (data not shown).

Table 2.7 Partial correlation between changes from week 0 to week 2 in metal and metabolism markers adjusted for fructose, glucose, BMI, and sex. $p < 0.05$ are shown in bold with r < 0 shown in red. TG AUC, triglyceride area under the curve; apoCIII, apolipoprotein CIII.

		Postprandial TG	TG AUC	Fasting apoCIII	Postprandial apoCIII	Glucose Amplitude	Insulin Amplitude	Lactate Amplitude
Copper	r	−0.001	−0.069	−0.250	−0.053	0.028	−0.116	−0.026
	p	0.994	0.504	**0.011**	0.606	0.788	0.261	0.800
Iron	r	0.029	−0.059	−0.165	−0.142	0.066	0.069	0.074
	p	0.777	0.565	0.109	0.169	0.525	0.504	0.473
Zinc	r	0.010	−0.061	0.023	−0.036	0.059	0.080	0.150
	p	0.922	0.555	0.823	0.728	0.566	0.436	0.144
Cp-ferrox	r	0.010	0.095	−0.089	0.0172	−0.260	−0.270	−0.300
	p	0.334	0.359	0.389	0.868	**0.007**	**0.007**	**0.003**
Cp	r	−0.056	−0.060	0.050	0.005	0.085	−0.077	−0.121
	p	0.586	0.559	0.630	0.959	0.411	0.457	0.240
Transferrin	r	−0.047	−0.069	−0.078	−0.200	−0.104	−0.059	0.007
	p	0.651	0.507	0.451	**0.046**	0.312	0.570	0.947
Ferritin	r	−0.220	−0.230	−0.290	−0.290	−0.210	0.096	−0.21
	p	**0.025**	**0.021**	**0.003**	**0.003**	0.934	0.351	**0.039**

2.4 Discussion

The current study provides insights on the relationship between the consumption of sweetened beverages in the diet and metal micronutrient regulation in humans. Our data propose connections between diet composition; copper, iron, and zinc metabolism; and metabolic biomarkers in healthy subjects. We found consumption of both glucose and fructose contributed to significant decreases in ceruloplasmin ferroxidase activity but had no effect on ceruloplasmin concentrations. We also found

consumption of glucose, but not fructose, contributed to decreases in serum copper and zinc concentrations.

The notable changes in ceruloplasmin ferroxidase activity and copper concentrations in the serum of subjects consuming sugar-sweetened beverages suggest a connection between sugar ingestion and copper metabolism. The role of copper in human health is poorly understood, with a majority of research investigating copper in patients with obesity. Our data point to healthy adults having increased serum copper levels with higher BMI. The association between serum copper concentration and adiposity status in healthy individuals was also noted by Olusi et al., who reported a positive association between copper and leptin in healthy adults.[38] Yang et al. reported that an increase in copper and ceruloplasmin serum concentrations was positively associated with BMI.[14] Additional studies have shown increased copper export along with decreased hepatic copper concentration in non-alcoholic fatty liver disease (NAFLD) and a relationship between elevated serum copper and liver cirrhosis or hepatocellular carcinoma.[10,39,40] While these studies relate elevated serum copper to obesity and associated conditions, our data suggest consumption of sugar-sweetened beverages, especially glucose containing beverages, by healthy subjects, decreases serum copper and ceruloplasmin ferroxidase activity. Similarly to our findings, Aigner et al. demonstrated patients with NAFLD present a decrease in both hepatic copper concentration and serum ceruloplasmin ferroxidase activity.[41] Previous in vivo studies indicate involved pathogenic factors may include reduced duodenal copper absorption due to inhibited transcription of *Ctr1*, concomitant hepatic iron accumulation, or alterations in gut microbiota composition possibly related to increased abundance of Firmicutes and reduced Akkermansia.[16,41,42] Other proposed mechanisms involve copper regulation of cyclic-AMP-dependent lipolysis or mitochondrial dysfunction associated with impaired cupro-enzymatic activity.[43-45] These mechanisms may be contributing factors to effects observed but not studied in our work.

To the best of our knowledge, this is the first study of the effects of glucose or HFCS on copper and its markers in healthy subjects. Previous studies have focused on fructose and indicated fructose may impact

copper metabolism in a unique way.[46,47] In rats, fructose-rich diets and copper-deficient diets showed exacerbations of NAFLD-like pathology, suggesting a potential crosstalk between copper metabolism and fructose.[46]. Recent studies have further corroborated this finding and revealed sex-specific differences, finding that a diet of 30% caloric intake from fructose altered copper only in males.[48] Our results suggest glucose consumption may also have a negative impact on copper metabolism and this impact may be more marked than that of fructose. More studies of the effects of glucose, HFCS, and fructose on copper metabolism are needed.

We found changes in copper were negatively associated with changes in fasting apoCIII, a lipoprotein implicated as a cardiovascular disease risk factor[49], and ceruloplasmin ferroxidase activity was negatively associated with increases in post-meal glucose, insulin, and lactate responses. These inverse associations, which were independent of the effects of fructose and glucose, suggest the possibility that adequate copper and ceruloplasmin ferroxidase activity is linked to fuel utilization and may have protective metabolic effects.

Traditionally it is thought that iron is linked to copper through the activity of ceruloplasmin, however, our data suggest that zinc may also be involved.[50] Serum zinc levels follow a pattern similar to copper, with glucose consumption contributing to decreased zinc concentrations. We also observed a strong positive association between the changes in zinc and copper independent of the effects of glucose and fructose. Baseline serum zinc concentrations were negatively correlated with ceruloplasmin concentration. A connection between sugar consumption and zinc has also been recently reported wherein rats consuming high fructose diets exhibited decreases in hepatic zinc concentrations.[48] These data strengthen the connection between copper and zinc, but also indicate that the interplay between them, especially in the context of dietary interventions, has yet to be fully understood.[51-53]

While we failed to observe any significant difference between beverage groups, or significant effects of fructose or glucose, on the decreases in iron and iron markers, we observed some interesting

relationships. Analysis of the change from baseline to intervention of iron and ferritin by repeated measures ANCOVA reveals that serum iron was significantly decreased in all four beverage groups. Ferritin, however, was significantly decreased in subjects consuming sugar-containing beverage, but not the subjects consuming aspartame. Literature is sparse regarding connections between serum iron and aspartame. As the aspartame-induced decrease in serum iron concentrations was not confirmed by an aspartame-induced decrease in ferritin, additional studies are required to determine whether aspartame consumption affects iron levels. We observed that subjects with BMI < 25 had higher serum iron concentrations at baseline than subjects with BMI ≥ 25. This difference requires further study as it was not observed at the end of the two-week intervention. However, the baseline relationship supports data reporting decreased serum iron concentration is associated with increased BMI.[54] Our data support the findings that NAFLD induces increased hepatic iron concentrations and increased hepatic hepcidin expression, which would result in decreased serum iron levels.[41] This relationship between hepcidin and diet merits additional research given the role of this peptide in the innate immune system.[55] Studying the interplay between diet, inflammatory cytokines, and transition metal regulation would add another piece to the puzzle of transition metals in biology.

We also observed that the changes in ferritin were negatively associated with the changes in postprandial TG and the changes in fasting and postprandial apoCIII. These effects, which were independent of fructose and glucose consumption, are contradicted by a recent observational study showing fasting ferritin levels were positively associated with TG and lipoproteins.[56] This discrepancy may be due to the much higher ferritin concentrations exhibited by the subjects studied by Zhou et al. They were divided into quartiles based on ferritin concentrations; only three of the subjects in our study met the criteria of the second-highest quartile and none fit in the highest quartile.

One important observation of the present study concerns the relationship between serum copper concentration, ceruloplasmin levels, and copper-dependent ceruloplasmin ferroxidase activity. Laboratory

tests for ceruloplasmin levels are widely used as a proxy for copper concentration in the serum.[29,57] While serum ceruloplasmin has been a key test for diagnosing Wilson disease, our findings suggest ceruloplasmin ferroxidase activity might be a more accurate representation for copper status given the observed strong correlation of copper concentration with ceruloplasmin ferroxidase activity and a weaker correlation with ceruloplasmin concentration. The differences between activity and concentration are even more apparent when considering the effects of the intervention. The change in serum copper was positively correlated with ceruloplasmin ferroxidase activity, yet negatively correlated with ceruloplasmin concentration. This accentuates the differences between the activity and concentration of a protein and the need for additional studies untangling how these parameters relate to one another and to copper metabolism.

Our study is limited by the post hoc nature of the analysis. Consumption of metal micronutrients were not controlled during the outpatient period of the study and the subjects were instructed to consume their normal diets. Thus, both metal consumption and bioavailability could have been altered by variables for which this study did not control. In addition to variabilities in the subjects' normal diets, it is possible that the added calories from the beverages could have displaced the consumption of metal-rich foods or nutrients that enhance metal bioavailability. It is also feasible that consumption of sweetened beverages affected metal absorption. Future studies may be informed by existing reports on the impacts of sugar intake on metal bioavailability.[58,59] In addition, given the assessment of metal markers was not initially planned, the study might also have been under-powered to assess certain effects of sugar consumption on metal metabolism. Future studies are warranted that control for metal micronutrient intake and being sufficiently powered to validate the trends observed in this study. Nevertheless, the short-term two-week intervention was sufficient to cause significant sugar-dependent changes in certain serum metal markers, offering support for a connection between sugar metabolism and metal homeostasis.

2.5 Conclusions

Our results suggest sugar consumption affects copper and zinc metabolism parameters within two weeks. Alterations in transition metal metabolism, in turn, can contribute to aberrant fuel utilization and potentially worsen the course of metabolic-related diseases. Glucose consumption may possibly have a more marked impact on transition metal metabolism than fructose consumption. Ceruloplasmin ferroxidase activity appears to correlate significantly with copper serum levels and may have broader applications in clinical practice than ceruloplasmin levels.

Our findings are the first evidence that consumption of sugar-sweetened beverages can alter clinical parameters of transition metal metabolism in healthy subjects. As sugar consumption has become entrenched in the Western diet, further study of the relationships between transition metal metabolism and glucose, fructose, HFCS, and also sucrose is warranted. Our findings represent the proverbial tip of the iceberg toward understanding the physiological impact of microminerals in the modern Western diet and highlight the need to further probe the clinical relationship between metal status and metabolic health.

2.6 Supplementary Material

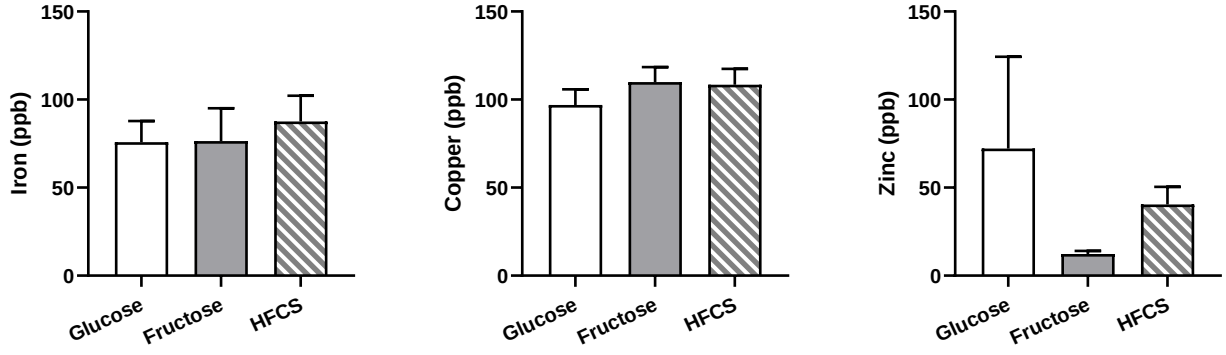

Figure 2.S1. Metal concentrations in glucose-, fructose-, or HFCS-sweetened beverages consumed by subjects (n=6). Mean ± SEM are shown. One-way ANOVA were used to analyze significance between metal levels in sweetened beverages; no significant differences were found.

2.7 References

(1) Hasan, N.M. Regulation of Copper Transporters in Human Cells. Curr. Top. Membr. 2012, 69, 137–161.

(2) Morrell, A.; Tallino, S.; Yu, L.; Burkhead, J.L. The role of insufficient copper in lipid synthesis and fatty-liver disease. IUBMB Life 2017, 69, 263–270.

(3) Han, M.; Lin, Z.; Zhang, Y. The Alteration of Copper Homeostasis in Inflammation Induced by Lipopolysaccharides. Biol. Trace Elem. Res. 2013, 154, 268–274.

(4) Kim, H.; Son, H.-Y.; Bailey, S.M.; Lee, J. Deletion of hepatic Ctr1 reveals its function in copper acquisition and compensatory mechanisms for copper homeostasis. AJP Gastrointest. Liver Physiol. 2008, 296, G356–G364.

(5) Lutsenko, S. Copper trafficking to the secretory pathway. Metallomics 2016, 8, 840–852.

(6) Linder, M.C. Ceruloplasmin and other copper binding components of blood plasma and their functions: An update. Metallomics 2016, 8, 887–905.

(7) Lutsenko, S.; Barnes, N.L.; Bartee, M.Y.; Dmitriev, O.Y. Function and Regulation of Human Copper-Transporting ATPases. Physiol. Rev. 2007, 87, 1011–1046.

(8) Członkowska, A.; Litwin, T.; Dusek, P.; Ferenci, P.; Lutsenko, S.; Medici, V.; Rybakowski, J.K.; Weiss, K.H.; Schilsky, M.L. Wilson disease. Nat. Rev. Dis. Prim. 2018, 4, 1–20.

(9) Roberts, E.A. Update on the Diagnosis and Management of Wilson Disease. Curr. Gastroenterol. Rep. 2018, 20, 1–12.

(10) Heffern, M.C.; Park, H.M.; Au-Yeung, H.Y.; van de Bittner, G.C.; Ackerman, C.M.; Stahl, A.; Chang, C.J. In vivo bioluminescence imaging reveals copper deficiency in a murine model of nonalcoholic fatty liver disease. Proc. Natl. Acad. Sci. USA 2016, 113, 14219–14224.

(11) Klevay, L.M. Is the Western diet adequate in copper? J. Trace Elem. Med. Biol. 2011, 25, 204–212.

(12) Lim, K.H.C.; Riddell, L.J.; Nowson, C.A.; Booth, A.O.; Szymlek-Gay, E.A. Iron and zinc nutrition in the economically-developed world: A review. Nutrients 2013, 5, 3184–3211.

(13) Fan, Y.; Zhang, C.; Bu, J. Relationship between selected serum metallic elements and obesity in children and adolescent in the U.S. Nutrients 2017, 9, 104.

(14) Yang, H.; Liu, C.N.; Wolf, R.M.; Ralle, M.; Dev, S.; Pierson, H.; Askin, F.; Steele, K.E.; Magnuson, T.H.; Schweitzer, M.A.; et al. Obesity is associated with copper elevation in serum and tissues. Metallomics 2019, 11, 1363–1371.

(15) Aigner, E.; Strasser, M.; Haufe, H.; Sonnweber, T.; Hohla, F.; Stadlmayr, A.; Solioz, M.; Tilg, H.; Patsch, W.; Weiss, G.; et al. A role for low hepatic copper concentrations in nonalcoholic fatty liver disease. Am. J. Gastroenterol. 2010, 105, 1978–1985.

(16) Song, M.; Schuschke, D.A.; Zhou, Z.; Chen, T.; Pierce, W.M.; Wang, R.; Johnson, W.T.; McClain, C.J. High fructose feeding induces copper deficiency in Sprague-Dawley rats: A novel mechanism for obesity related fatty liver. J. Hepatol. 2012, 56, 433–440.

(17) Lane, D.J.R.; Ayton, S.; Bush, A.I. Iron and Alzheimer's Disease: An Update on Emerging Mechanisms. J. Alzheimers Dis. 2018, 64, S379–S395.

(18) Datz, C.; Müller, E.; Aigner, E. Iron overload and non-alcoholic fatty liver disease. Miner. Endocrinol. 2017, 42, 173–183.

(19) Brabin, B.J.; Hakimi, M.; Pelletier, D. An Analysis of Anemia and Pregnancy-Related Maternal Mortality. J. Nutr. 2001, 131, 604S–615S.

(20) Burggraf, L.W.; Hansen, S.D.; Bleckmann, C.A. Metabolic inhibition by transition metal ions in a slow-growing, toluene-enriched microbial population. Environ. Toxicol. Water Qual. 1998, 13, 249–261.

(21) Salaye, L.; Bychkova, I.; Sink, S.; Kovalic, A.J.; Bharadwaj, M.S.; Lorenzo, F.; Jain, S.; Harrison, A.V.; Davis, A.T.; Turnbull, K.; et al. A Low Iron Diet Protects from Steatohepatitis in a Mouse Model. Nutrients 2019, 11, 2172.

(22) Tamaki, M.; Fujitani, Y.; Hara, A.; Uchida, T.; Tamura, Y.; Takeno, K.; Kawaguchi, M.; Watanabe, T.; Ogihara, T.; Fukunaka, A.; et al. The diabetes-susceptible gene SLC30A8/ZnT8 regulates hepatic insulin clearance. J. Clin. Investig. 2013, 123, 4513–4524.

(23) Daru, J.; Colman, K.; Stanworth, S.J.; de La Salle, B.; Wood, E.M.; Pasricha, S.R. Serum ferritin as an indicator of iron status: What do we need to know? Am. J. Clin. Nutr. 2017, 106, 1634S–1639S.

(24) Viveiros, A.; Finkenstedt, A.; Schaefer, B.; Mandorfer, M.; Scheiner, B.; Lehner, K.; Tobiasch, M.; Reiberger, T.; Tilg, H.; Edlinger, M.; et al. Transferrin as a predictor of survival in cirrhosis. Liver Transpl. 2018, 24, 343–351.

(25) Coleman, J.E. Zinc Proteins: Enzymes, Storage Proteins, Transcription Factors, and Replication Proteins. Annu. Rev. Biochem. 1992, 61, 897–946.

(26) Ahmed, U.; Latham, P.S.; Oates, P.S. Interactions between hepatic iron and lipid metabolism with possible relevance to steatohepatitis. World J. Gastroenterol. 2012, 18, 4651–4658.

(27) Meerarani, P.; Reiterer, G.; Toborek, M.; Hennig, B. Zinc modulates PPARgamma signaling and activation of porcine endothelial cells. J. Nutr. 2003, 133, 3058–3064.

(28) Temple, K.A.; Cohen, R.N.; Wondisford, S.R.; Yu, C.; Deplewski, D.; Wondisford, F.E. An intact DNA-binding domain is not required for peroxisome proliferator-activated receptor γ (PPARγ) binding and activation on some PPAR response elements. J. Biol. Chem. 2005, 280, 3529–3540.

(29) Kelly, D.; Crotty, G.; O'Mullane, J.; Stapleton, M.; Sweeney, B.; O'Sullivan, S.S. The Clinical Utility of a Low Serum Ceruloplasmin Measurement in the Diagnosis of Wilson Disease. Ir. Med. J. 2016, 109, 341–343.

(30) Twomey, P.J.; Viljoen, A.; Reynolds, T.M.; Wierzbicki, A.S. Non-ceruloplasmin-bound copper in routine clinical practice in different laboratories. J. Trace Elem. Med. Biol. Organ Soc. Min. Trace Elem. 2008, 22, 50–53.

(31) Hellman, N.E.; Gitlin, J.D. Ceruloplasmin metabolism and function. Annu. Rev. Nutr. 2002, 22, 439–458.

(32) Członkowska, A.; Rodo, M.; Wierzchowska-Ciok, A.; Smolinski, L.; Litwin, T. Accuracy of the radioactive copper incorporation test in the diagnosis of Wilson disease. Liver Int. 2018, 38, 1860–1866.

(33) Woimant, F.; Djebrani-Oussedik, N.; Poujois, A. New tools for Wilson's disease diagnosis: Exchangeable copper fraction. Ann. Transl. Med. 2019, 7, S70.

(34) Stanhope, K.L.; Medici, V.; Bremer, A.A.; Lee, V.; Lam, H.D.; Nunez, M.V.; Chen, G.X.; Keim, N.L.; Havel, P.J. A dose-response study of consuming high-fructose corn syrup–sweetened beverages on

lipid/lipoprotein risk factors for cardiovascular disease in young adults. Am. J. Clin. Nutr. 2015, 101, 1144–1154.

(35) Stanhope, K.L.; Bremer, A.A.; Medici, V.; Nakajima, K.; Ito, Y.; Nakano, T.; Chen, G.; Fong, T.H.; Lee, V.; Menorca, R.I.; et al. Consumption of fructose and high fructose corn syrup increase postprandial triglycerides, LDL-cholesterol, and apolipoprotein-B in young men and women. J. Clin. Endocrinol. Metab. 2011, 96, E1596.

(36) Mifflin, M.D.; St Jeor, S.T.; Hill, L.A.; Scott, B.J.; Daugherty, S.A.; Koh, Y.O. A new predictive equation for resting energy expenditure in healthy individuals. Am. J. Clin. Nutr. 1990, 51, 241–247.

(37) Ramanujam, V.M.S. Riboflavin as an Oral Tracer for Monitoring Compliance in Clinical Research. Open Biomark. J. 2011, 4, 1–7.

(38) Olusi, S.; Al-Awadhi, A.; Abiaka, C.; Abraham, M.; George, S. Serum copper levels and not zinc are positively associated with serum leptin concentrations in the healthy adult population. Biol. Trace Elem. Res. 2003, 91, 137–144.

(39) Tallino, S.; Duffy, M.; Ralle, M.; Cortés, M.P.; Latorre, M.; Burkhead, J.L. Nutrigenomics analysis reveals that copper deficiency and dietary sucrose up-regulate inflammation, fibrosis and lipogenic pathways in a mature rat model of nonalcoholic fatty liver disease. J. Nutr. Biochem. 2015, 26, 996–1006.

(40) Porcu, C.; Antonucci, L.; Barbaro, B.; Illi, B.; Nasi, S.; Martini, M.; Licata, A.; Miele, L.; Grieco, A.; Balsano, C. Copper/MYC/CTR1 interplay: A dangerous relationship in hepatocellular carcinoma. Oncotarget 2018, 9, 9325–9343.

(41) Aigner, E.; Theurl, I.; Haufe, H.; Seifert, M.; Hohla, F.; Scharinger, L.; Stickel, F.; Mourlane, F.; Weiss, G.; Datz, C. Copper Availability Contributes to Iron Perturbations in Human Nonalcoholic Fatty Liver Disease. Gastroenterology 2008, 135, 680–688.

(42) Song, M.; Li, X.; Zhang, X.; Shi, H.; Vos, M.B.; Wei, X.; Wang, Y.; Gao, H.; Rouchka, E.C.; Yin, X.; et al. Dietary copper-fructose interactions alter gut microbial activity in male rats. Am. J. Physiol. Gastrointest. Liver Physiol. 2018, 314, G119–G130.

(43) Krishnamoorthy, L.; Cotruvo, J.A.; Chan, J.; Kaluarachchi, H.; Muchenditsi, A.; Pendyala, V.S.; Jia, S.; Aron, A.T.; Ackerman, C.M.; Vander Wal, M.N.; et al. Copper regulates cyclic-AMP-dependent lipolysis. Nat. Chem. Biol. 2016, 12, 586–592.

(44) Prohaska, J.R. Changes in Cu,Zn-Superoxide Dismutase, Cytochrome c Oxidase, Glutathione Peroxidase and Glutathione Transferase Activities in Copper-Deficient Mice and Rats. J. Nutr. 1991, 121, 355–363.

(45) Gallagher, C.H.; Reeve, V.E.; Wright, R. Copper deficiency in the rat. Effect on the ultrastructure of hepatocytes. Aust. J. Exp. Biol. Med. Sci. 1973, 51, 181–189.

(46) Song, M.; Vos, M.; McClain, C. Copper-Fructose Interactions: A Novel Mechanism in the Pathogenesis of NAFLD. Nutrients 2018, 10, 1815.

(47) Fields, M.; Lewis, C.G. Dietary Fructose but Not Starch is Responsible for Hyperlipidemia Associated with Copper Deficiency in Rats: Effect of High-Fat Diet. J. Am. Coll. Nutr. 1999, 18, 83–87.

(48) Morrell, A.; Tripet, B.P.; Eilers, B.J.; Tegman, M.; Thompson, D.; Copié, V.; Burkhead, J.L. Copper modulates sex-specific fructose hepatoxicity in nonalcoholic fatty liver disease (NALFD) Wistar rat models. J. Nutr. Biochem. 2020, 78, 108316.

(49) Hieronimus, B.; Griffen, S.C.; Keim, N.L.; Bremer, A.A.; Berglund, L.; Nakajima, K.; Havel, P.J.; Stanhope, K.L. Effects of Fructose or Glucose on Circulating ApoCIII and Triglyceride and Cholesterol Content of Lipoprotein Subfractions in Humans. J. Clin. Med. 2019, 8, 913.

(50) Jiang, B.; Liu, G.; Zheng, J.; Chen, M.; Maimaitiming, Z.; Chen, M.; Liu, S.; Jiang, R.; Fuqua, B.K.; Dunaief, J.L.; et al. Hephaestin and ceruloplasmin facilitate iron metabolism in the mouse kidney. Sci. Rep. 2016, 6, 1–11.

(51) Navarro, J.A.; Schneuwly, S. Copper and zinc homeostasis: Lessons from Drosophila melanogaster. Front. Genet. 2017, 8, 223.

(52) Latorre, M.; Low, M.; Gárate, E.; Reyes-Jara, A.; Murray, B.E.; Cambiazo, V.; González, M. Interplay between copper and zinc homeostasis through the transcriptional regulator Zur in Enterococcus faecalis. Metallomics 2015, 7, 1137–1145.

(53) Panemangalore, M.; Bebe, F.N. Effect of high dietary zinc on plasma ceruloplasmin and erythrocyte superoxide dismutase activities in copper-depleted and repleted rats. Biol. Trace Elem. Res. 1996, 55, 111–126.

(54) Ausk, K.J.; Ioannou, G.N. Is obesity associated with anemia of chronic disease? A population-based study. Obesity 2008, 16, 2356–2361.

(55) Ganz, T. Hepcidin—A Peptide Hormone at the Interface of Innate Immunity and Iron Metabolism. In Antimicrobial Peptides and Human Disease; Springer: Berlin, Germany, 2006; Volume 306, pp. 183–198.

(56) Zhou, B.; Ren, H.; Zhou, X.; Yuan, G. Associations of iron status with apolipoproteins and lipid ratios: A cross-sectional study from the China Health and Nutrition Survey. Lipids Health Dis. 2020, 19, 1–12.

(57) Mak, C.M.; Lam, C.-W. Diagnosis of Wilson's disease: A comprehensive review. Crit. Rev. Clin. Lab. Sci. 2008, 45, 263–290.

(58) Pollack, S.; Kaufman, R.M.; Crosby, W.H. Iron Absoption: Effects of Sugars and Reducing Agents. Blood 1964, 24, 577–581.

(59) Christides, T.; Sharp, P. Sugars increase non-heme iron bioavailability in human epithelial intestinal and liver cells. PLoS ONE 2013, 8, e83031.

Chapter 3: Glucose control on ceruloplasmin activity

This work is in collaboration with Samuel Janisse. As such, portions of work will also be found in his thesis.

3.1 Introduction

Ceruloplasmin plays an important role in copper metabolism, copper transport, iron metabolism, and acute phase response.[1–4] The protein is a glycoprotein that contains 6-8 copper atoms, with at least two type 1 copper centers and a trinuclear copper center composed of two type 3 copper centers and one type 2 copper center.[5,6] These 6 coppers are responsible for its catalytic activity through a series of intramolecular electron transfer leading to the 4-electron reduction of O_2 to H_2O.[7,8] One of the more established roles of this activity is the facilitation of serum iron bioavailability.[2] The catalytic activity enables the oxidation of Fe(II) to Fe(III), allowing for transferrin to bind and transport iron throughout the body.[2,9,10] Despite ceruloplasmin's key roles in metal regulation throughout the body, the functions and mechanics of this protein remain relatively unknown. Work in the past 20 years has begun to uncover the intricacies of this protein, from the crystallization of the protein to recent work on uncovering the mechanisms of electron transfer that lead to the protein's activity.[6–8] Yet, the regulation of the protein is still poorly understood. Mainly synthesized in the liver, ceruloplasmin is loaded with copper by the copper transporter ATP7B.[1,11,12] Diseases like Wilson's disease, arising from a loss of function mutation of ATP7B, can be assessed by the reduced concentration of ceruloplasmin in the serum of affected individuals.[13–15] Left untreated, Wilson's Disease will lead to copper accumulation in organs, resulting in organ failure and death.[15,16]

It is not only genetic factors that are responsible for the altered regulation of ceruloplasmin, but the Heffern lab recently demonstrated that sugar consumption influences the plasma protein.[17] Human subjects undergoing a two-week dietary intervention of glucose, fructose, or high fructose corn syrup exhibit decreases in both serum copper concentration and copper-dependent ceruloplasmin ferroxidase activity, despite ceruloplasmin concentrations remaining constant. This hints at a connection between the copper loading of the protein, copper homeostasis, and sugars. The link between copper metabolism and nutrients has been highlighted in other studies, demonstrating modified hepatic and serum copper status in models of nutrient overload.[18–22] These studies have been relatively observational and do not provide insight into

the ability of diet to directly influence ceruloplasmin. From cell, to rodent, to human studies, an interplay between ceruloplasmin, copper, and sugars has been noted, leading to presently more questions than answers.

Along with changes in intracellular regulation, one possible area of interplay between sugars and ceruloplasmin can be the formation of non-enzymatic glycation products[23,24]. Diabetes and other nutrient overload diseases can result in hyperglycemia which, over time, leads to the non-enzymatic glycation of proteins, also called advanced glycation end products (AGEs).[25] The effects of these can be deleterious and lead to the degradation of proteins in the blood, as well as increased reactive oxygen species.[26] These glycation products have been hypothesized to influence ceruloplasmin wherein the protein exposed to an excess of glucose results in the release of bound copper.[23] It is posited that the fragmentation of the protein is linked to the release of copper wherein reactive oxygen species are evolved, reacting with ceruloplasmin and leading to cleavage of the peptide backbone, however, the mechanisms of copper release have yet to be established. The addition of the copper chelator EDTA with glucose and ceruloplasmin ablated the effects of copper on fragmentation, solidifying the role of copper in the fragmentation of the protein.[23,24] However, further studies are needed to establish the biological impacts of cleavage.

In the work presented in this chapter, we probed the ability of glucose to alter the activity of ceruloplasmin. These effects are studied mainly through two courses, one as the ability of glucose to alter the activity of ceruloplasmin in short-term incubations, and the other as an investigation of long-term exposure of ceruloplasmin to glucose. The effects of glucose on the protein that we observe in these studies may be the cause of previously observed changes in ceruloplasmin activity in human subjects. We propose through binding and cleavage of the protein, in short- and long-term exposures respectively, glucose may have significant impacts on ceruloplasmin with larger implications for iron and copper metabolism under hyperglycemic conditions.

3.2 Methods

3.2.1 Ceruloplasmin incubation with glucose

Ceruloplasmin (239799-1MG, Millipore Sigma) was resuspended in 500 uL nanopure water and dialyzed (Slide-A-Lyzer™ Dialysis Cassettes 20K MWCO 0.5 mL, ThermoFisher Scientific) with 500 mL PBS (BP3991, ThermoFisher Scientific) overnight at 25 ˚C and then for 2 hours at 25 ˚C with constant light agitation. After dialysis, the protein was brought to a volume of 1mL and split into two 500 uL samples where 170 uL nanopure water was added to the control and 103 uL of nanopure water and 67 uL 1M glucose (G8270-1KG, Millipore Sigma) in nanopure water was added to the glucose treated sample, for a total of 0.1M glucose. Both samples, control, and glucose were further split into two for a total of 4 samples of 335 uL. Samples designated as day 0 were immediately frozen at -80 ˚C while day 10 samples were incubated at 37 ˚C for 10 days before being frozen.

3.2.2 UV-Vis experiments

Ceruloplasmin absorption was assessed by UV-Visible spectroscopy (Shimadzu 1900i) from a range of 200 to 800 nm wavelengths at 0.5 s per read every 0.5 nm. Spectra were corrected to buffer absorbance and the ratio of 610:280 nm was assessed per sample. Samples were processed using Excel (Microsoft) as a subtraction of PBS buffer and PBS with glucose subtracted from the relevant spectrum.

3.2.3 Gel and Western blots

10ul sample was added 2 uL LDS sample buffer (B0007, ThermoFisher Scientific) and 10 uL was added to a Bis-Tris 4-12% gel (NW04125BOX, ThermoFisher Scientific). Protein gels were assessed using a Coomassie-based Imperial Stain (PI24615, ThermoFisher Scientific) with a Silver Stain (24612, ThermoFisher Scientific) used to detect low abundant protein fragments. For western blots, samples were transferred onto a low fluorescent PVDF membrane (1704274, Bio-Rad) using a Trans-Blot Turbo Transfer System (Bio-Rad). Blots were blocked in 5% BSA in TBST (9997S, Cell Signaling Technology) for 1 hour at room temperature and left in anti-Ceruloplasmin (1:1000 sc-365205, SCBT) primary antibody overnight at 4˚C. Membranes were

washed 3 times 5 minutes before the addition of anti-mouse Alexafluor 555 (1:2000 A28180 ThermoFisher Scientific) secondary antibody for 1 hour in 5% milk powder in TBST. Membranes were imaged by fluorescence imaging on the Chemidoc MP (BioRad).

3.2.4 Ceruloplasmin ELISA

Human anti-ceruloplasmin ELISA (EC4201-1, Assaypro) was used to assess clinical assay-based readouts of ceruloplasmin. Samples were diluted 1:10000 in provided dilution buffer. Assays were read at 450 nm and 650 nm on the Spectramax i3x plate reader (Molecular devices). Data are normalized to the control sample at day 0 and processed in Excel (Microsoft).

3.2.5 Ceruloplasmin ferroxidase activity

Ceruloplasmin activity (EIACPLC, ThermoFisher Scientific) was assessed by the colorimetric assay of the ferroxidase activity of the protein. The sample was diluted 1:20 and data were normalized to the control sample at day 0. Assays were read on the Spectramax i3x plate reader (Molecular Devices) and processed on Excel (Microsoft).

3.3 Results

3.3.1 Glucose induces changes in ceruloplasmin

The physiological ranges of glucose in serum range from 1 to 5 mM at fasting concentrations, and 10 to 15 mM at post-prandial concentrations. In healthy adults, the glucose concentration remains at post-prandial levels for an hour, while in diabetic patients, it may last significantly longer.[27] To this end, we sought to investigate the effects of these physiological states of glucose on ceruloplasmin. In the presence of glucose at fasting levels, the activity of ceruloplasmin is decreased to 90.6 ± 1.8 percent and 98.1 ± 2.8 percent of baseline for 1 and 5 mM glucose respectively, where the baseline is defined as the activity of ceruloplasmin without glucose (Figure 1A and B). Conversely, ceruloplasmin exposed to post-prandial levels of glucose lead to an increase of 115.4 ± 5.6 and 111.9 ± 2.6 percent for 10 and 15 mM glucose respectively. This phenomenon indicates an interaction between glucose and ceruloplasmin influencing the protein by

reducing its catalytic activity at lower concentrations of glucose and increasing activity at higher concentrations. Glucose appears to have a certain level of control over the activity of the protein. At excess levels of glucose, 100 mM, the activity of ceruloplasmin returns to the levels of 0 mM glucose, 104 ± 0.5 percent. This effect may point to a concentration of glucose wherein the activation of the protein plateaus and decreases at excess levels of glucose. It is important to note that the sample size for these experiments is not sufficiently large for statistical tests and additional biological replicates are required to confirm the effects of glucose on ceruloplasmin.

Examinations of the type I copper centers of the protein demonstrate slight glucose-dependent shifts in absorbance of the catalytic centers of ceruloplasmin. The type I copper centers are characterized by a sulfur-copper bond, giving the protein its signature blue color with an absorbance of around 610 nm. In ceruloplasmin, two of the three type I copper centers are responsible for the ferroxidase activity of the protein enabling spectroscopic studies to inform on the status of the protein.[7,28–30] Absorption spectroscopy of the protein demonstrates a slight, but notable shift in the shape of the absorbance (Figure 1C). While there is no shift in the maximum wavelength with the addition of glucose, the change in shape may correlate to alterations of the structure of the type 1 copper center. We hypothesize that glucose is complexing with ceruloplasmin, altering the structure of the catalytic copper site either through direct coordination or through an allosteric site. This might occur through minor shifts in the tetrahedral geometry of the copper site or changes in the secondary coordination environment rather than a change in the species of atoms coordinated to the copper centers. All structural determinations of ceruloplasmin and glucose complexation require additional studies for validation and assessment of the binding modes.

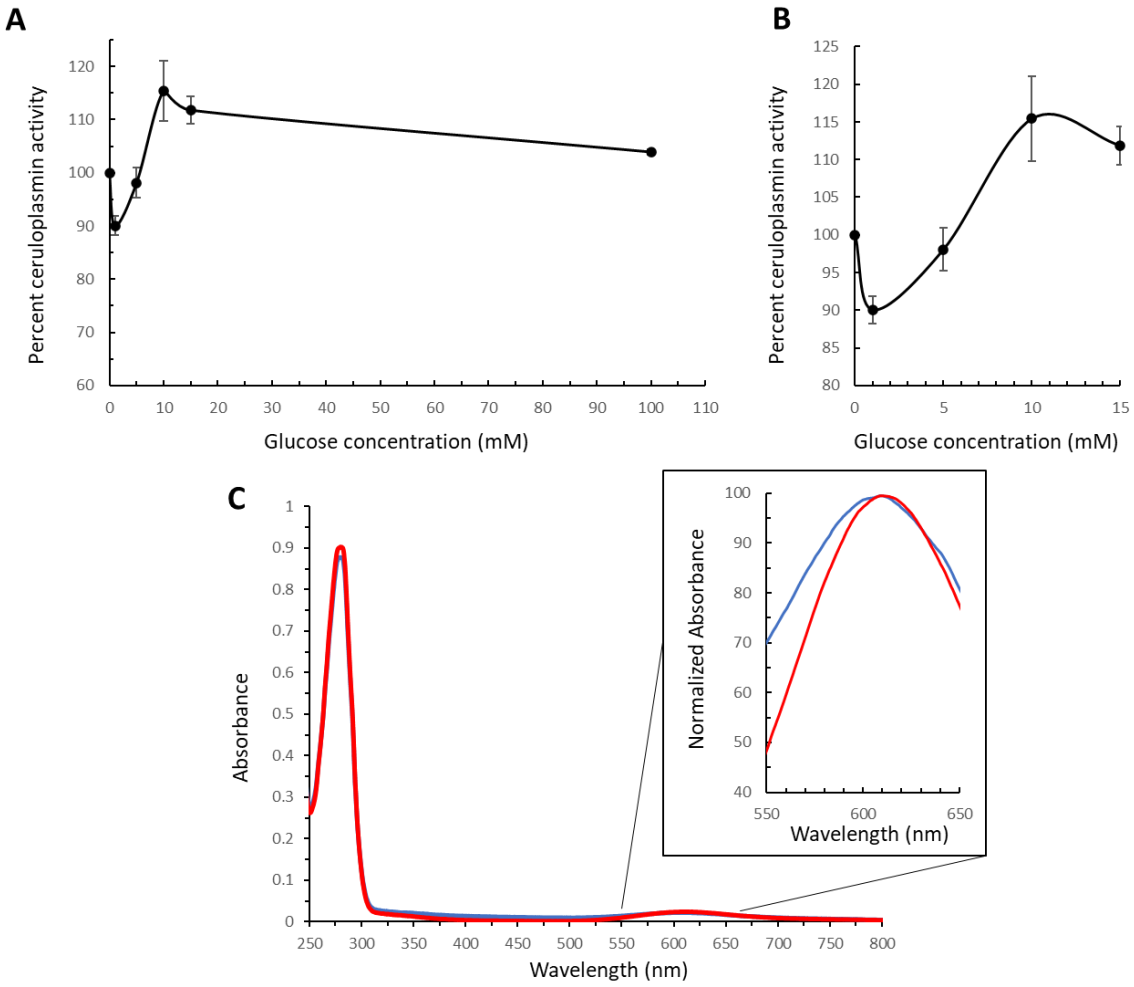

Figure 3.1. Effects of glucose on activity and copper centers of ceruloplasmin. A) 30-minute incubations of ceruloplasmin with 0, 1, 5, 10, 15, and 100 mM glucose alters ferroxidase activity. B) Activity of ceruloplasmin with 0 to 15 mM glucose. Data is normalized to the activity protein at 0 mM glucose, Mean ± SD are shown, n = 2. C) Absorption spectrum from 250 to 800 nm of 0 (blue) and 100 (red) mM glucose. A picture-in-picture of normalized absorbance demonstrates the effects of glucose on type I copper centers.

3.3.2 Future work for changes glucose-induced changes in ceruloplasmin

To further investigate the effects of glucose on ceruloplasmin, the type I copper centers will be assessed using EPR.[31] The technique allows for the determination of the coordination environments of the paramagnetic copper center as well as the molecular shape of copper.[32] This will inform on the effects of glucose on the binding environment and may be able help explain changes in activity. Initial studies will investigate ceruloplasmin with high concentrations of glucose for validation, which will then extend to a

concentration gradient that can determine if low and high glucose concentrations exhibit alternative binding. The changes in the copper environment observed by spectroscopic studies may also be examined through computational chemistry. Computer modeling can be a powerful tool in conjunction with experimental data and can inform on the nature of ligands and environments around the copper centers of ceruloplasmin.

Structural changes in the secondary structure of ceruloplasmin upon glucose stimulation will be assessed by circular dichroism (CD). This technique may not be able to detect minimal changes in protein structure but could inform on the magnitude of any changes in the protein. CD has previously been used to observe the stability of ceruloplasmin at a range of temperatures and thus may provide information towards uncovering structural alterations or stabilizing properties of glucose on ceruloplasmin.[33,34] To uncover the nature of glucose and ceruloplasmin interactions, incubation of the protein followed by dialysis to understand the strength of the interactions of ceruloplasmin and glucose. This will also be detected using ESI-MS or MALDI-TOF. In conjunction with MS, isothermal calorimetry (ITC) will be used to assess the binding stoichiometries of ceruloplasmin and glucose. ITC is an analytical method to determine binding stoichiometry and kinetics that would uncover how glucose may influence the protein.

Alternative probes for the activity of the ferroxidase activity of ceruloplasmin will be used to directly measure reactions with iron, rather than the use of p-phenylenediamine as is used in the experiments highlighted above. This will provide an increased level of specificity for the reaction of Fe(II) to Fe(III) by the use of tracking changes in the absorbance of a Fe(II) TAR, 4-(2-thiazolylazo)resorcinol, complex.[35] This complex has been proposed as a direct measure of ferroxidase activity while allowing for low background data collection. The complex demonstrates a decrease in the 700nm range as Fe(II) oxidizes to Fe(III) and would inform on the iron bioavailability activity of the protein. Additionally, ceruloplasmin in serum should be assessed to ensure that the changes in activity are not only present *in vitro,* but *ex vivo* as well.

There are several considerations with experiments that we have undertaken that must be addressed for future work. One of the largest considerations is the auto-oxidation of ceruloplasmin in aerobic conditions that the samples have been run in which may lead to inconsistent states of the copper within ceruloplasmin. To overcome this, future work should include either air-free conditions that validate previously collected data or the addition of an oxidizing agent to maintain the redox state of the protein. [7,36] Additionally, ceruloplasmin has been commercially purchased from serum isolates, however, sample-to-sample variability may influence ceruloplasmin's interactions with glucose. We have attempted to overcome this through biological replicates; however, the lot differences must be considered when processing data. We additionally plan on probing whether ceruloplasmin is only affected by glucose or other sugars and upon validation of preliminary data, we will use other monosaccharides like fructose.

3.3.3 Long-term exposure to glucose leads to ceruloplasmin degradation

Previously published studies found an increase in the fragmentation of copper with the incubation of glucose for 10 days.[23] This effect was posited to be due to increased degradation and redox activity from the reducing sugar and their interactions with the copper centers of the protein. These data were corroborated in our lab with imperial and silver stains of gels comparing ceruloplasmin at days 0 and 10 with and without glucose (Figure 2A). The gels demonstrate an appearance of markers at lower molecular weights and a decrease in the intensity of holo-ceruloplasmin over the course of the glucose incubation. An increase in protein bands appearing around 50 and 70 kDa in glucose samples point to a regular and consistent location of glucose-induced fragmentations. Additional biological replicates (not shown) confirm the consistent cleavage of the protein.

Western blot analysis of ceruloplasmin demonstrates bands in samples incubated with glucose for 10 days that are not in the 10-day control sample, insinuating a certain degree of recognition of ceruloplasmin (figure 2B). Western blots of the ceruloplasmin fragmentation also highlight changes observed in the imperial stains as there is a clear increase in bands at 50 kDa with the addition of glucose.

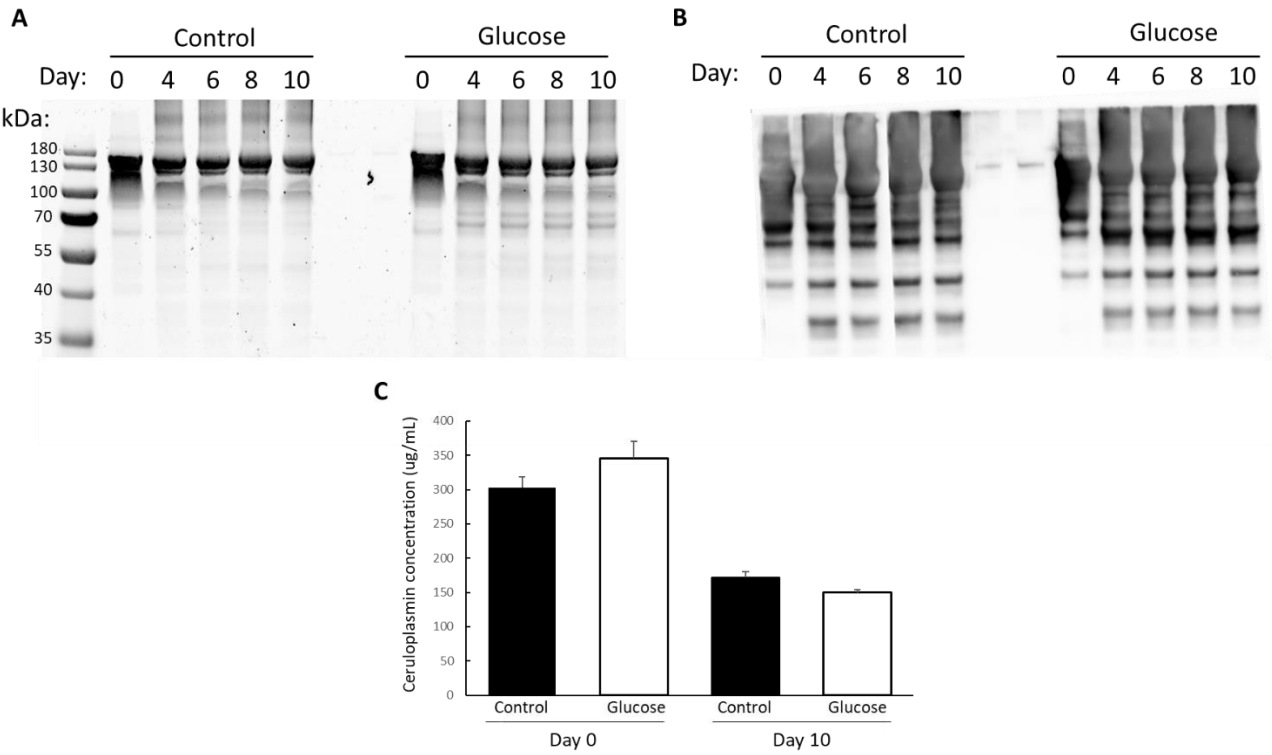

Figure 3.2. Glucose facilitates ceruloplasmin fragmentation. Ceruloplasmin was incubated with 100 mM glucose for 0, 4, 6, 8, and 10 days. Fragmentation was analyzed by A) an imperial stain for total protein detection, and B) western blot analysis to determine antibody recognition of ceruloplasmin fragments. C) ELISA analysis of ceruloplasmin at days 0 and 10 show Mean ± SEM are shown, n=5. Significance was assessed by unpaired t-tests, *P>0.05.

Work highlighted in Chapter 2 demonstrates a change in ceruloplasmin activity in human serum that was not reflected by a change in concentration by ELISA assay.[17] ELISA assays are the most common method of identification of ceruloplasmin concentration in the serum and are often used as a proxy for the status of copper clinically.[14] We hypothesized that this difference may be due to the ELISA antibody recognition of ceruloplasmin that does not differentiate between apo- and holo- ceruloplasmin and is noted with western blot analysis of glucose-induced fragmentation (Figure 2B). To examine the antibody recognition, an ELISA assay was run on the ceruloplasmin exposed to glucose for 10 days. Ceruloplasmin without glucose decreases from 302.2 ± 16.5 to 171.9 ± 8.6 ug/mL; glucose exacerbates this effect from 345 ± 25.0 to 149 ± 3.7 ug/mL. The decreases from 0 to 10 days were statistically significant, whether it was with and without glucose. Comparison of the concentration of ceruloplasmin with and without glucose demonstrated a non-

significant effect in antibody recognition at day 0 and was not statistically significantly different at day 10 (P=0.054). These data may agree with observations in human samples as a decrease in registered concentration was not observed with glucose consumption. It is thus possible that copper metabolism changes in human serum relate to the interactions of glucose with ceruloplasmin in the serum. However, it does not rule out considerations that the decreases observed in human samples arise from intracellular processing.

The absorbance spectra of ceruloplasmin collected at day 0 and day 10 demonstrates a decrease in the absorption at 610 nm with the addition of glucose after 10 days, pointing to a change in the copper center potentially related to a release of copper from the protein. It is important to note a decrease in 610 nm in the control sample at day 10 relative to day 0, which may be due to the natural degradation of the protein as the half-life of ceruloplasmin is 4 to 5 days. These changes are more pronounced with consideration of the ratio of 610:280 nm. This ratio has previously been used to assess protein purity with a value of 0.045 established as pure.[37] With the addition of glucose, there is a significant decrease in the ratio with the addition of glucose after 10 days compared to the control sample at 10 days, reinforcing the changes in copper loading and status by the incubation of glucose.

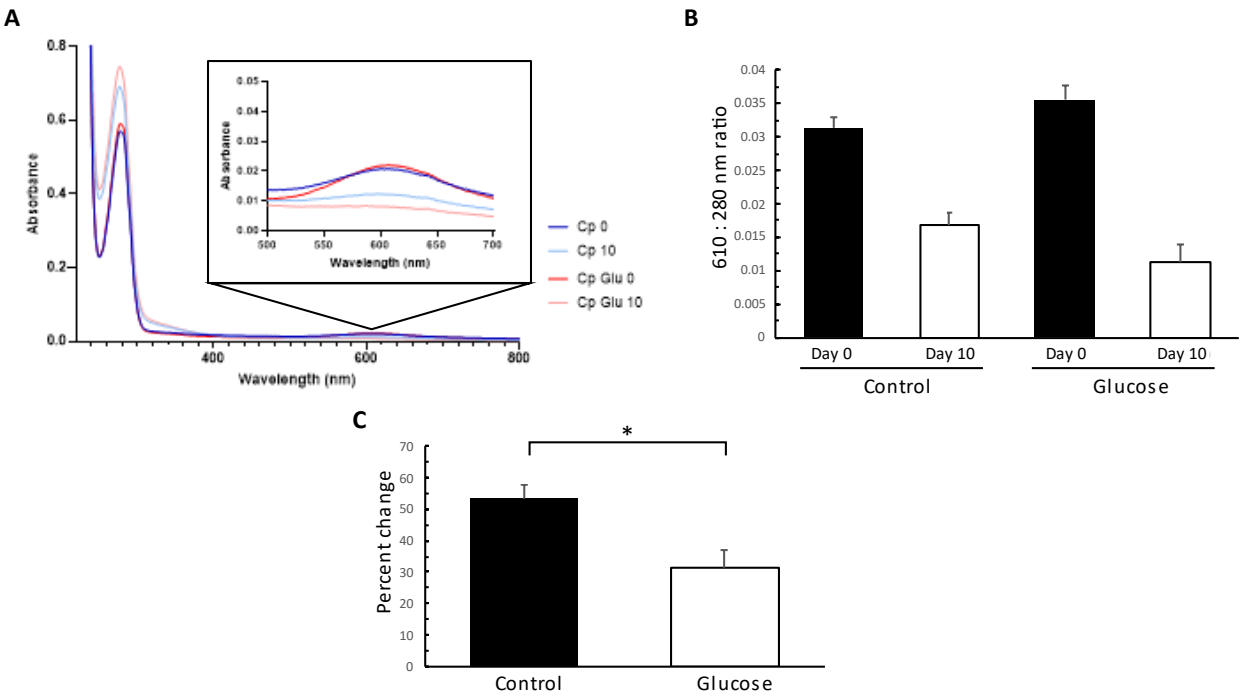

Figure 3.3. Glucose fragmentation leads to copper release from ceruloplasmin's type I copper center. Ceruloplasmin was incubated with 100 mM glucose for 0 and 10 days. A) Type 1 copper centers were assessed by UV-vis spectroscopy with spectrum inset highlighting changes at 610 nm. B) The ratio of spectra at 610 to 280 nm demonstrates changes in the copper loading of ceruloplasmin. C) The percent change in the 610:280 nm ratio from day 0 to day 10. Mean ± SEM are shown, n=5. Significance was assessed by paired t-tests, *P>0.05.

With changes in the copper centers of ceruloplasmin, we anticipate observing an analogous decrease in activity. The ferroxidase activity of ceruloplasmin with and without glucose demonstrates a decrease from day 0 to 10. These changes in activity at day 10 are not significantly different, yet follow trends observed with ceruloplasmin concentration. Of note is a change in the activity of the protein at day 0 with glucose. Experiments with ceruloplasmin with short-term glucose incubations demonstrate at 100 mM glucose, the protein activity should not be significantly different than the protein without glucose (Figure 1), however, the activity is increased nearly 2-fold, from 3977 ± 1256 to 7574 ± 2613 mU/uL. Factoring in the concentrations measured by ELISA, the specific activity of ceruloplasmin hints at structural changes in the protein as a function of glucose incubation. We hypothesize that freeze-thaw cycles of the proteins with glucose are protective of activity, explaining the increase of activity at day 0 with glucose.[38] These changes

emphasize the need for future experiments for validation but also to probe the mechanics behind the effects of glucose as a ceruloplasmin cryoprotectant.

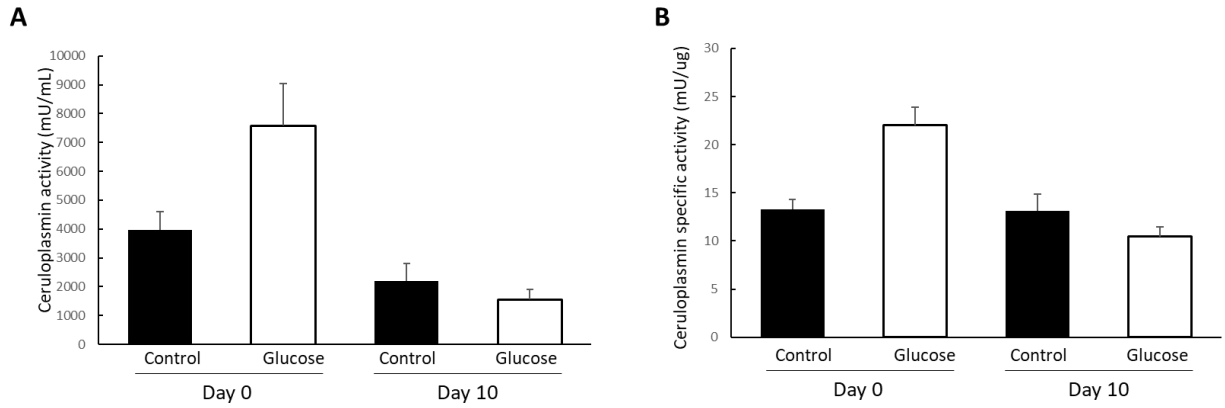

Figure 3.4. Long-term incubation of ceruloplasmin with glucose alters activity. Ceruloplasmin was incubated with 100 mM glucose for 0 and 10 days. A) Activity of ceruloplasmin with and without glucose at days 0 and 10. The activity was assessed by colorimetric assays and expressed as mU/mL. B) Specific activity of ceruloplasmin samples expressed as the activity of the protein over the concentration. Mean ± SEM are shown, n=5. Significance was assessed by unpaired t-tests, *P>0.05.

3.3.4 Future work for long-term exposure of glucose on ceruloplasmin

Current work focuses on establishing the state of copper with the incubation of ceruloplasmin with glucose. This will be assessed by EPR of ceruloplasmin with the addition of glucose for 10 days. Preliminary tests of ceruloplasmin EPR yielded low signal-to-noise ratios (data not shown) that, in collaboration with the Britt lab, are being optimized using tris buffer rather than PBS. The change of buffers allows for the detection of non-ceruloplasmin-bound copper that may be released. Copper ions are minimally soluble in PBS and as such tris offers a buffer wherein labile copper may be detected. Assessment of ceruloplasmin in tris buffer demonstrates similar effects by gel fragmentation and absorbance. This upcoming data collection aims to establish changes in the copper environment in the protein as well as the state of copper released in the buffer.

While antibody recognition conveys a certain level of sequence information based on the epitope of the antibody, mass spectrometry-based analysis will be used to identify the fragments of the glucose-incubated

ceruloplasmin. MALDI-TOF is an incredibly powerful tool for protein analysis that has been used to detect and determine the identity of protein sequences.[39] We intend to isolate protein fragments from imperial-stained gels which will be subjected to tryptic digestion. These digested fragments of ceruloplasmin can then be used to identify the sequences that appear from glucose-induced fragmentation. The identity of the fragments may uncover a biological relevance of the fragmentation with sequences that are similar to other copper proteins in the blood as well as highlight the mechanisms of copper release from non-enzymatic ceruloplasmin degradation.

Similar considerations must be taken for longer terms stimulations of ceruloplasmin as with short-term stimulations. Namely the sensitivity of the protein to oxidation by oxygen in the environment. To overcome these challenges, experiments should be controlled by restricting oxygen to the protein as well as investigating the long-term effects of a reducing agent on ceruloplasmin. On top of the effect of oxygen on the protein, glucose appears to have a protective effect on ceruloplasmin through freeze-thaw cycles that need to be considered in the future experiments. To this end, we plan on investigating the effects of freeze-thaw cycles and timing on ceruloplasmin activity and copper centers.

3.4 Discussion

The effects of glucose on metal micronutrients appear to be more significant than previously reported, which hypothesized that sugars may alter the metabolism of organs linked to the changes in metal regulation.[17,40,41] The studies presented here demonstrate that glucose may interact with ceruloplasmin, in a mechanism that can alter the protein's activity and functionality through direct coordination. While the biological relevance of the effects of glucose on ceruloplasmin requires additional studies, it appears that glucose exhibits a significant control over ceruloplasmin through changes in activity to fragmentation of the protein. Glycation products may form with long-term exposures to glucose that lead to alterations in

the structure and function of the protein, however, this is currently speculative with no preliminary data to support this hypothesis.

Glucose exhibits an effect on ceruloplasmin catalytic activity as short-term exposure of ceruloplasmin to glucose induces inhibition and activation of the protein. This hints at a mechanism wherein with fasting levels of glucose, ceruloplasmin may be less active in the circulatory system, while at elevated, post-prandial or diabetic levels of glucose ceruloplasmin will be more catalytically active. This has implications not only for copper but iron metabolism as well. Changes in the activity of ceruloplasmin have a direct effect on iron bioavailability and loading into transferrin.[2,35] Future work will address changes in iron regulation as a result of ceruloplasmin's interaction with glucose. While the structural effects of glucose on the protein have yet to be established, it is difficult to understand the implications of this interaction mechanistically and biologically. We hope to uncover the nature of glucose interactions with the protein, either through direct coordination to the metal or through allosteric interactions.

In agreement with previous studies, glucose facilitated the fragmentation of ceruloplasmin.[23] These fragments are detected by ELISA, implying that a lack of change in quantified ceruloplasmin in human samples may be due to the preservation of antibody recognition of ceruloplasmin fragments. However, we did not observe significant changes in activity after 10 days with or without glucose incubation. This does not agree with the data in chapter 2 and implies alternative forms of ceruloplasmin and copper regulation in addition to fragmentation of the protein.[17] Interesting phenomena were observed with the incubation of ceruloplasmin with glucose. Of note is the dramatic increase in ceruloplasmin activity in the frozen samples at day 0. With a freeze-thaw to consider, the activity of ceruloplasmin at day 0 was significantly increased with the incubation of glucose compared to the control. This effect was not observed with the short-term incubation of ceruloplasmin with 100 mM of the sugar with a 30-minute incubation and may be related to the stabilizing or glassing properties of glucose that protects the protein.[38] This requires

additional assays to investigate how glucose may facilitate the stability of the protein or protection from freeze cycles.

Much of the data presented in this chapter are preliminary and require additional biological replicates to ensure sufficient scientific rigor is met before we can expand on the hypothesis. Despite this preliminary nature, the data points to the unique effects of glucose on ceruloplasmin, in both short- and long-term exposures. The implications of glucose on ceruloplasmin and metal micronutrients is an emerging topic in the field of metals in biology and as the field continues to develop, many questions brought forth in this chapter will be answered.

3.5 References

(1) Linder, M. C. Copper Homeostasis in Mammals, with Emphasis on Secretion and Excretion. A Review. *Int. J. Mol. Sci.* 2020, *21* (14), 1–22.

(2) Vashchenko, G.; MacGillivray, R. T. A. Multi-Copper Oxidases and Human Iron Metabolism. *Nutrients* . 2013.

(3) Charlie-Silva, I.; Klein, A.; Gomes, J. M. M.; Prado, E. J. R.; Moraes, A. C.; Eto, S. F.; Fernandes, D. C.; Fagliari, J. J.; Junior, J. D. C.; Lima, C.; et al. Acute-Phase Proteins during Inflammatory Reaction by Bacterial Infection: Fish-Model. *Sci. Rep.* 2019, *9* (1), 1–13.

(4) Ramos, D.; Mar, D.; Ishida, M.; Vargas, R.; Gaite, M.; Montgomery, A.; Linder, M. C. Mechanism of Copper Uptake from Blood Plasma Ceruloplasmin by Mammalian Cells. *PLoS One* 2016, *11* (3), e0149516.

(5) Bento, I.; Peixoto, C.; Zaitsev, V. N.; Lindley, P. F. Ceruloplasmin Revisited: Structural and Functional Roles of Various Metal Cation-Binding Sites. *Acta Crystallogr. Sect. D Biol. Crystallogr.* 2007, *63* (Pt 2), 240.

(6) Samygina, V. R.; Sokolov, A. V.; Bourenkov, G.; Schneider, T. R.; Anashkin, V. A.; Kozlov, S. O.; Kolmakov, N. N.; Vasilyev, V. B. Rat Ceruloplasmin: A New Labile Copper Binding Site and Zinc/Copper Mosaic. *Metallomics* 2017, *9* (12), 1828–1838.

(7) Solomon, E. I.; Tian, S.; Jones, S. M. Role of a Tyrosine Radical in Human Ceruloplasmin Catalysis. *ACS Cent. Sci.* 2020, *6* (10), 1835–1843.

(8) Tian, S.; Jones, S. M.; Jose, A.; Solomon, E. I. Chloride Control of the Mechanism of Human Serum Ceruloplasmin (Cp) Catalysis. *J. Am. Chem. Soc.* 2019, *141* (27), 10736–10743.

(9) Hellman, N. E.; Gitlin, J. D. Ceruloplasmin Metabolism and Function. *Annu. Rev. Nutr.* 2002, *22* (1), 439–458.

(10) Aigner, E.; Theurl, I.; Haufe, H.; Seifert, M.; Hohla, F.; Scharinger, L.; Stickel, F.; Mourlane, F.; Weiss,

G.; Datz, C. Copper Availability Contributes to Iron Perturbations in Human Nonalcoholic Fatty Liver Disease. *Gastroenterology* 2008, *135* (2).

(11) de Bie, P.; van de Sluis, B.; Burstein, E.; van de Berghe, P. V. E.; Muller, P.; Berger, R.; Gitlin, J. D.; Wijmenga, C.; Klomp, L. W. J. Distinct Wilson's Disease Mutations in ATP7B Are Associated With Enhanced Binding to COMMD1 and Reduced Stability of ATP7B. *Gastroenterology* 2007, *133* (4), 1316–1326.

(12) Hasan, N. M.; Gupta, A.; Polishchuks, E.; Yu, C. H.; Polishchuks, R.; Dmitriev, O. Y.; Lutsenko, S. Molecular Events Initiating Exit of a Copper-Transporting ATPase ATP7B from the Trans-Golgi Network. *J. Biol. Chem.* 2012, *287* (43), 36041–36050.

(13) Woimant, F.; Djebrani-Oussedik, N.; Poujois, A. New Tools for Wilson's Disease Diagnosis: Exchangeable Copper Fraction. *Ann. Transl. Med.* 2019, *7* (S2), S70–S70.

(14) Mak, C. M.; Lam, C.-W. Diagnosis of Wilson's Disease: A Comprehensive Review. *Crit. Rev. Clin. Lab. Sci.* 2008, *45* (3), 263–290.

(15) Członkowska, A.; Litwin, T.; Dusek, P.; Ferenci, P.; Lutsenko, S.; Medici, V.; Rybakowski, J. K.; Weiss, K. H.; Schilsky, M. L. Wilson Disease. *Nature Reviews Disease Primers*. Nature Publishing Group December 1, 2018.

(16) Zischka, H.; Einer, C. Mitochondrial Copper Homeostasis and Its Derailment in Wilson Disease. *Int. J. Biochem. Cell Biol.* 2018, *102*, 71–75.

(17) Harder, N. H. O.; Hieronimus, B.; Stanhope, K. L.; Shibata, N. M.; Lee, V.; Nunez, M. V.; Keim, N. L.; Bremer, A.; Havel, P. J.; Heffern, M. C.; et al. Effects of Dietary Glucose and Fructose on Copper, Iron, and Zinc Metabolism Parameters in Humans. *Nutrients* 2020, *12* (9), 1–14.

(18) Harder, N. H. O.; Lee, H. P.; Flood, V. J.; Juan, J. A. S.; Gillette, S. K.; Heffern, M. C. Fatty Acid Uptake in Liver Hepatocytes Induces Relocalization and Sequestration of Intracellular Copper. *Front. Mol. Biosci.* 2022, *9*.

(19) Song, M.; Schuschke, D. A.; Zhou, Z.; Chen, T.; Pierce, W. M.; Wang, R.; Johnson, W. T.; McClain, C. J. High Fructose Feeding Induces Copper Deficiency in Sprague-Dawley Rats: A Novel Mechanism for Obesity Related Fatty Liver. *J. Hepatol.* 2012, *56* (2), 433–440.

(20) Morrell, A.; Tallino, S.; Yu, L.; Burkhead, J. L. The Role of Insufficient Copper in Lipid Synthesis and Fatty-Liver Disease. *IUBMB Life* 2017, *69* (4), 263–270.

(21) Morrell, A.; Tripet, B. P.; Eilers, B. J.; Tegman, M.; Thompson, D.; Copié, V.; Burkhead, J. L. Copper Modulates Sex-Specific Fructose Hepatoxicity in Nonalcoholic Fatty Liver Disease (NALFD) Wistar Rat Models. *J. Nutr. Biochem.* 2020, *78*, 108316.

(22) Song, M.; Vos, M.; McClain, C. Copper-Fructose Interactions: A Novel Mechanism in the Pathogenesis of NAFLD. *Nutrients* 2018, *10* (11), 1815.

(23) Nazrul Islam, K.; Takahashi, M.; Higashiyama, S.; Myint, T.; Uozumi, N.; Kayanoki, Y.; Kaneto, H.; Kosaka, H.; Taniguchi, N. Fragmentation of Ceruloplasmin Following Non-Enzymatic Glycation Reaction 1. *J. Biochem* 1995, *118*, 1054–1060.

(24) Jung, H. K. Oxidative Modification of Human Ceruloplasmin by Methylglyoxal: An in Vitro Study. *BMB Rep.* 2006, *39* (3), 335–338.

(25) Vlassara, H.; Uribarri, J. Advanced Glycation End Products (AGE) and Diabetes: Cause, Effect, or Both? *Curr. Diab. Rep.* 2014, *14* (1), 453.

(26) Nowotny, K.; Jung, T.; Höhn, A.; Weber, D.; Grune, T. Advanced Glycation End Products and Oxidative Stress in Type 2 Diabetes Mellitus. *Biomolecules* 2015, *5* (1), 194.

(27) Monnier, L.; Colette, C.; Dunseath, G. J.; Owens, D. R. The Loss of Postprandial Glycemic Control Precedes Stepwise Deterioration of Fasting With Worsening Diabetes. *Diabetes Care* 2007, *30* (2), 263–269.

(28) Arnal, N.; De Alaniz, M. J. T.; Marra, C. A. Cytotoxic Effects of Copper Overload on Human-Derived Lung and Liver Cells in Culture. *Biochim. Biophys. Acta - Gen. Subj.* 2012, *1820* (7), 931–939.

(29) Dawson, J. H.; Dooley, D. M.; Clark, R.; Stephens, P. J.; Gray, H. B. Spectroscopic Studies of Ceruloplasmin. Electronic Structures of the Copper Sites. *J. Am. Chem. Soc.* 1979, *101* (17), 5046–5053.

(30) Chapman, A. L. P.; Mocatta, T. J.; Shiva, S.; Seidel, A.; Chen, B.; Khalilova, I.; Paumann-Page, M. E.; Jameson, G. N. L.; Winterbourn, C. C.; Kettle, A. J. Ceruloplasmin Is an Endogenous Inhibitor of Myeloperoxidase. *J. Biol. Chem.* 2013, *288* (9), 6465.

(31) Kubiak, T.; Krzyminiewski, R.; Dobosz, B. EPR Study of Paramagnetic Centers in Human Blood. *Curr. Top. Biophys.* 2013, *36* (1), 7–13.

(32) Onori, S.; Rosati, A.; Cannistraro, S. Electron Paramagnetic Resonance Study of Storage Effects on Ceruloplasmin in Human Serum Compared with Purified Ceruloplasmin in Aqueous Solution. *Physiol. Chem. Phys.* 1981, *13* (5), 439–446.

(33) Noyer, M.; Putnam, F. W. A Circular Dichroism Study of Undegraded Human Ceruloplasmin. *Biochemistry* 1981, *20* (12), 3536–3542.

(34) Sedlák, E.; Žoldák, G.; Wittung-Stafshede, P. Role of Copper in Thermal Stability of Human Ceruloplasmin. *Biophys. J.* 2008, *94* (4), 1384.

(35) Cortes, L.; Roberts, B. R.; Wedd, A. G.; Xiao, Z. Molecular Aspects of a Robust Assay for Ferroxidase Function of Ceruloplasmin. *Inorg. Chem.* 2017, *56* (9), 5275–5284.

(36) Machonkin, T. E.; Solomon, E. I. The Thermodynamics, Kinetics, and Molecular Mechanism of Intramolecular Electron Transfer in Human Ceruloplasmin. *J. Am. Chem. Soc.* 2000, *122* (50), 12547–12560.

(37) Rydbn, L. Comparison of Polypeptide-Chain Structure of Four Mammalian Ceruloplasmins by Gel Filtration in Guanidine Hydrochloride Solutions. *Eur. J. Biochem* 1972, *28*, 46–50.

(38) Tsai, S.; Chong, G.; Meng, P. J.; Lin, C. Sugars as Supplemental Cryoprotectants for Marine Organisms. *Rev. Aquac.* 2018, *10* (3), 703–715.

(39) Boivin, S.; Aouffen, M.; Fournier, A.; Mateescu, M. A. Molecular Characterization of Human and Bovine Ceruloplasmin Using MALDI-TOF Mass Spectrometry. *Biochem. Biophys. Res. Commun.* 2001, *288* (4), 1006–1010.

(40) Song, M.; Vos, M. B.; McClain, C. J. Copper-Fructose Interactions: A Novel Mechanism in the Pathogenesis of NAFLD. *Nutrients*. MDPI AG November 1, 2018.

(41) Lowe, J.; Taveira-da-Silva, R.; Hilário-Souza, E. Dissecting Copper Homeostasis in Diabetes Mellitus. *IUBMB Life* 2017, *69* (4), 255–262.

Chapter 4: Fatty acid uptake in liver hepatocytes induces the relocalization and sequestration of intracellular copper.

Adapted with Permission from:

Nathaniel H. O. Harder, Hannah P. Lee, Valerie J. Flood, Jessica A. San Juan, Skyler Gillette, Marie C. Heffern

4.1 Introduction

Excess consumption of high-calorie diets rich in fats and sugars are linked to adverse physiological effects, such as increased oxidative stress and inflammation [1–5]. The increased prevalence of such diets is strongly associated with the rise of metabolic diseases including diabetes and non-alcoholic fatty liver disease (NAFLD) [6–9]. Recent literature suggests that excess macronutrient load may result in disruptions in copper trafficking [10–13]. The essential metal micronutrient, copper, serves vital roles in signaling as well as in enzymatic cofactors for key biological processes ranging from mitochondrial respiration to radical scavenging [14–16]. However, due to its redox activity, misregulated copper can also be deleterious via increased radical formation and DNA damage. Thus, copper must be tightly regulated via an intricate network of transporters and chaperones to maintain proper levels and control its localization [14,17,18]. Copper is introduced into cells via membrane importers, then trafficked with dedicated chaperones to their directed targets, including metallothioneins, mitochondrial enzymes, and exporter proteins such as ATP7A and ATP7B [17,19,20]. The importance of proper copper homeostasis is evidenced in diseases like Menkes disease and Wilson's disease, deadly disorders resulting from mutations in the copper transporters ATP7A and ATP7B, respectively [20–22]. These diseases show remarkably similar phenotypes to diseases induced by high-fat and high-sugar diets, insinuating a link between copper and macronutrient-derived metabolic misregulation.

In addition to its central role in energy metabolism, the liver is the primary organ for maintaining copper balance in the body. The majority of dietary copper is trafficked to the liver for storage, distribution, and utilization [14]. It is in this organ that the copper-binding serum protein, ceruloplasmin, is synthesized and metalated [23–25]. Additionally, the liver plays a key role in copper excretion via biliary export [17,24]. Recent research suggests that dietary fats may affect hepatic copper metabolism. In one study, mice fed high-fat diets showed significant decreases in hepatic copper. In another study, researchers found that human

hepatocyte (HepG2) cells exposed to a mix of palmitic and oleic acids displayed decreases in intracellular copper levels akin to the trends seen in the mice study [11,26]. The prevailing hypothesis is that changes in copper metabolism are attributed to increased levels of copper transporter ATP7B, inducing copper efflux from the cell [11,26]. Yet, what instigates alterations to ATP7B, the consequence to intracellular copper pathways, and the interplay with fat consumption and energy metabolism is not well understood.

In this work, we scrutinized how fat accumulation impacts molecular pathways of copper metabolism and sequestration. Our goal was to determine associations between ATP7B expression and cellular copper status in response to fatty acid exposure. We assessed time-dependent changes in gene expression, levels, and localization of major copper proteins in HepG2 cells treated with palmitic acid (PA), a 16:0 unsaturated fatty acid. At early time points of PA exposure, we identified elevations in upstream regulators of the ATP7B export machinery alongside protein changes typically associated with cellular states copper overload. This is accompanied by perturbations in mitochondrial health and mitochondrial copper proteins. Prolonged exposure shifts the cellular state to one resembling copper deficiency at later time points, alongside increased expressions of protein indicative of lysosomal sequestration and membrane localization of copper. From this data, we propose a scheme wherein fat accumulation induces miscompartmentalization of copper to induce a state resembling cytosolic copper overload, activating sequestration and export of copper from the cytosol, leading to a cytosolic state of copper deficiency.

4.2 Materials and Methods

4.2.1 Cell culture and maintenance

Human hepatocyte carcinoma cells (HepG2) were grown in complete DMEM media (31053036, ThermoFisher Scientific) with 10% Avantor Seradigm Premium Grade Fetal Bovine Serum (97068-085, VWR), 1 mM sodium pyruvate (11360070, ThermoFisher Scientific), 100 IU penicillin and 100 µg/mL streptomycin (MT30002CI, ThermoFisher Scientific), and 2 mM L-glutamine (25-030-081, Gibco). Cells were

subcultured every 2 to 3 days at 70% confluence. HepG2 cells were generously gifted to us from Dr. Patricia Oteiza's laboratory. All experiments were performed on cells between passages 10 and 20. Sterile culturing and assay plates were used for the following experiments. Cells were regularly tested for mycoplasma every 6 months with the MycoAlert assay (LT07-701, Lonza).

4.2.2 General procedure for cell stimulations

HepG2 cells were stimulated with 250 µM PA solution in MEM media [27]. The stock PA stimulation solution (stock concentration of 8 mM) was prepared by the addition of sodium palmitate (P9767, MilliporeSigma) to a 10.5% w/w solution of fatty acid-free bovine serum albumin (BP9704100, ThermoFisher Scientific) in DMEM (31053036, ThermoFisher Scientific) and 25 mM HEPES (15630-080, Gibco). The solution was stirred for at least 4 hours at 50 °C until the sodium palmitate was completely incorporated. The solution was filtered through a 0.22 µm cellulose acetate filter (976134, ThermoFisher Scientific) and diluted to a final concentration of 250 µM in MEM (51200038, ThermoFisher Scientific) solution with 10% Avantor Seradigm Premium Grade Fetal Bovine Serum (97068-085, VWR), 1 mM sodium pyruvate (11360070, ThermoFisher Scientific), 100 IU penicillin and 100 µg/mL streptomycin (MT30002CI, ThermoFisher Scientific), and 2 mM L-glutamine (25-030-081, Gibco). Solutions of $CuCl_2$ were prepared in nanopure water (Millipore) at 200 mM and diluted to 200 µM in the BSA control media. Solutions of bathocuproinedisulfonic acid disodium salt (B1125, Millipore Sigma) were prepared at 20 mM in nanopure water and diluted to 200 µM in BSA control media (10.5% w/w solution of fatty acid-free bovine serum albumin in DMEM and 25 mM HEPES). For each stimulation, HepG2 cells were seeded (see description of experiments below for cell counts) and left to adhere overnight in complete DMEM media. Media was aspirated and cells were then washed once with PBS warmed to 37 ºC. PBS was aspirated and stimulation media was added to cells as described for each experiment below.

4.2.3 Cell viability and lipid staining assays

Cell viability was assessed with an MTS assay (G3582, Promega) at 24 hours. HepG2 cells were seeded in a clear bottom 96-well plate at 10,000 cells per well and stimulated as described above. MTS reagent was added and incubated at 37 ˚C for 1 hour before detection via absorbance at 490 nm on a platereader (SpectraMax i3x, Molecular Devices). Oil O Red was used to assess intracellular fat accumulation with cells plated at 300,000 cells per well in 6-well plates. Cells were stimulated as previously described, washed with PBS, and fixed with 4% paraformaldehyde for 30 minutes. The Oil O Red stock solution was prepared as 0.5% Oil O Red (NC0961554, ThermoFisher Scientific) in isopropanol and diluted to 60% in nanopure water fresh for each use. The working Oil O Red solution was filtered before staining for 10 minutes at room temperature. After staining, cells were washed three times with PBS and then imaged (EVOS Core XL, Thermofisher Scientific). To elute dye for quantification, 250 µL of 100% isopropanol was added to stained cells. Cells were then rocked at room temperature for 10 minutes in isopropanol before transferring 75 µL of the isopropanol solution from each well to a 96-well plate. The absorbance of eluted dye was measured at 540 nm on a platereader (SpectraMax i3x, Molecular Devices). Statistics were carried out on Prism 9.1 (Graphpad).

4.2.4 Western blot analysis

HepG2 cells were plated at 300,000 cells per well in a 6-well plate. Cells were stimulated as described above and then lysed at 1, 6, 12, and 24 hours in RIPA buffer (150 mM NaCl, 1% NP-40, 0.5% sodium deoxycholate, 0.1% SDS, 50 mM Tris-Cl pH 7.4) with EDTA-free protease inhibitor (PIA32955, ThermoFisher Scientific) and phosphatase inhibitor (4906845001, MilliporeSigma). Lysates were vortexed on ice for 20 minutes before being cleared by centrifugation at 15000 x g at 4 ºC. Lysates were frozen at -20 ºC prior to protein quantification by BCA assay (71285-3, Invitrogen). 20 µg protein was prepared with 2-mercaptoethanol (1610710, BioRad), PBS (Gibco), and LDS sample buffer (NP0007, Invitrogen) according to the manufacturer's protocols but without heating and loaded into a 4-12% Bis-Tris 15-well gel (NW04125BOX, Invitrogen) for probing all proteins except CCS and SCO2. To probe CCS, Mt2A, and SCO2, protein solutions

were run on a 16% Tricine gel (EC66952BOX, Invitrogen). In all cases gels were run in MES buffer at 100 V for 1 hour and transferred onto a low fluorescence PVDF membrane (1704274, BioRad) using a Trans-Blot Turbo Transfer System (BioRad). Membranes were blocked with 5% BSA in TBST (9997S, Cell Signaling Technology) for 1 hour at room temperature and incubated with primary antibodies overnight at 4 °C. Membranes were washed 3 x 5 minutes with TBST at room temperature and blotted with secondary antibody in 5% dry milk (31FZ82, Grainger) in TBST. Membranes were washed 3 x 5 minutes with TBST and submerged in Crescendo HRP substrate solution (Millipore) for 5 minutes prior to imaging on a Chemidoc MP Imager (BioRad). Primary antibodies used included anti-ATP7B (ab124973, 1:2000 Abcam), anti-CCS (sc-55561, 1:1000 Santa Cruz Biotechnology), anti-SCO2 (ab113758, 1:1000 Abcam), anti-β Actin (mouse IgG, sc-47778, 1:5000 SCBT or rabbit IgG, 4970S, 1:5000 Cell Signaling Technology), anti-SLC46A3 (NBP1-85054, 1:1000 Novus Biologicals), anti-Mt2A (PA5-102549, 1:1000 Invitrogen), and anti-hephaestin (sc-393701 ,1:1000 Santa Cruz Biotechnology). For secondary antibodies, anti-rabbit IgG HRP-conjugated antibody (7074S, 1:2000 Cell Signaling Technology) was used for SCO2, and ATP7B, anti-mouse IgG HRP-conjugated antibody (7076S, 1:1000 Cell Signaling Technology) for CCS, anti-rabbit IgG AlexaFluor 555 (A21428, 1:5000 Invitrogen) and anti-mouse IgG AlexaFluor 800 (A32789, 1:5000 Invitrogen) for β-Actin. Images were processed using the ImageLab software (Biorad). Densitometry analysis was carried out on ImageLab software (Biorad), all analysis was normalized to the baseline condition, BSA at1 hour.

4.2.5 Gene expression analysis

HepG2 cells were plated at 300,000 cells per well in a 6-well plate. Cells were then stimulated as described above and mRNA was isolated at 1, 6, 12, and 24 hours using the RNeasy PLUS RNA isolation kit (74136, Qiagen). mRNA was quantified on a QuickDrop spectrophotometer (Molecular Devices), and 1000 ng was added to iScript Reverse Transcription Supermix (1708841, Biorad). A C1000 thermocycler (Biorad) was used for reverse transcription. 0.2 ng cDNA was loaded into a master mix of amplification primer and iQ SYBR green (1708882, Biorad) before amplification and observation of gene expression by a CFX Connect

Real-Time PCR system (Biorad). Data were processed on Microsoft Excel by $2^{-\Delta\Delta Ct}$ method using β-Actin as the housekeeping gene. TBP (TATA binding protein) was used as a secondary housekeeping gene to ensure β-Actin was stably expressed over the PA stimulation. Primers for real-time PCR analysis are listed in Supplemental Table 4.S1. Statistics were carried out on Prism 9.1 (Graphpad) while colocalization analysis were carried out on ImageJ (FIJI) using Coloc 2 (79).

4.2.6 Ceruloplasmin activity and quantification

Media was collected from qPCR and western blot stimulations for analysis of ceruloplasmin activity and concentration. Collected media was spun at 500 x g for 10 minutes at room temperature prior to being aliquoted and frozen at -20 ˚C. Undiluted media was assessed for ceruloplasmin concentration by ELISA (EC4201-1, Assaypro) while media for ceruloplasmin ferroxidase activity was diluted 1:3 in assay buffer for colorimetric quantification of activity (EIACPLC, Invitrogen). All experiments were run in four independent biological replicates. Statistics were carried out on Prism 9.1 (Graphpad).

4.2.7 Immunofluorescence imaging

HepG2 cells were plated at 150,000 cells per well on acid-washed and sterilized glass coverslips in a 12-well plate. Cells were stimulated as described above and then washed at 1, 6, 12, and 24 hours in cold PBS (Gibco) and fixed for 10 minutes in 4% paraformaldehyde (AAJ19943K2, ThermoFisher Scientific). Cells were blocked in 10% BSA and permeabilized with Triton X-100. 1:600 anti-ATP7B (ab124973, Abcam) and 1:600 anti-TGN46 (GTX74290, GeneTex) antibodies were used to stain the copper transporter and trans-Golgi network marker respectively, and anti-rabbit IgG AlexaFluor 488 (R37116, Invitrogen) and anti-sheep IgG AlexaFluor 647 (A21448, Invitrogen) were used as secondary antibodies to fluorescently label the proteins. A DAPI dye (R37606, Invitrogen) was used to stain the nucleus, and coverslips were sealed to glass slides along with Prolong Gold Antifade Mountant (P36930, Invitrogen). Fixed and mounted cells were

imaged using a laser scanning confocal microscope (Olympus FluoView FV1000) with a 60x oil immersion lens at the UC Davis Molecular and Cellular Biology Light Microscopy Imaging Facility.

4.2.8 Glutathione oxidation

Oxidized and total glutathione levels were assessed by the GSH-Glo Glutathione assay (V6611, Promega). HepG2 cells were plated at 10,000 cells per well in white 96-well plates. Cells were stimulated for 1, 6, 12, and 24 hours before addition of glutathione detection reagents. Oxidized and total glutathione levels were assessed by bioluminescent signal on the i3x Plate reader (Molecular Devices) with an integration of 1000 ms. Data is expressed as the ratio of oxidized glutathione over total glutathione. Statistics were carried out on Prism 9.1 (Graphpad).

4.2.9 Mitochondrial membrane potential

Mitochondrial membrane potential was assessed by the JC-1 probe assay (ab113850, Abcam). HepG2 cells were plated at HepG2 cells were plated at 10,000 cells per well in black, clear-bottom 96-well plates. Cells were stimulated for 1, 6, 12, and 24 hours before addition of 1 mM JC-1 solution in the corresponding stimulation media. Cells were incubated for 10 minutes in the dark at 37˚C and washed twice with PBS. Stained cells were imaged on the i3x Plate reader (Molecular Devices) with 535 nm excitation and 590 nm emission for aggregates and 475 nm excitation and 530 nm emission for monomers. Statistics were carried out on Prism 9.1 (Graphpad).

4.2.10 Metal analysis

Metal analysis was performed at the Northwestern University Quantitative Bio-element Imaging Center generously supported by NASA Ames Research Center NNA06CB93G. Intra- and extracellular copper was assessed by inductively-coupled plasma mass spectrometry (Thermo iCap Qc ICP-MS). Cells were seeded at 300,000 cells per well and stimulated for 1, 6, 12, and 24 hours. Media was collected and spun at 500 x

g for 10 minutes. 250 µL media was added to pre-weighed metal-free 15 mL conical tubes (89049-170, VWR) and 250 µL analytical grade 70% nitric acid (A509P500, ThermoFisher) was added and left at room temperature for 24 hours. Cells were washed two times with cold PBS and digested in 250 µL analytical grade 70% nitric acid. After 24 hours of acid digestion, 225 µL of cell lysate was transferred to pre-weighed metal-free 15 mL conical tubes. All samples were diluted to 5 mL with 3% analytical grade nitric acid. Copper and phosphorus were assessed by ICP-MS. Intracellular copper concentration is expressed as the ratio of concentrations of copper over phosphorus while copper concentration in media samples is expressed as the concentration of copper over the mass of the sample.

4.3 Results

4.3.1 PA alters copper transporter levels with a time dependence prompting copper export mechanisms.

Previous work showed that high-fat diets perturb hepatic copper metabolism in mice as manifested by an increase in hepatic copper transporter ATP7B [11]. Considered the main copper efflux transporter in liver hepatocytes, elevation in ATP7B expression is typically associated with increased copper export [17,19]. We first sought to establish whether a hepatocellular model could recapitulate these fat-induced effects on ATP7B expression. HepG2, a human hepatocellular carcinoma cell line, has been extensively used to study metabolic processes at the molecular level; in particular, these cells accumulate fat when treated with fatty acids via similar mechanisms as the livers of rodents and human patients given high-fat diets [4,10,26,28,29]. With this precedence, we elected to utilize the well-documented model of treating these cells with sodium palmitate, a sodium salt of PA, for 24 hours using bovine serum albumin (BSA) as a carrier and solubilizer [10,30]. Sodium palmitate has been used extensively to model fatty acid exposure liver due to its ability to represent models of lipid accumulation and steatosis in cells, and as such, provides a basis to study lipid-induced copper misregulation [31,32]. A 24-hour treatment of HepG2 with 250 µM PA indeed resulted in an elevation of ATP7B expression as measured by western blotting (Figure 4.1A, Supplemental Figure 4.S1A).

This change in ATP7B was accompanied by an increase in lipid droplets as measured by Oil O Red staining (Supplemental Figure 4.S2A-B), suggesting that this cell-based model could emulate a similar fat-induced change in copper biology that was previously observed in the mouse models [11]. No changes in cell viability were observed under these treatment conditions (Supplemental Figure 4.S3). Comparison of metal content of BSA and PA stimulation media showed no difference in copper levels between the two, ensuring that changes in copper metabolism are due to the fatty acid content of the PA treatment (Supplemental Figure 4.S4).

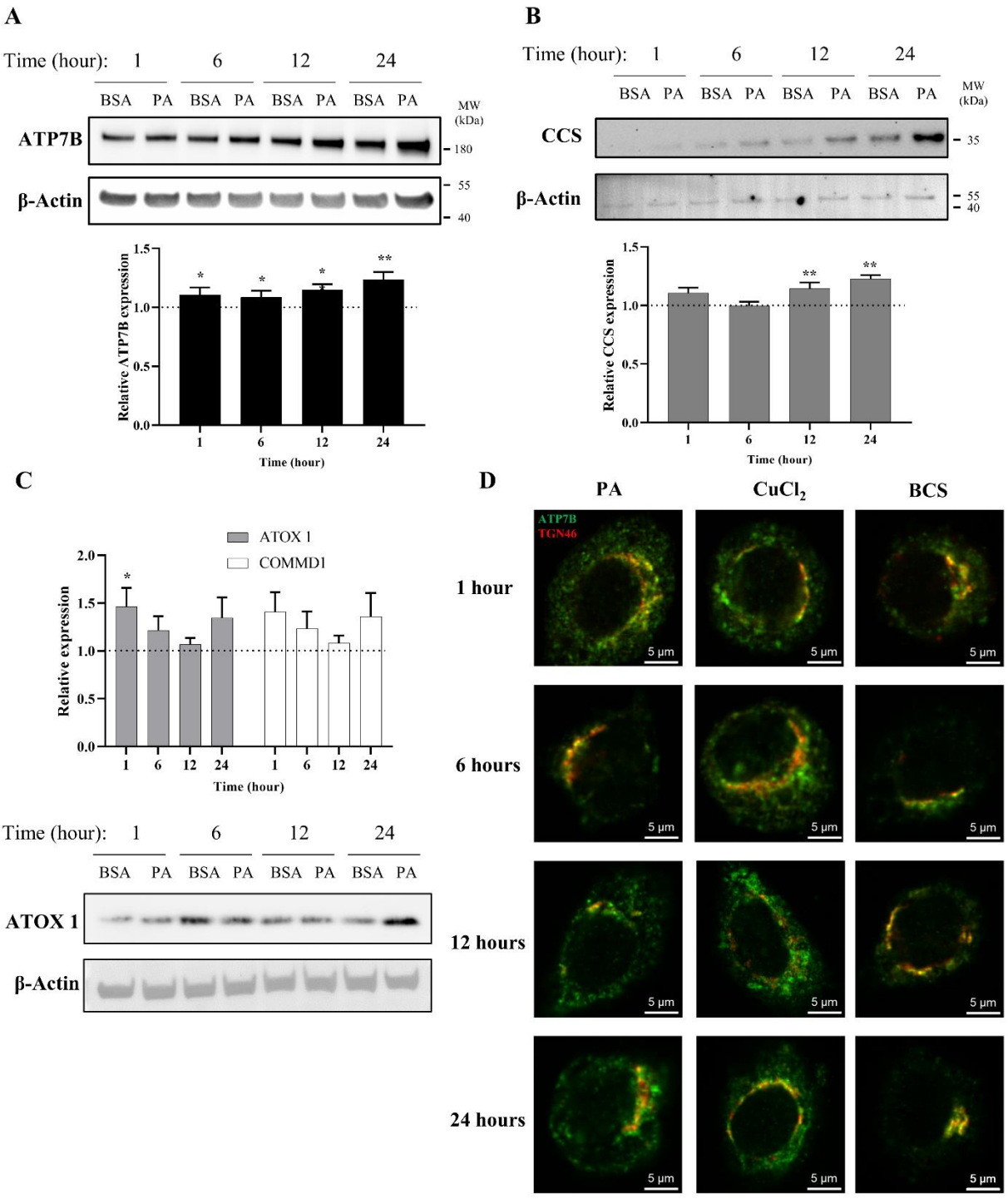

Figure 4.1. PA induces changes in proteins associated with copper export and induces a subcellular localization of ATP7B that resembles cytosolic copper overload in liver cells. Representative western blot images, densitometry, and gene expression analysis of A) ATP7B (n = 10) and B) CCS (n = 9) C) ATOX1 (n = 10), and COMMD1 (n = 10) from lysates collected at different stimulation times with PA. Densitometry is

shown in Supplementary Figure 4.1A-C. Gene expression analysis is provided as the levels from PA stimulation relative to BSA stimulation with normalization to β-Actin as the housekeeping gene. Mean ± SEM are shown. Mann-Whitney *U* Test was used to assess significance (*p < 0.05, **p<0.01). D) HepG2 cells were stimulated with PA, 200 µM $CuCl_2$ to induce a state of copper overload, or 200 µM BCS to induce a state of copper deficiency for 1, 6, 12, and 24 hours. Cells were fixed and immunostained, and immunofluorescence imaging was used to capture the subcellular localization of ATP7B (green) and TGN46 (red). Cells were imaged by laser scanning confocal microscopy with a 60x oil immersion lens. Colocalization is observed by the overlap of signals of ATP7B and TGN46 (yellow).

With a viable model in hand, we applied this system to assess the time-dependent effects of fat accumulation on copper metabolism. We tracked the time-dependent changes in both ATP7B protein and mRNA levels in cell lysates as well as cellular lipid content at 1, 6, 12, and 24 hours of stimulation with 250 µM PA. Both ATP7B protein levels and gene expression (Figure 4.1A, Supplemental Figure 4.S1A), as revealed by western blotting and qPCR analysis respectively, are elevated with PA treatment relative to the BSA vehicle at all time points with the most pronounced changes observed at 12 and 24 hours ($p = 0.0015$ and $p = 0.000011$ respectively for relative gene expression analysis). The 12-hour point at which notable elevation in ATP7B is observed corresponds to the time frame in which elevated fat accumulation is initially observed by Oil O Red staining (Supplemental Figure 4.S2A-B), suggesting a possible correlation between intracellular fat stores and copper regulation.

To determine how the ATP7B changes may correlate with cellular copper status, we evaluated the protein and gene expression levels of the copper chaperone of superoxide dismutase 1 (CCS). Copper-deficient states induce the upregulation of CCS, allowing the protein to serve as a marker for cytosolic copper status [33–36]. Previous work has shown that CCS expression increased in the livers of mice fed high-fat diets [11]. When we stimulated the HepG2 cells with PA, we observed an increase in CCS protein and gene expression levels relative to the vehicle with a time-dependence similar manner to ATP7B, with the most notable increases at 12 and 24 hours ($p = 0.0040$ for 12 hours, $p = 0.000041$ for 24 hours for relative gene expression analysis)

(Figure 4.1B, Supplemental Figure 4.S1B). This elevation in CCS expression suggests that the PA-induced elevation in ATP7B is accompanied by the onset of a cytosolic copper-deficient state.

To further understand copper trafficking pathways associated with PA addition, we evaluated the changes in two copper chaperones associated with ATP7B, ATOX1, and COMMD1. ATOX1 acts upstream to ATP7B in the copper export machinery and is responsible for loading copper into ATP7B [37,38]. COMMD1, while somewhat elusive in terms of its exact function, is linked to ATP7B both as a possible upstream regulator of ATP7B stability, as well as in supporting the bile-dependent export of copper downstream of interactions with ATP7B and independent of ATOX1 [39–42]. Upon PA treatment, both ATOX1 and COMMD1 showed changes in gene expression with similar time-dependent trends to one another but at earlier time points than ATP7B, with initial increases at 1 and 6 hours relative to the vehicle, followed by a drop in the expression (albeit still modestly elevated above the vehicle) at 12 hours which increases at 24 hours (Figure 4.1C, Supplemental Figure 4.S1C). Western blot analysis of ATOX1 reveals similar trends between expression and protein levels, with clear increases in PA-stimulated cells at 1 and 24 hours. We note that for ATP7B, CCS, and ATOX1, BSA treatment alone increases expression over time (Figure 4.1 A-C, Supplemental Figure 4.S1A-C). Such BSA-dependent changes have not previously been noted in the literature and warrant further exploration beyond this study. Nonetheless, the PA-associated changes occur over this baseline increase with the BSA vehicle. The concomitant changes in these proteins, as well as the earlier time points at which they occur support the notion that PA perturbs the copper shuttling machinery upstream of ATP7B.

While classically associated with copper excretion, post-translational regulation of ATP7B plays a role in altering the cellular localization of the metal as reflected in its subcellular localization, which is modulated by cellular copper status [19,43,44]. Under copper-deficient conditions, hepatocytic ATP7B localizes to the trans-Golgi network (TGN) where it is presumed to load copper into membrane and serum derived proteins

[38]. In contrast, excess cytosolic copper prompts a delocalization of ATP7B from the TGN into dispersed cytosolic vesicles and moves to the cell periphery [43–45]. The delocalization of ATP7B away from the TGN has been associated with the transfer or removal of copper away from the cytosol [43]. We thus probed the localization of ATP7B in HepG2 cells treated with PA and compared it to induced copper-overload or copper-deficient conditions, which were achieved by respective treatments with 200 μM $CuCl_2$ or the copper chelator, bathocuproine-disulfonate (BCS). The cells were fixed at 1, 6, 12, and 24 hours after treatment and stained for immunofluorescence imaging of ATP7B (green) as well as TGN46 (red) as a marker for the TGN (Figure 4.1D). As expected, BCS-treated cells exhibited ATP7B localization to the TGN while ATP7B of $CuCl_2$-treated showed dispersed localization away from the TGN. When the same experiment was performed in cells treated with PA, we observed that ATP7B initially localizes to the TGN at the 6-hour time point, consistent with a copper-deficient state. However, at 12 and 24 hours, ATP7B localizes to the cell periphery in a distribution akin to that seen in $CuCl_2$-treated cells, indicating that the observed increase in ATP7B expression may be pointing towards the removal of copper from the cytosol. Colocalization analysis highlights the similarities between PA and $CuCl_2$ stimulated cells (Supplemental Figure 4.S5A-D) in decreasing TGN/ATP7B colocalization, particularly at the 12-hour time point. The similarity between the two treatments suggests that PA induces a cellular response that is observed under copper-overload conditions, despite expressing markers associated with copper deficiency. This data points to a PA-induced shift in copper metabolism that is distinct from chances altering the overall copper levels of the cell as produced by $CuCl_2$ or BCS. Furthermore, the time-dependent changes in ATP7B localization within the cell over the course of the stimulations highlights the plasticity of copper trafficking in the cell in response to fatty acid overload.

4.3.2 PA sequesters copper into the membrane and lysosomes.

The changes in ATP7B localization points to the ability of PA to induce a removal or sequestration of copper from the cytosol. One of the primary known roles of ATP7B for loading of copper is the multi-copper oxidase proteins ceruloplasmin (Cp) and hephaestin [17,24,46]. These homologous multi-copper oxidases are cuproenzymes that contain 6-8 copper atoms per protein. Cp is secreted from the cell, and is the most abundant serum copper chaperone, carrying 50-90% of copper in the blood [25,47,48]. In contrast, hephaestin is anchored to the membrane, presenting copper at the cell surface [49]. Both ferroxidases influence iron availability through their copper-dependent ferroxidase activity [23,50,51]. Having observed the PA-induced elevation ATP7B expression as well as its delocalization from the TGN at 12 and 24 hours, we assessed whether these changes were associated with changes in either ferroxidase at these time points. Extracellular Cp concentration and activity were examined from media taken from the cell supernatant while cellular hephaestin was assessed by western blotting. No significant differences were observed in either extracellular Cp concentration or copper-dependent extracellular ferroxidase activity upon PA treatment (Figure 4.2A-B). This is reflected in a similar lack of change in total extracellular copper levels in the media nor in total cellular copper levels of whole cell pellets, as measured by ICP-MS (Supplemental Figure 4.S6). In contrast, we observe an increase in the protein levels of hephaestin at 24 hours of stimulation with PA (Figure 4.2C). The concomitant changes in hephaestin, ATP7B, and ATP7B-associated chaperones suggest that PA may induce translocation of copper from the cytosol to the membrane via loading into hephaestin, consequently reducing the cytosolic copper content.

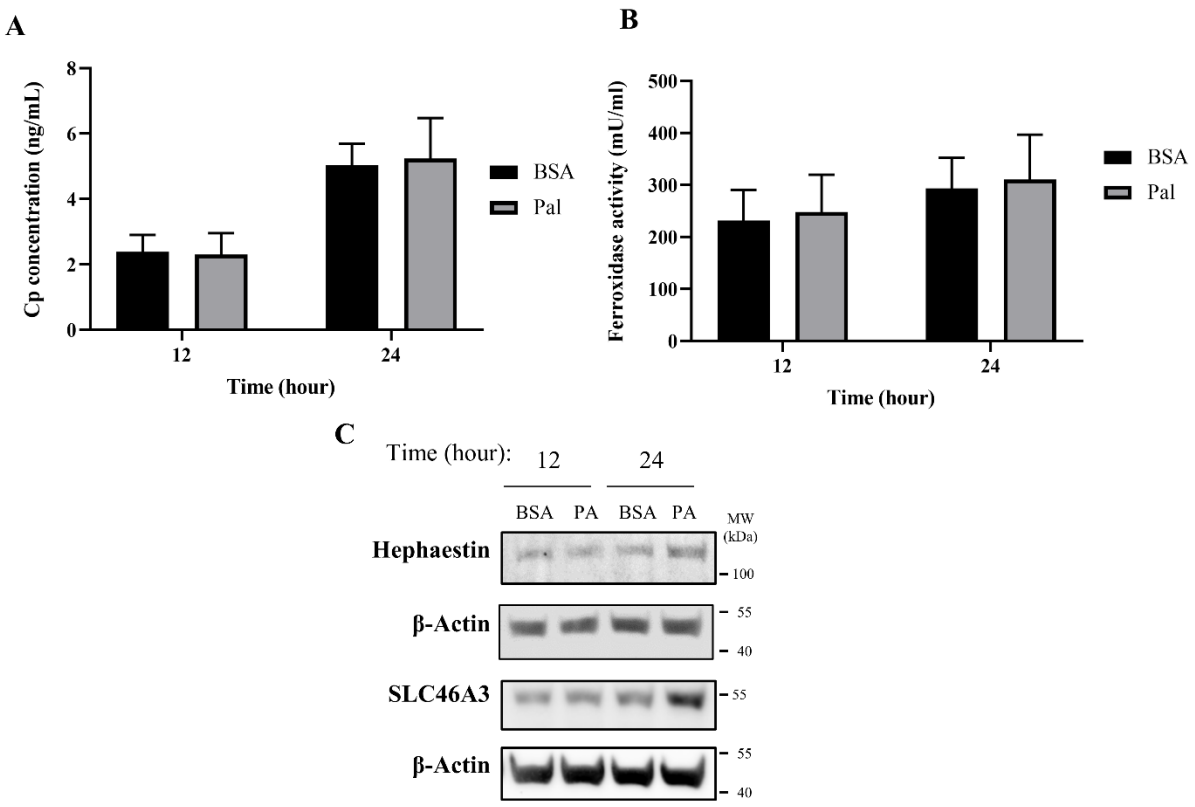

Figure 4.2 PA does not alter serum copper proteins but induces copper membrane localization and sequestration. A) Cp concentration measured by ELISA (n = 4). B) Copper-dependent ferroxidase activity of Cp in media collected from HepG2 cells treated with PA or BSA for 12 and 24 hours (n = 4). Mean ± SEM are shown. Mann-Whitney *U* Test was used to assess significance (**p < 0.01). C) Representative western blot images of hephaestin and SLC46A3.

Alongside the increases in hephaestin, we investigated other mechanisms involved in the sequestering and redistribution of copper in the cell. Recent research has highlighted SLC46A3 as a protein that is responsible for copper loading into lysosomal units in the liver; as such, we aimed to investigate how SLC46A3 is altered with PA stimulation [52]. As with hephaestin, PA induces an increase in SLC46A3 protein levels at 24 hours of PA stimulation relative to the BSA control (Figure 4.2C). Thus, in addition to the translocation of copper to the membrane, our data also hints at a PA-induced increase in lysosomal copper sequestration. Taken together, the increases of both hephaestin and SLC46A3 expression at 24 hours points to a cellular response

to PA involving the mobilization of copper away from the cytosol towards the membrane and lysosomal units.

4.3.3 PA stimulation perturbs intracellular copper balance and redox status.

When cytosolic copper levels are perturbed, to counteract oxidative stress and cell damage, the cell utilizes chelators and chaperones to traffic and maintain homeostasis of copper both in terms of overall levels and subcellular distribution [14,34,53]. To this end, we first investigated the effects of PA on Metallothionein 2A (Mt2A), a protein implicated in both copper chelation and storage, to establish the cell's copper buffering dynamics with fatty acid accumulation [11,34,54,55]. Mt2A levels are initially elevated upon stimulation of PA (Figure 4.3A-B), possibly pointing to an initial state of copper overload. This increase subsides with 6 hours of PA stimulation and continues to decrease at 12 hours, consistent with depression in cytosolic copper levels. By 24 hours, we observe a return to Mt2A levels that is similar to those of the control, implying a level of homeostasis. mRNA expression of Mt2A matches the trends observed by Western blot wherein there is an initial increase upon stimulation with PA, 1 ($p = 0.0015$) and 6-hour treatments but that decreases upon extended PA exposure with 12 and 24 ($p = 0.023$) hour treatments (Figure 4.3B). As a comparison, we assessed Mt2A gene expression with cells treated with 200 µM $CuCl_2$ or 200 µM of the copper chelator BCS. As expected, the addition of $CuCl_2$ increases Mt2A expression, whereas BCS decreases Mt2A expression (Supplemental Figure 4.S7). The dynamics of Mt2A suggest that PA treatment initially places the cell's cytosol in a state of copper overload, prompting the cell to remove copper from the cytosol. This reduction in cytosolic copper then prompts a release of copper stores from Mt2A to restore copper balance.

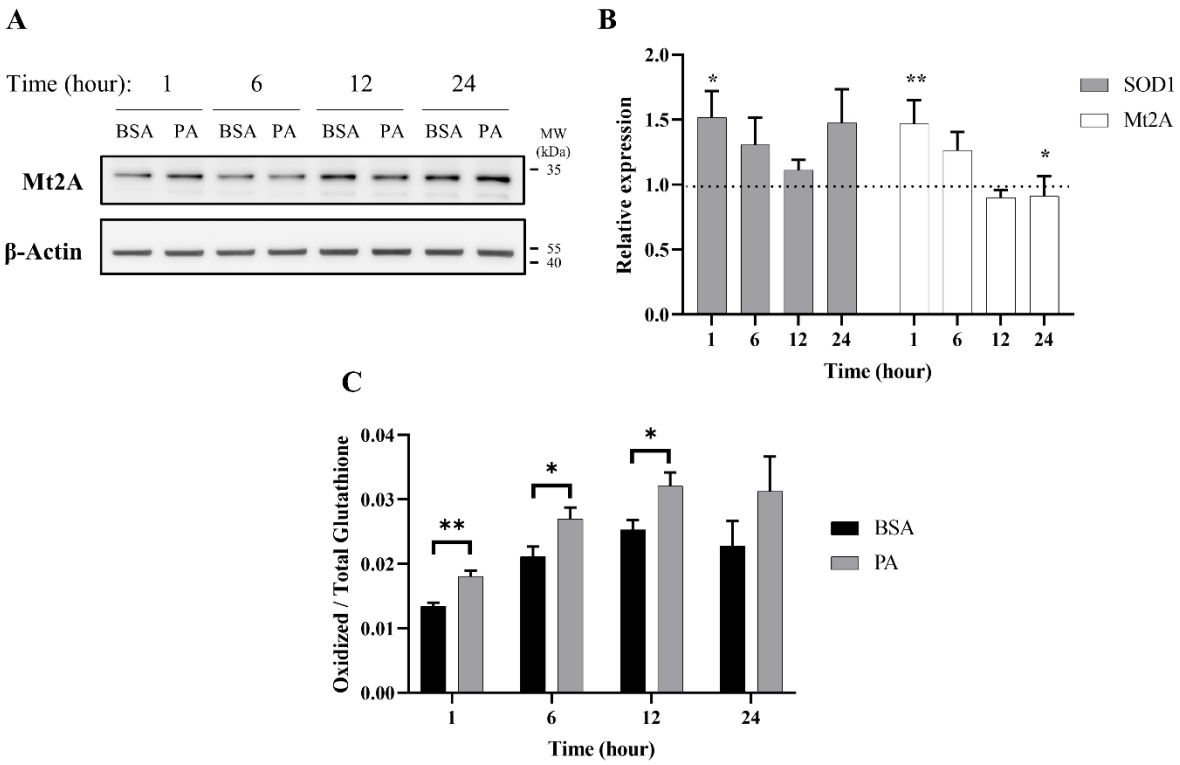

Figure 4.3 Palmitate stimulations induce changes in cytosolic markers of copper status. Analysis of copper chaperones in the lysates of cells treated with PA or BSA for 1, 6, 12, and 24 hours. A) Representative western blot images of Mt2A. B) Gene expression analysis of SOD1 (n = 10), and Mt2A (n = 10) of PA-stimulated cells relative to BSA stimulated cells at the same time points (normalized to β-Actin as the housekeeping gene). Mann-Whitney *U* Test was used to assess the statistical significance. (*p < 0.05, **p<0.01). Mean ± SEM are shown. C) Ratio of oxidized-to-total glutathione in PA-stimulated cells. Unpaired Student's *t* test was used to assess significance.

Intracellular copper levels are integral to maintaining redox balance in the cytosol. Given the perturbation in cytosolic copper homeostasis by PA, we assessed the consequences of the treatment to cellular oxidative status. We evaluated the expression of Cu, Zn-superoxide dismutase (SOD1), a copper-dependent enzyme responsible for scavenging radical and reactive oxygen species [35]. SOD1 gene expression increases at 1 (p = 0.023), 6, and 24 hours of PA stimulation, corroborating previous research relating copper and oxidative stress in liver fat accumulation (Figure 4.3B) [10,56]. We also tracked changes in intracellular glutathione oxidative activity. Glutathione is an intracellular peptide that plays a significant role as an intracellular buffer

as well as maintaining the overall reducing environment of the cytosol due to its free thiols and susceptibility to oxidation by radicals [53,56–58]. Alongside its redox control, glutathione is responsible for chelating labile metal pools in the cell to reduce Fenton-like chemistry [59]. Upon PA addition, we observed an increase in oxidized glutathione at all time points, with significant increases at 1 ($p = 0.0072$), 6 ($p = 0.049$), and 12 ($p = 0.043$) hours (Figure 4.3C). This may be indicative of either an increase in the overall redox state of the cell, which has been previously observed in fatty acid overload in HepG2 cells, or an increase in the labile copper within the cytoplasm of the cell, or both [10].

4.3.4 PA induces mitochondrial dysfunction linked to cytosolic copper overload.

Our data points to an initial state of cytosolic copper overload with PA stimulation, that the cell compensates for by removing copper from the cytosol. However, as the PA stimulation solution does not contain exogenous copper, the elevation in cytosolic copper may stem from release of copper from intracellular compartments. Excess fat accumulation is strongly associated with disruptions in proper function of the mitochondria, an organelle that plays a critical role in energy processing from fatty acid oxidation to ATP production [6,9,60,61]. PA-induced mitochondrial fission, that is, the splitting of the organelle, has been proposed as a main contributor to mitochondrial fragmentation and dysfunction [62]. As mitochondria contain high levels of copper as the metal plays critical functions in the electron transport chain, we investigated whether mitochondrial fission occurs at early time points of PA stimulation to potentially release copper in the cytosol [57,60,63]. We monitored time-dependent changes in the protein FIS1, a marker for mitochondrial fission, in response to PA stimulation [64,65]. FIS1 levels are increased at 1 and 24 hours with stimulation of PA (Figure 4.4A). The early change in FIS1 levels may thus support a mechanism wherein the excess cytosolic copper originates from release of the metal from mitochondrial fission. In support of the changes in mitochondrial fission, we observe changes in mitochondrial membrane potential. This potential was measured by the JC-1 dye, which aggregates in healthy mitochondria and is monomeric

in depolarized membranes, is perturbed by the accumulation of fatty acids in the cell as previously reported [32]. The changes show a slight increase at 1 hour, that subsides at 6 hours, but becomes significantly increased at 12 ($p = 0.0109$) and 24 hours ($p = 0.00597$), all of which coincides with changes in copper metabolism (Figure 4.4B). Moreover, PA induces changes in COX17, a copper chaperone that facilitates copper transport to the mitochondria, and SCO2, a chaperone responsible for copper loading into cytochrome c oxidase in the electron transport chain [16,44,66,67]. COX17 and SCO2 gene expression are increased in cells stimulated with PA at all time points (Figure 4.4C), with notable increases at 1, 6, and 24 hours, whereas SCO2 protein levels do not noticeably increase until the 12- and 24-hour time points (Figure 4.4A). Similar increases in SCO2 protein and mRNA levels have been previously observed by Arciello et al. when HepG2 cells are stimulated with 500 μM of a mixed fatty acid (oleic acid and PA) solution [26]. The degree and direction of changes in these genes at the different time points follow a similar trend as the copper proteins ATOX1, COMMD1, and SOD1 expression, corroborating an overall disruption in copper-associated respiration associated with oxidative imbalance. Taken together, the data supports an initial disruption in copper mitochondrial health that may then induce alterations in the copper subcellular localization.

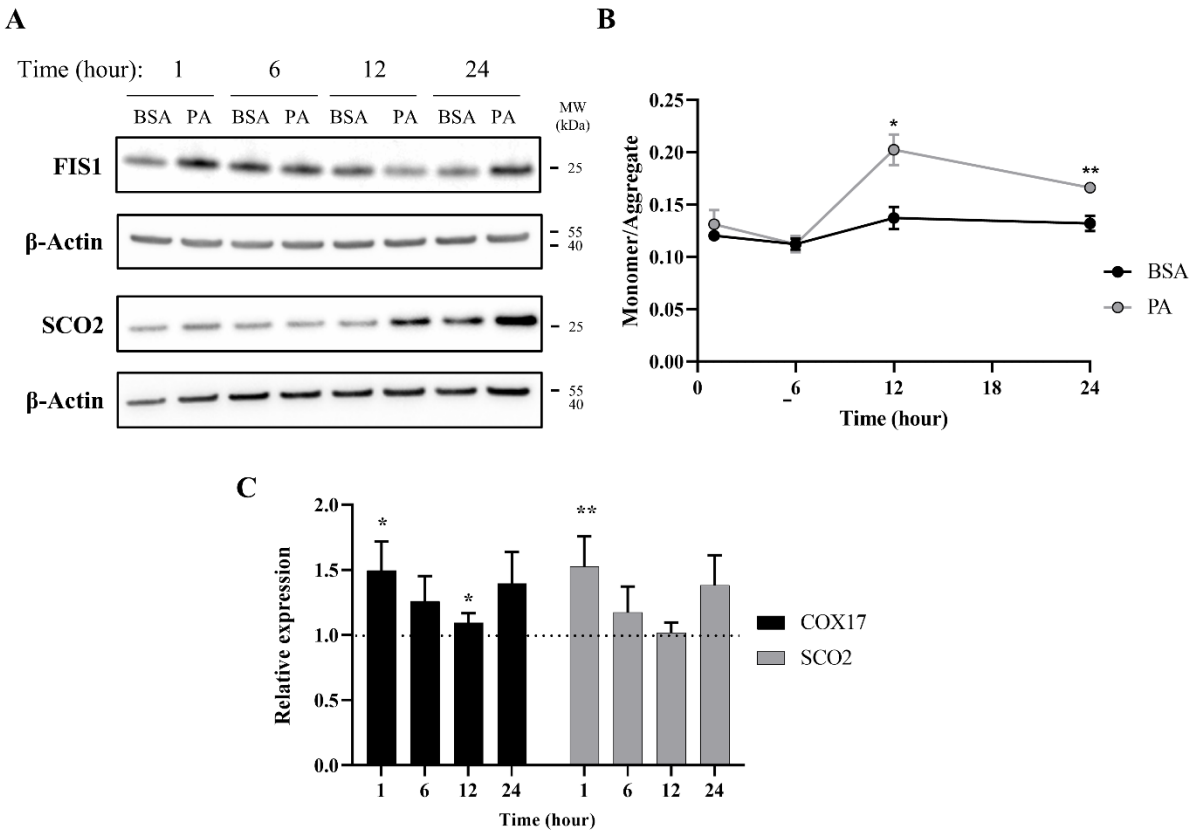

Figure 4.4 Palmitate stimulations induce changes in mitochondria copper protein regulation. A) Representative western blot images of SCO2 and FIS1 of cells stimulated with BSA or PA. B) Mitochondrial membrane potential was measured using the JC-1 fluorescent dye. Data is shown as monomer/aggregate fluorescence of BSA and PA stimulated cells (n = 4). Mean ± SEM are shown. Unpaired *t*-test was used to assess significance (*p < 0.05, **p < 0.01). C) Gene expression of COX17 and SCO2 with PA-stimulated HepG2 cells relative to BSA-stimulated cells (n = 10) with normalization to β-Actin as the housekeeping gene. Mean ± SEM are shown. Mann Whitney *U* Test was used to assess significance (*p < 0.05, **p < 0.01).

4.4 Discussion

Emerging studies on copper metabolism are illuminating its vital roles in energy regulation and nutrient processing. In particular, research is revealing homeostatic perturbations in copper metabolism in relation to obesity-related conditions in rodent models and human physiology [11,13,66,68]. Previous studies have observed increased expression of ATP7B and hepatic copper deficiency in association with hepatic fat accumulation [11,26]. In this study, we profiled the changes in copper trafficking that accompanies this change in ATP7B using a cellular model, with stimulations HepG2 cells with PA. Our observations point to a

mechanism wherein fatty acids may induce a response akin to cytosolic copper overload that triggers copper transport mechanisms to subsequently generate a copper-deficient-like state. At shorter time points of stimulation, the cell initially demonstrates an increase in copper trafficking and chaperone proteins associated with copper overload, including the elevated expression of proteins involved in the copper export machinery as well an increase of Mt2A levels and expression, a putative copper storage protein. This in turn results in a subsequent shift of markers towards a state of copper deficiency, including downregulation and reduced levels of Mt2A, which may indicate the release of copper stores, an increase in protein levels and gene expression of CCS, and an increase in ATP7B. Overexpression of CCS is an established marker of copper-deficient states and is posited to occur as a means for the cell to redirect the limited available copper towards redox balance mechanisms [34,54,56]. Despite the expression of molecular markers of cytosolic copper deficiency at these later time points, the subcellular localization of ATP7B is delocalized from the TGN, a phenotype that is observed in the presence of excess copper [43,44]. This localization is also accompanied by the increased expression of total ATP7B. While increased ATP7B is typically associated with the activation of copper export, we do not observe changes in total copper concentration of cell pellets, nor do we observe increases in extracellular Cp levels or activity. This might suggest that the regulation of ATP7B may instead be functioning towards sequestering or redistributing copper within or at the surface of, rather than exporting the metal from, the cell [44,69]. In support of this hypothesis, we observed an increase in SLC46A3, a protein proposed to play a role in copper loading into lysosomes and potential sequestration [52]. This membrane protein may be responsible for the changes in cytosolic copper status as copper is redistributed within the cell towards lysosomes. Additionally, we observed an increase in protein expression of hephaestin, the membrane-anchored homolog of Cp, supporting a movement of copper to the membrane surface away from the intracellular space (Figure 4.5) [23,49,70]. In a mouse model of NAFLD, hepatic hephaestin was significantly increased in mice fed a high-fat and high-cholesterol diet [70]. This increase correlates with our observations in HepG2 cells exposed to PA

and highlights the relationship of hephaestin and copper redistribution in nutrient overload. While implications of copper loading into the lysosome and hephaestin are not fully understood and require further investigations, their changes may point to a cellular response to either reduce or utilize cytosolic copper [49,71,72]. We noted that COMMD1, which has a posited role in biliary copper export, is altered by PA stimulations [38,40,73]; however, as HepG2 cells have altered biliary export mechanisms, our model may be limited in its ability to capture this particular trafficking mechanism [74].

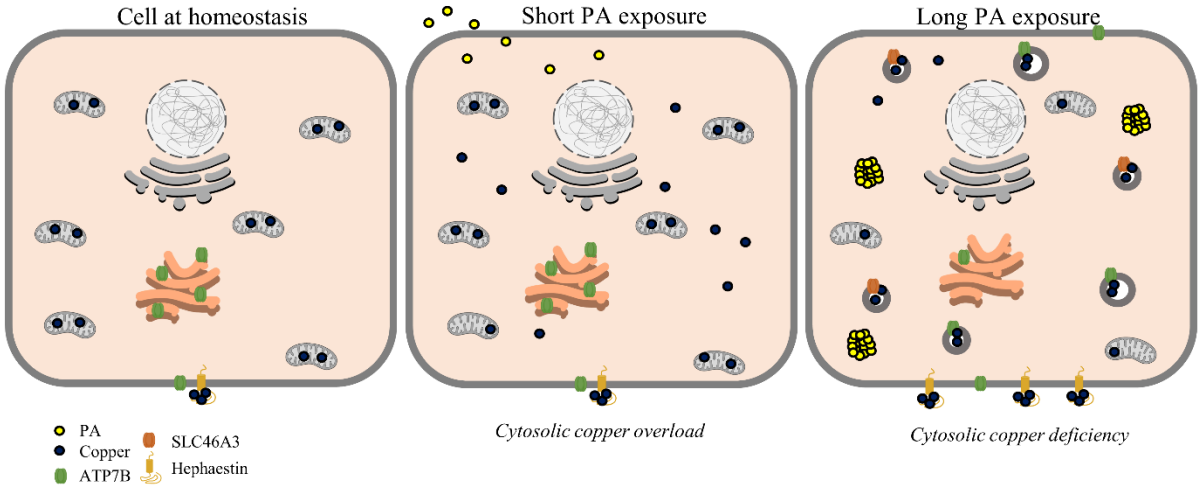

Figure 4.5 Proposed scheme for possible perturbations of copper homeostasis by PA. At homeostasis (left), copper is mostly sequestered in proteins and organelles with a large concentration in the mitochondria. At short time points of PA exposure (middle), cytosolic copper levels are increased alongside mitochondrial dysfunction, leading to a state resembling cytosolic copper overload. With longer PA (right), copper is relocalized towards export by ATP7B and sequestering mechanisms by SLC46A3 and hephaestin resulting in a copper-deficient state.

In further investigating potential mechanisms by which PA perturbs cytosolic copper, we identified alterations in mitochondrial copper proteins. Copper plays a critical role in the electron transport chain and is thus tightly regulated within the mitochondria [4,26,75]. It has even been proposed that the organelle has the ability to store copper within its matrix [14,16,60]. We observed changes in the gene expression of the

mitochondrial copper proteins COX17 and SCO2 with PA addition alongside an increase in the mitochondrial fission protein, FIS1, and mitochondrial membrane depolarization. Additionally, the time-dependence of the changes of the mitochondrial proteins correlate with the increases in Mt2A, denoting a link between PA-induced effects on mitochondrial health and perturbations to cytosolic copper. Our data agrees with published data wherein changes to SCO2 expression were observed alongside fatty acid treatments in cell culture [26]. A hypothesis of SCO-dependent regulation of copper export from the mitochondria may agree with the observed increases in SCO2 protein and point to a loss of mitochondrial copper [67]. Mutations and knockout of SCO2 have been implicated in fatty acid processing and insulin resistance in mouse models, further implicating mitochondrial copper dysfunction in fat accumulation [61]. Our data complements these findings, as we observed increased glutathione oxidation with the PA treatments, which can relate both to altered copper metabolism as well as changes in the overall redox state of the intracellular environment [53,56]. While implications of copper misregulation within the mitochondria are not fully understood, fat overload diseases like NAFLD have been strongly linked to mitochondrial dysfunction, further connecting such diseases to disruptions in intracellular copper balance [9,76]. Taken together, our data may point to mitochondrial fission as a potential source for miscompartmentalized copper that triggers subsequent copper shuttling pathways to restore homeostasis. Future studies are required to firmly establish the links between mitochondrial copper regulation and fat accumulation as well as their implications on cell health and disease pathologies.

Diseases that arise alongside fat accumulation are hypothesized to progress in a “multiple-hit” system, with an increase in reactive oxygen species and the accumulation of fat in the liver contributing to disease pathogenesis [9,77,78]. However, the mechanisms behind these phenotypes have yet to be uncovered [9,78,79]. As copper can play a role in oxidative stress, the shifts in hepatic copper metabolism that we have observed in response to PA exposure may play a role in the exacerbation of fat-induced cellular stress [80–82]. This cytosolic copper overload in turn leads to copper detoxification that appears through export or

sequestration as evidenced by increases in SLC46A3 and hephaestin [14,43,49,52]. Previous models of copper deficiency demonstrate altered lipid synthesis and metabolism, leading to increased lipid biogenesis and hepatic fat accumulation which could be triggered by the miscompartmenalization of copper observed at later time points [83]. This increase in expression of markers of copper deficiency alongside increases in fat accumulation implicates copper misregulation in the process of lipid biogenesis.

From this study, we propose the following as a mechanism by which copper is misregulated within the liver cell upon PA stimulation (Figure 4.5). Fatty acid stimulation and subsequent uptake initiates a mislocalization of copper, possibly related to mitochondrial dysfunction. This mislocalization triggers an initial cytosolic response similar to copper overload states, initiating export pathways involving ATOX1, COMMD1, and ATP7B to restore copper balance. This results in sequestration and redistribution of copper, likely to the lysosomes and cell membrane, leading to a state of cytosolic copper deficiency corresponding to increases in CCS levels and decreased levels and expression of Mt2A. This copper deficiency may be exacerbated by export induced by overexpression and relocalization of ATP7B.

In conclusion, our studies reveal mechanistic insights regarding how the cellular copper distribution of hepatocytes is dynamically perturbed by fat accumulation. We suggest that the dynamic shift towards copper export or sequestration is due to cells sensing a state of cytosolic copper overload to restore a level of copper homeostasis. This perceived copper overload activates copper export or sequestering pathways, which subsequently induce a state that resembles copper deficiency. We note that this study is not an exhaustive study of all the proteins that are potentially involved in copper regulation in the cell and focused primarily on regulatory pathways that were established in the literature. Proteins of note that deserve a deeper study with regard to their function in hepatic copper trafficking and consequent effects of macronutrients like fatty acids include but are not limited to ATP7A (which recent studies have highlighted as being expressed in the liver) and CUTC (a protein hinted at playing a role in cytosolic copper balance).

Nonetheless, the present study provides a starting point to broaden our mechanistic understanding of how macronutrients like fat can alter the regulation and compartmentalization of micronutrients like copper within the cell.

4.5 Supplementary Materials

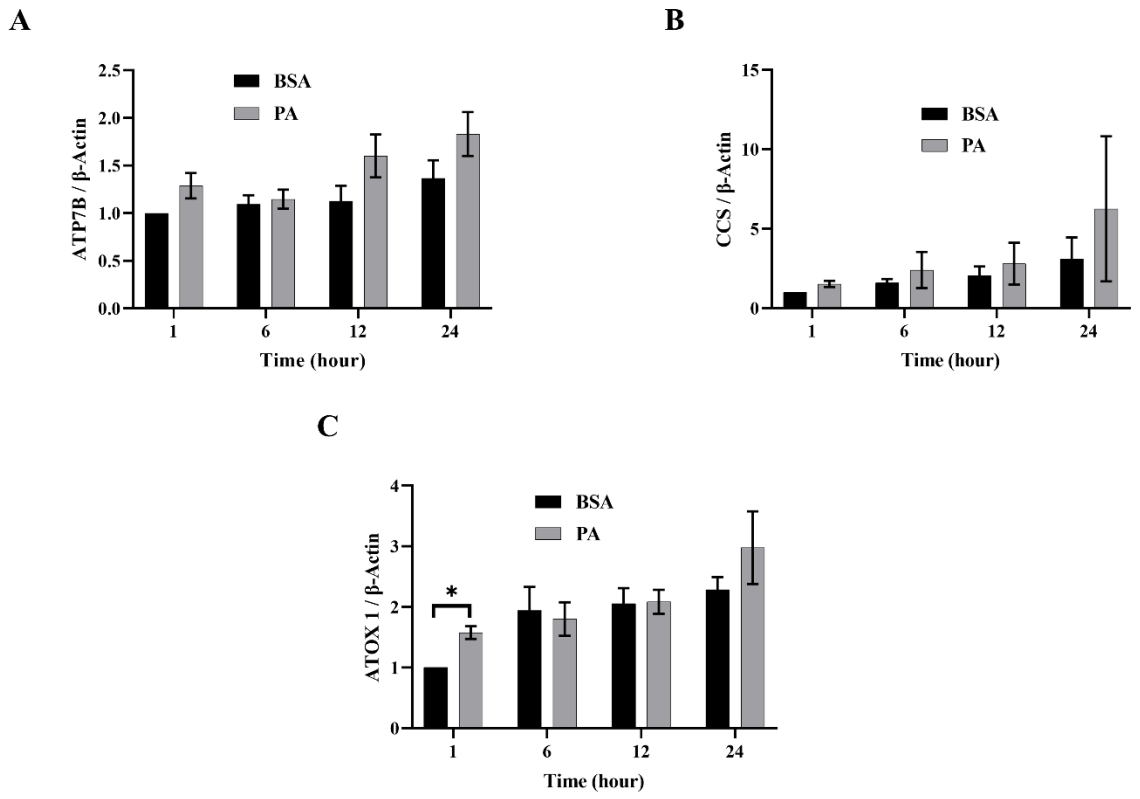

Supplemental Figure 4.S1. Densitometry of representative blots are shown in Figure 4.1. Densitometry analysis of the Western blots of A) ATP7B (n = 7), B) CCS (n = 5), and C) ATOX1 (n=5). Mean ± SEM are shown. Unpaired Student's *t*-test, *p<0.05 was used to assess significance.

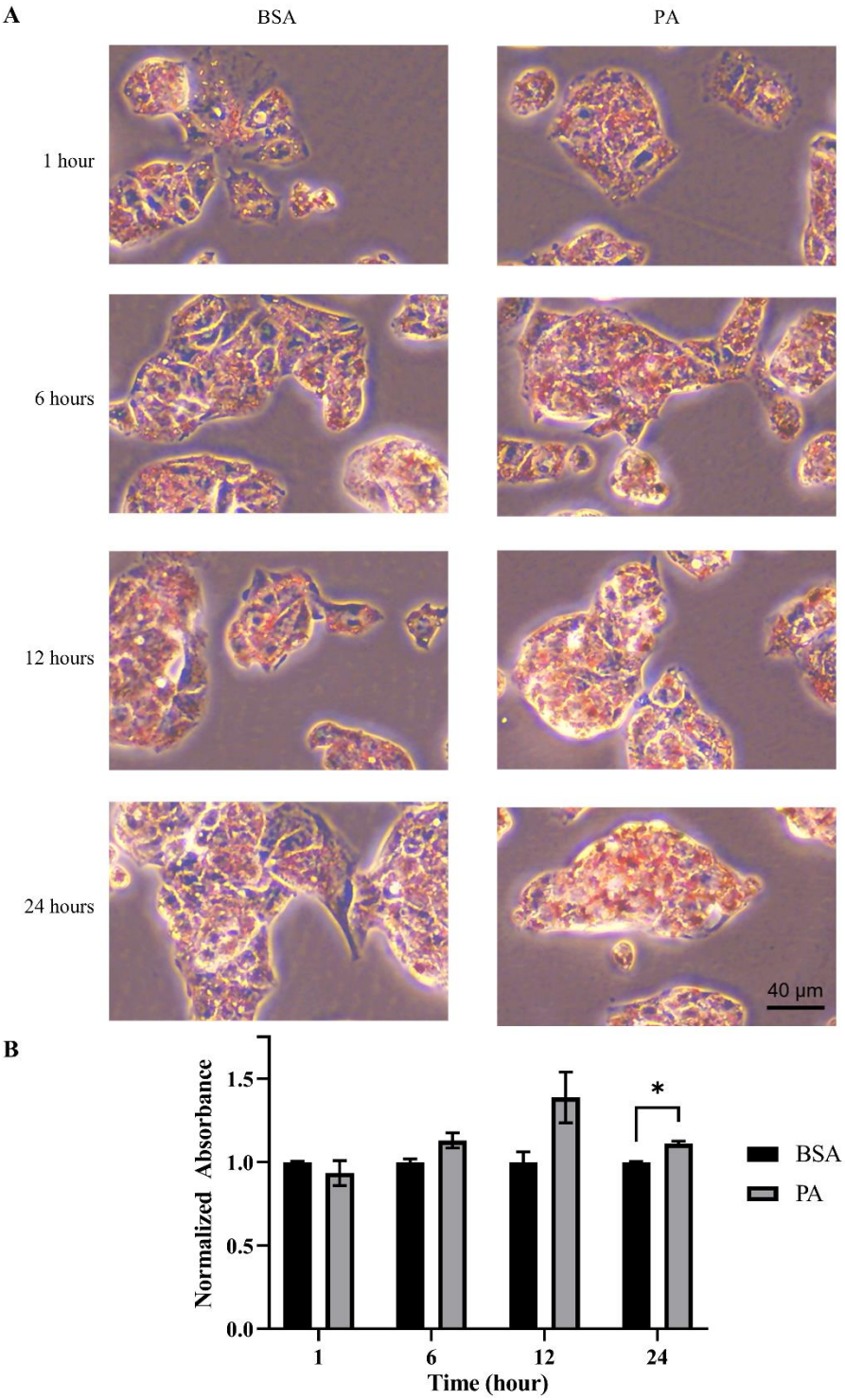

Supplemental Figure 4.S2. PA induces fat accumulation in HepG2 cells. Oil O Red staining of HepG2 cells demonstrating intracellular fat accumulation in cells stimulated with 250 µM PA for 1, 6, 12, and 24 hours. A) Representative images of HepG2 cells are shown. B) Eluted Oil O Red dye from stained cells was measured at 540 nm to assess relative levels of fat accumulation within the cell (n = 4). Absorbance was

normalized to BSA control at each time point. Mean ± SEM are shown. Unpaired Student's *t*-test, *p<0.05 was used to assess significance.

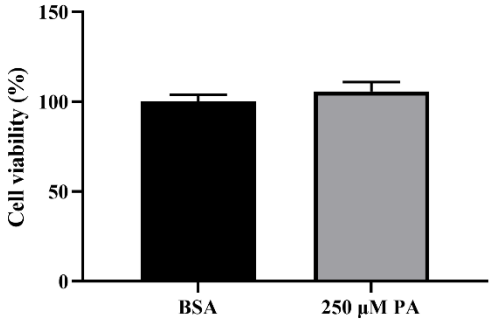

Supplemental Figure 4.S3. Fat accumulation in HepG2 cells does not impact cell viability. HepG2 cells were stimulated for 24 hours with 250 µM PA. Cell viability was assessed by MTS assay (n = 4). Mean ± SEM are shown. Unpaired Student's *t*-test, **p<0.01 was used to assess significance.

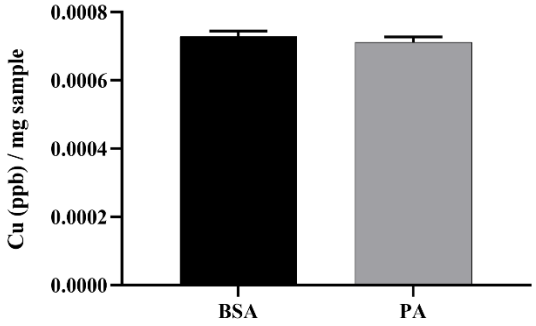

Supplemental Figure 4.S4. No difference is observed in the copper levels between the BSA and PA stimulation media. ICP-MS analysis of stimulation media demonstrates no significant differences in the copper levels of the control (BSA) and PA stimulation media (n = 5). Mean ± SEM are shown.

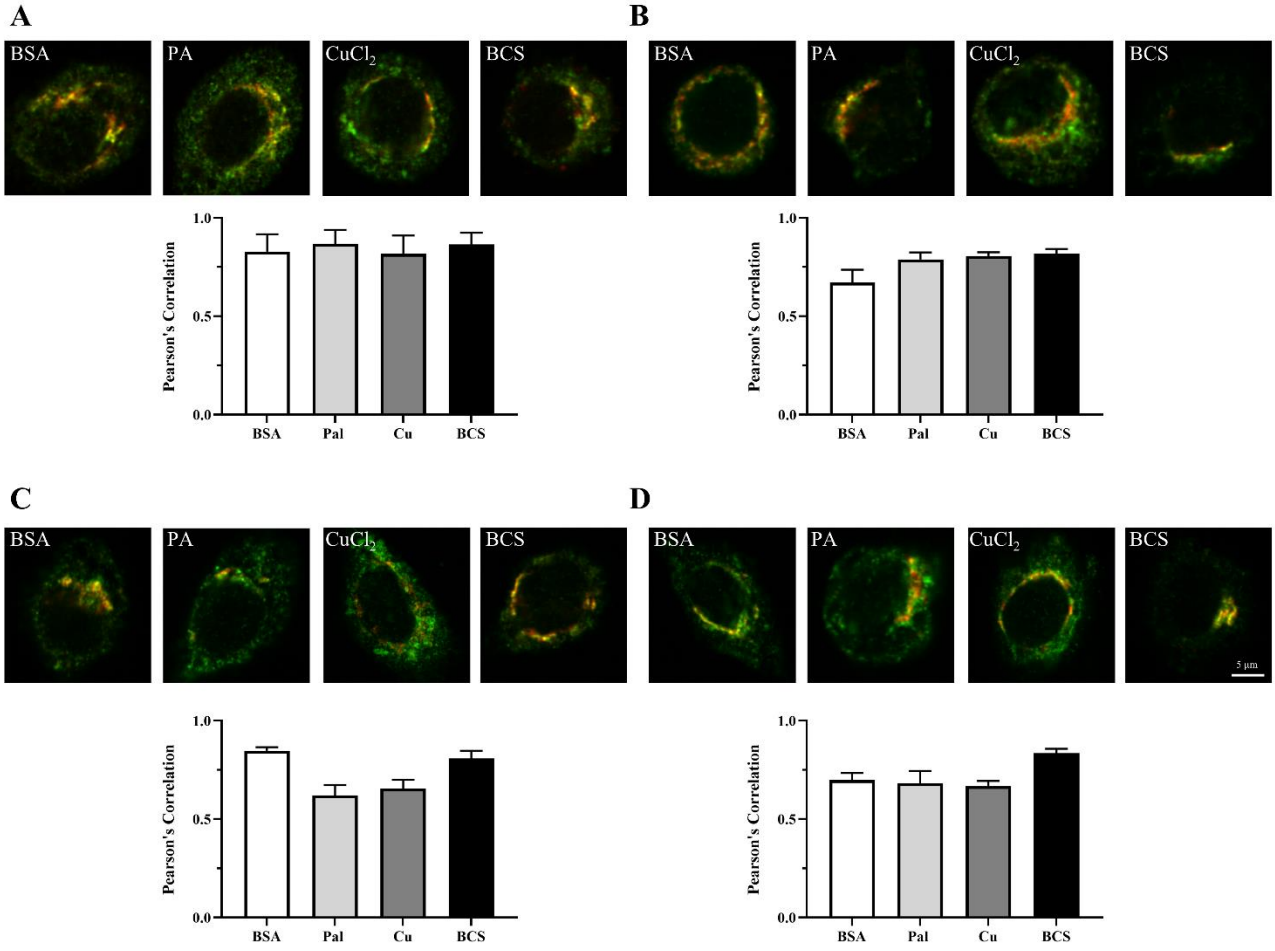

Supplemental Figure 4.S5. Palmitate stimulation induces localization of ATP7B similar to copper deficient and copper overload states and early and late time points respectively. HepG2 cells were stimulated with PA, BSA, 200 µM $CuCl_2$ to induce a state of copper overload, or 200 µM BCS to induce a state of copper deficiency for A) 1, B) 6, C) 12, and D) 24 hours. Cells were fixed and immunostained, and immunofluorescence imaging was used to capture the subcellular localization of ATP7B (green) and TGN46 (red). Cells were imaged by laser scanning confocal microscopy with a 60x oil immersion lens. Colocalization is observed by the overlap of signals of ATP7B and TGN46 (yellow). Bar graphs demonstrate Pearson correlation coefficient used to assess colocalization of ATP7B and TGN 46 (n = 9). Mean ± SEM are shown.

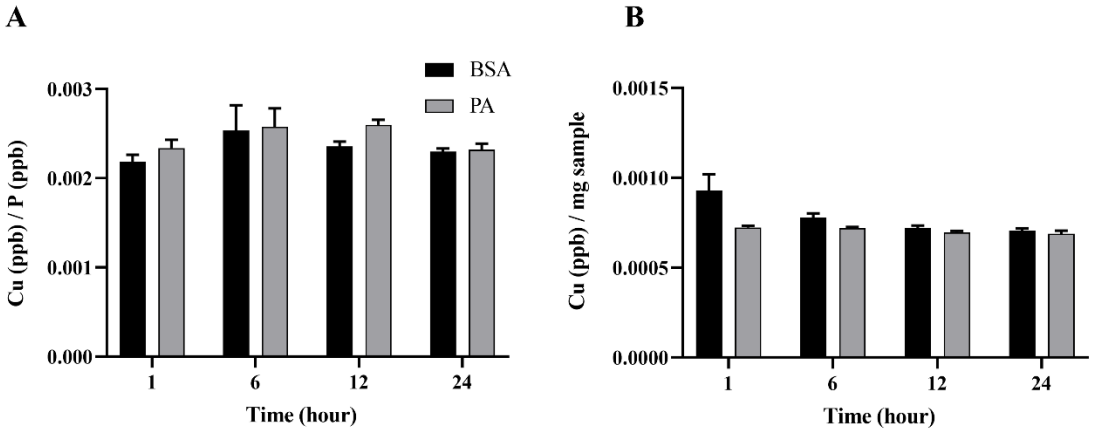

Supplemental Figure 4.S6. PA stimulations do not induce significant changes in intra- or extracellular copper concentrations. Total copper levels analyzed by ICP-MS. A) Copper levels of whole cell pellets are expressed as copper concentration (ppb) over phosphorus concentration (ppb) (n = 5). B) Extracellular copper levels from the cell culture media are expressed as copper concentration (ppb) over mg sample (n = 5). Mean ± SEM are shown.

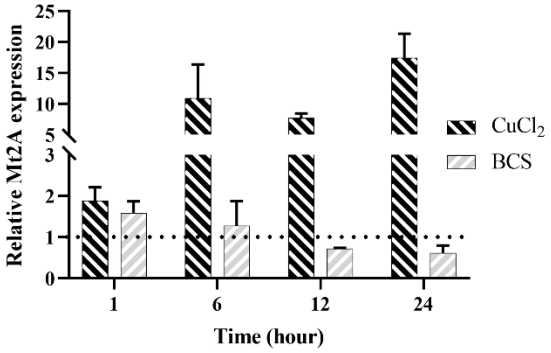

Supplemental Figure 4.S7. Mt2A gene expression is sensitive to copper-modulating treatments. Gene expression analysis of Mt2A of cells treated with 200 µM $CuCl_2$ or 200 µM BCS relative to BSA-stimulated cells (n = 3) with normalization to β-Actin as the housekeeping gene. Mean ± SEM are shown.

Gene	Sequence (5’-3’)
B-actin Forward	GGACGACATGGAGAAAATCTGGCA
B-actin Reverse	GTAGATGGGCACAGTGTGGGTG
TBP Forward	CAGCCTTCCACCTTATGCTC
TBP Reverse	TGCTGCTGTCTTTGTTGCTC
CCS Forward	GACCCTCTGCACGTTGGAGTT
CCS Reverse	GTGGTGTGTACCAAGACCATCTG
ATP7B Forward	CTCATTAAAGCTACCCACG
ATP7B Reverse	GACAAAATATCCACTAAACCG
SOD1 Forward	ACTCTCAGGAGACCATTGCATCA
SOD1 Reverse	TCCTGTCTTTGTACTTTCTTCATTTCC
SCO2 Forward	TCCATTGCCATCTACCTGCTCAAC
SCO2 Reverse	TCAAGACAGGACACTGCGGAA
COX17 Forward	AGGAGAAGAAGCCGCTGAAG
COX17 Reverse	GGCCTCAATTAGATGTCCACAGT
Mt2A Forward	AAAGGGGCGTCGGACAAGT
Mt2A Reverse	TAGCAAACGGTCACGGTCAG
ATOX1 Forward	CTCTCGGGTCCTCAATAAGC
ATOX1 Reverse	GTTGCAAGCAGAGTGTCCAT
COMMD1 Forward	GCTGGAGAGTTGATGGCAAGTC
COMMD1 Reverse	GACCTCATCAAATTCCAAACACAG
Cp Forward	TCCCTGGAACATACCAAACC
Cp Reverse	CCAATTTATTTCATTCAGCCGA

Supplemental Table 4.S1. RT-qPCR primer sequences

4.6 References

(1) Klevay, L. M. Is the Western Diet Adequate in Copper? *Journal of Trace Elements in Medicine and Biology*. J Trace Elem Med Biol December 2011, pp 204–212.

(2) Hieronimus, B.; Griffen, S. C.; Keim, N. L.; Bremer, A. A.; Berglund, L.; Nakajima, K.; Havel, P. J.; Stanhope, K. L. Effects of Fructose or Glucose on Circulating ApoCIII and Triglyceride and Cholesterol Content of Lipoprotein Subfractions in Humans. *J. Clin. Med.* 2019, *8* (7), 913.

(3) Perdomo, C. M.; Frühbeck, G.; Escalada, J. Impact of Nutritional Changes on Nonalcoholic Fatty Liver Disease. *Nutrients* 2019, *11* (3).

(4) Joshi-Barve, S.; Barve, S. S.; Amancherla, K.; Gobejishvili, L.; Hill, D.; Cave, M.; Hote, P.; McClain, C. J. Palmitic Acid Induces Production of Proinflammatory Cytokine Interleukin-8 from Hepatocytes. *Hepatology* 2007, *46* (3), 823–830.

(5) Statovci, D.; Aguilera, M.; MacSharry, J.; Melgar, S. The Impact of Western Diet and Nutrients on the Microbiota and Immune Response at Mucosal Interfaces. *Frontiers in Immunology*. Frontiers Media S.A. July 28, 2017, p 838.

(6) Softic, S.; Cohen, D. E.; Kahn, C. R. Role of Dietary Fructose and Hepatic De Novo Lipogenesis in Fatty Liver Disease. *Digestive Diseases and Sciences*. Springer New York LLC May 1, 2016, pp 1282–1293.

(7) Cusi, K. Role of Insulin Resistance and Lipotoxicity in Non-Alcoholic Steatohepatitis. *Clinics in Liver Disease*. Clin Liver Dis November 2009, pp 545–563.

(8) Lomonaco, R.; Chen, J.; Cusi, K. An Endocrine Perspective of Nonalcoholic Fatty Liver Disease (NAFLD). *Therapeutic Advances in Endocrinology and Metabolism*. SAGE Publications 2011, pp 211–225.

(9) Antonucci, L.; Porcu, C.; Iannucci, G.; Balsano, C.; Barbaro, B. Non-Alcoholic Fatty Liver Disease and Nutritional Implications: Special Focus on Copper. *Nutrients* 2017, *9* (10).

(10) Cremonini, E.; Oteiza, P. I. (-)-Epicatechin and Its Metabolites Prevent Palmitate-Induced NADPH Oxidase Upregulation, Oxidative Stress and Insulin Resistance in HepG2 Cells. *Arch. Biochem. Biophys.* 2018, *646*, 55–63.

(11) Heffern, M. C.; Park, H. M.; Au-Yeung, H. Y.; Van de Bittner, G. C.; Ackerman, C. M.; Stahl, A.; Chang, C. J. In Vivo Bioluminescence Imaging Reveals Copper Deficiency in a Murine Model of Nonalcoholic Fatty Liver Disease. *Proc. Natl. Acad. Sci. U. S. A.* 2016, *113* (50), 14219–14224.

(12) Song, M.; Vos, M. B.; McClain, C. J. Copper-Fructose Interactions: A Novel Mechanism in the Pathogenesis of NAFLD. *Nutrients*. MDPI AG November 1, 2018.

(13) Harder, N. H. O.; Hieronimus, B.; Stanhope, K. L.; Shibata, N. M.; Lee, V.; Nunez, M. V.; Keim, N. L.; Bremer, A.; Havel, P. J.; Heffern, M. C.; et al. Effects of Dietary Glucose and Fructose on Copper, Iron, and Zinc Metabolism Parameters in Humans. *Nutrients* 2020, *12* (9), 1–14.

(14) Lutsenko, S. Human Copper Homeostasis: A Network of Interconnected Pathways. *Curr. Opin. Chem. Biol.* 2010, *14* (2), 211–217.

(15) Ackerman, C. M.; Chang, C. J. Copper Signaling in the Brain and Beyond. *Journal of Biological Chemistry*. American Society for Biochemistry and Molecular Biology Inc. March 30, 2018, pp 4628–4635.

(16) Nevitt, T.; Ohrvik, H.; Thiele, D. J. Charting the Travels of Copper in Eukaryotes from Yeast to Mammals. *Biochim. Biophys. Acta* 2012, *1823* (9), 1580–1593.

(17) Lutsenko, S. Copper Trafficking to the Secretory Pathway. *Metallomics* 2016, *8* (9), 840–852.

(18) Bost, M.; Houdart, S.; Oberli, M.; Kalonji, E.; Huneau, J.-F.; Margaritis, I. Dietary Copper and Human Health: Current Evidence and Unresolved Issues. *J. Trace Elem. Med. Biol.* 2016, *35*, 107–115.

(19) Lutsenko, S.; Barnes, N. L.; Bartee, M. Y.; Dmitriev, O. Y. Function and Regulation of Human Copper-Transporting ATPases. *Physiol. Rev.* 2007, *87* (3), 1011–1046.

(20) Członkowska, A.; Litwin, T.; Dusek, P.; Ferenci, P.; Lutsenko, S.; Medici, V.; Rybakowski, J. K.; Weiss, K. H.; Schilsky, M. L. Wilson Disease. *Nature Reviews Disease Primers*. Nature Publishing Group December 1, 2018.

(21) Cope-Yokoyama, S.; Finegold, M. J.; Sturniolo, G. C.; Kim, K.; Mescoli, C.; Rugge, M.; Medici, V. Wilson Disease: Histopathological Correlations with Treatment on Follow-up Liver Biopsies. *World J. Gastroenterol.* 2010, *16* (12), 1487–1494.

(22) Horn, N.; Wittung-Stafshede, P. ATP7A-Regulated Enzyme Metalation and Trafficking in the Menkes Disease Puzzle. *Biomedicines* 2021, *9* (4).

(23) Jiang, B.; Liu, G.; Zheng, J.; Chen, M.; Maimaitiming, Z.; Chen, M.; Liu, S.; Jiang, R.; Fuqua, B. K.; Dunaief, J. L.; et al. Hephaestin and Ceruloplasmin Facilitate Iron Metabolism in the Mouse Kidney. *Sci. Rep.* 2016, *6* (1), 1–11.

(24) Linder, M. C. Copper Homeostasis in Mammals, with Emphasis on Secretion and Excretion. A Review. *Int. J. Mol. Sci.* 2020, *21* (14), 1–22.

(25) Linder, M. C. Ceruloplasmin and Other Copper Binding Components of Blood Plasma and Their Functions: An Update. *Metallomics* 2016, *8* (9), 887–905.

(26) Arciello, M.; Longo, A.; Viscomi, C.; Capo, C.; Angeloni, A.; Rossi, L.; Balsano, C. Core Domain Mutant Y220C of P53 Protein Has a Key Role in Copper Homeostasis in Case of Free Fatty Acids Overload. *BioMetals* 2015, *28* (6), 1017–1029.

(27) Cremonini, E.; Oteiza, P. I. (-)-Epicatechin and Its Metabolites Prevent Palmitate-Induced NADPH Oxidase Upregulation, Oxidative Stress and Insulin Resistance in HepG2 Cells. *Arch. Biochem. Biophys.* 2018, *646*, 55–63.

(28) Park, J. Y.; Kim, Y.; Im, J. A.; Lee, H. Oligonol Suppresses Lipid Accumulation and Improves Insulin Resistance in a Palmitate-Induced in HepG2 Hepatocytes as a Cellular Steatosis Model. *BMC*

Complement. Altern. Med. 2015, *15* (1).

(29) Di Bella, L. M.; Alampi, R.; Biundo, F.; Toscano, G.; Felice, M. R. Copper Chelation and Interleukin-6 Proinflammatory Cytokine Effects on Expression of Different Proteins Involved in Iron Metabolism in HepG2 Cell Line. *BMC Biochem.* 2017, *18* (1), 1.

(30) Alsabeeh, N.; Chausse, B.; Kakimoto, P. A.; Kowaltowski, A. J.; Shirihai, O. Cell Culture Models of Fatty Acid Overload: Problems and Solutions. *Biochim. Biophys. Acta* 2018, *1863* (2), 143.

(31) Gómez-Lechón, M. J.; Donato, M. T.; Martínez-Romero, A.; Jiménez, N.; Castell, J. V.; O'Connor, J. E. A Human Hepatocellular in Vitro Model to Investigate Steatosis. *Chem. Biol. Interact.* 2007, *165* (2), 106–116.

(32) Eynaudi, A.; Díaz-Castro, F.; Bórquez, J. C.; Bravo-Sagua, R.; Parra, V.; Troncoso, R. Differential Effects of Oleic and Palmitic Acids on Lipid Droplet-Mitochondria Interaction in the Hepatic Cell Line HepG2. *Front. Nutr.* 2021, *8*, 901.

(33) Brady, D. C.; Crowe, M. S.; Turski, M. L.; Hobbs, G. A.; Yao, X.; Chaikuad, A.; Knapp, S.; Xiao, K.; Campbell, S. L.; Thiele, D. J.; et al. Copper Is Required for Oncogenic BRAF Signalling and Tumorigenesis. *Nature* 2014, *509* (7501), 492–496.

(34) Bertinato, J.; Iskandar, M.; L'Abbé, M. R. Copper Deficiency Induces the Upregulation of the Copper Chaperone for Cu/Zn Superoxide Dismutase in Weanling Male Rats. *J. Nutr.* 2003, *133* (1), 28–31.

(35) Culotta, V. C.; Klomp, L. W.; Strain, J.; Casareno, R. L.; Krems, B.; Gitlin, J. D. The Copper Chaperone for Superoxide Dismutase. *J. Biol. Chem.* 1997, *272* (38), 23469–23472.

(36) Lassi, K. C.; Prohaska, J. R. Erythrocyte Copper Chaperone for Superoxide Dismutase Is Increased Following Marginal Copper Deficiency in Adult and Postweanling Mice. *J. Nutr.* 2012, *142* (2), 292–297.

(37) Zaccak, M.; Qasem, Z.; Gevorkyan-Airapetov, L.; Ruthstein, S. An EPR Study on the Interaction between the Cu(I) Metal Binding Domains of ATP7B and the Atox1 Metallochaperone. *Int. J. Mol. Sci.* 2020, *21* (15), 1–13.

(38) Shanmugavel, K. P.; Wittung-Stafshede, P. Copper Relay Path through the N-Terminus of Wilson Disease Protein, ATP7B. *Metallomics* 2019, *11* (9), 1472–1480.

(39) de Bie, P.; van de Sluis, B.; Burstein, E.; van de Berghe, P. V. E.; Muller, P.; Berger, R.; Gitlin, J. D.; Wijmenga, C.; Klomp, L. W. J. Distinct Wilson's Disease Mutations in ATP7B Are Associated With Enhanced Binding to COMMD1 and Reduced Stability of ATP7B. *Gastroenterology* 2007, *133* (4), 1316–1326.

(40) Stewart, D. J.; Short, K. K.; Maniaci, B. N.; Burkhead, J. L. COMMD1 and PtdIns(4,5)P2 Interaction Maintain ATP7B Copper Transporter Trafficking Fidelity in HepG2 Cells. *J. Cell Sci.* 2019, *132* (19).

(41) Fleming, R. E.; Whitman, I. P.; Gitlin, J. D. Induction of Ceruloplasmin Gene Expression in Rat Lung during Inflammation and Hyperoxia. *Am. J. Physiol. - Lung Cell. Mol. Physiol.* 1991, *260* (2 4-1).

(42) Gitlins, J. D. *THE JOURNAL OF BIOLOGICAL CHEMISTRY Transcriptional Regulation of Ceruloplasmin Gene Expression during Inflammation**; 1988; Vol. 263.

(43) Barnes, N.; Bartee, M. Y.; Braiterman, L.; Gupta, A.; Ustiyan, V.; Zuzel, V.; Kaplan, J. H.; Hubbard, A. L.; Lutsenko, S. Cell-Specific Trafficking Suggests a New Role for Renal ATP7B in the Intracellular Copper Storage. *Traffic* 2009, *10* (6), 767–779.

(44) Polishchuk, E. V.; Concilli, M.; Iacobacci, S.; Chesi, G.; Pastore, N.; Piccolo, P.; Paladino, S.; Baldantoni, D.; van IJzendoorn, S. C. D.; Chan, J.; et al. Wilson Disease Protein ATP7B Utilizes Lysosomal Exocytosis to Maintain Copper Homeostasis. *Dev. Cell* 2014, *29* (6), 686.

(45) Weiss, K. H.; Wurz, J.; Gotthardt, D.; Merle, U.; Stremmel, W.; Füllekrug, J. Localization of the Wilson Disease Protein in Murine Intestine. *J. Anat.* 2008, *213* (3), 232–240.

(46) Guttmann, S.; Nadzemova, O.; Grü Newald, I.; Lenders, M.; Brand, E.; Zibert, A.; Schmidt, H. H. ATP7B Knockout Disturbs Copper and Lipid Metabolism in Caco-2 Cells. 2020.

(47) Hellman, N. E.; Gitlin, J. D. Ceruloplasmin Metabolism and Function. *Annu. Rev. Nutr.* 2002, *22* (1), 439–458.

(48) Aigner, E.; Theurl, I.; Haufe, H.; Seifert, M.; Hohla, F.; Scharinger, L.; Stickel, F.; Mourlane, F.; Weiss, G.; Datz, C. Copper Availability Contributes to Iron Perturbations in Human Nonalcoholic Fatty Liver Disease. *Gastroenterology* 2008, *135* (2).

(49) Vashchenko, G.; MacGillivray, R. T. A. Multi-Copper Oxidases and Human Iron Metabolism. *Nutrients* . 2013.

(50) Freestone, D.; Denoyer, D.; Jakab, M.; Leigh Ackland, M.; Cater, M. A.; Michalczyk, A. Ceruloplasmin Is Regulated by Copper and Lactational Hormones in PMC42-LA Mammary Epithelial Cell Culture Models. *Metallomics* 2016, *8* (9), 941–950.

(51) Tapryal, N.; Mukhopadhyay, C.; Das, D.; Fox, P. L.; Mukhopadhyay, C. K. Reactive Oxygen Species Regulate Ceruloplasmin by a Novel MRNA Decay Mechanism Involving Its 3-Untranslated Region IMPLICATIONS IN NEURODEGENERATIVE DISEASES * □ S. *J. Biol. Chem.* 2009, *284*, 1873–1883.

(52) Kim, J. H.; Matsubara, T.; Lee, J.; Fenollar-Ferrer, C.; Han, K.; Kim, D.; Jia, S.; Chang, C. J.; Yang, H.; Nagano, T.; et al. Lysosomal SLC46A3 Modulates Hepatic Cytosolic Copper Homeostasis. *Nat. Commun.* 2021, *12* (1).

(53) Maryon, E. B.; Molloy, S. A.; Kaplan, J. H. Cellular Glutathione Plays a Key Role in Copper Uptake Mediated by Human Copper Transporter 1. *Am. J. Physiol. - Cell Physiol.* 2013, *304* (8), C768.

(54) Kumar, A.; Sharma, A.; Duseja, A.; Das, A.; Dhiman, R. K.; Chawla, Y. K.; Kohli, K. K.; Bhansali, A. Patients with Nonalcoholic Fatty Liver Disease (NAFLD) Have Higher Oxidative Stress in Comparison to Chronic Viral Hepatitis. *J. Clin. Exp. Hepatol.* 2013, *3* (1), 12–18.

(55) Ostrakhovitch, E. A.; Song, Y. P.; Cherian, M. G. Basal and Copper-Induced Expression of Metallothionein Isoform 1,2 and 3 Genes in Epithelial Cancer Cells: The Role of Tumor Suppressor P53. *J. Trace Elem. Med. Biol.* 2016, *35*, 18–29.

(56) Freedman$#, J. H.; Ciriolo$, M. R.; Peisach, J. *THE JOURNAL OF BIOLOGICAL CHEMISTRY The Role of Glutathione in Copper Metabolism and Toxicity**; 1989; Vol. 264.

(57) Gallagher, C. H.; Reeve, V. E.; Wright, R. Copper Deficiency in the Rat. Effect on the Ultrastructure of Hepatocytes. *Aust. J. Exp. Biol. Med. Sci.* 1973, *51* (2), 181–189.

(58) Ngamchuea, K.; Batchelor-McAuley, C.; Compton, R. G. The Copper(II)-Catalyzed Oxidation of Glutathione. *Chem. - A Eur. J.* 2016, *22* (44), 15937–15944.

(59) Thomas, C.; Mackey, M. M.; Diaz, A. A.; Cox, D. P. Hydroxyl Radical Is Produced via the Fenton Reaction in Submitochondrial Particles under Oxidative Stress: Implications for Diseases Associated with Iron Accumulation. *Redox Rep.* 2009, *14* (3), 102–108.

(60) Cobine, P. A.; Pierrel, F.; Winge, D. R. Copper Trafficking to the Mitochondrion and Assembly of Copper Metalloenzymes. *Biochimica et Biophysica Acta - Molecular Cell Research*. Elsevier July 1, 2006, pp 759–772.

(61) Hill, S.; Deepa, S. S.; Sataranatarajan, K.; Premkumar, P.; Pulliam, D.; Liu, Y.; Soto, V. Y.; Fischer, K. E.; Van Remmen, H. Sco2 Deficient Mice Develop Increased Adiposity and Insulin Resistance. *Mol. Cell. Endocrinol.* 2017, *455*, 103–114.

(62) Sergi, D.; Luscombe-Marsh, N.; Naumovski, N.; Abeywardena, M.; O'Callaghan, N. Palmitic Acid, but Not Lauric Acid, Induces Metabolic Inflammation, Mitochondrial Fragmentation, and a Drop in Mitochondrial Membrane Potential in Human Primary Myotubes . *Frontiers in Nutrition* . 2021.

(63) Leary, S. C.; Cobine, P. A.; Kaufman, B. A.; Guercin, G. H.; Mattman, A.; Palaty, J.; Lockitch, G.; Winge, D. R.; Rustin, P.; Horvath, R.; et al. The Human Cytochrome c Oxidase Assembly Factors SCO1 and SCO2 Have Regulatory Roles in the Maintenance of Cellular Copper Homeostasis. *Cell Metab.* 2007, *5* (1), 9–20.

(64) Koch, A.; Yoon, Y.; Bonekamp, N. A.; McNiven, M. A.; Schrader, M. A Role for Fis1 in Both Mitochondrial and Peroxisomal Fission in Mammalian Cells. *Mol. Biol. Cell* 2005, *16* (11), 5077.

(65) Swapna Sasi, U. S.; Sindhu, G.; Raghu, K. G. Fructose-Palmitate Based High Calorie Induce Steatosis in HepG2 Cells via Mitochondrial Dysfunction: An in Vitro Approach. *Toxicol. Vitr.* 2020, *68*, 104952.

(66) Morrell, A.; Tripet, B. P.; Eilers, B. J.; Tegman, M.; Thompson, D.; Copié, V.; Burkhead, J. L. Copper Modulates Sex-Specific Fructose Hepatoxicity in Nonalcoholic Fatty Liver Disease (NALFD) Wistar Rat Models. *J. Nutr. Biochem.* 2020, *78*, 108316.

(67) Cobine, P. A.; Moore, S. A.; Leary, S. C. Getting out What You Put in: Copper in Mitochondria and Its Impacts on Human Disease. *Biochim. Biophys. Acta - Mol. Cell Res.* 2021, *1868* (1), 118867.

(68) Lowe, J.; Taveira-da-Silva, R.; Hilário-Souza, E. Dissecting Copper Homeostasis in Diabetes Mellitus. *IUBMB Life* 2017, *69* (4), 255–262.

(69) Cater, M. A.; La Fontaine, S.; Shield, K.; Deal, Y.; Mercer, J. F. B. ATP7B Mediates Vesicular Sequestration of Copper: Insight Into Biliary Copper Excretion. *Gastroenterology* 2006, *130* (2),

493–506.

(70) Higuchi, T.; Moriyama, M.; Fukushima, A.; Matsumura, H.; Matsuoka, S.; Kanda, T.; Sugitani, M.; Tsunemi, A.; Ueno, T.; Fukuda, N. Association of MRNA Expression of Iron Metabolism-Associated Genes and Progression of Non-Alcoholic Steatohepatitis in Rats. *Oncotarget* 2018, *9* (40), 26183–26194.

(71) Bacchi, M.; Berggren, G.; Niklas, J.; Veinberg, E.; Mara, M. W.; Shelby, M. L.; Poluektov, O. G.; Chen, L. X.; Tiede, D. M.; Cavazza, C.; et al. Cobaloxime-Based Artificial Hydrogenases. *Inorg. Chem.* 2014, *53* (15), 8071–8082.

(72) Polishchuk, E. V; Polishchuk, R. S. The Emerging Role of Lysosomes in Copper Homeostasis. *Metallomics* 2016, *8* (9), 853–862.

(73) De Bie, P.; Van De Sluis, B.; Klomp, L.; Wijmenga, C. The Many Faces of the Copper Metabolism Protein MURR1/COMMD1. *Journal of Heredity*. Oxford Academic November 1, 2005, pp 803–811.

(74) Woolbright, B. L.; McGill, M. R.; Yan, H.; Jaeschke, H. Bile Acid-Induced Toxicity in HepaRG Cells Recapitulates the Response in Primary Human Hepatocytes. *Basic Clin. Pharmacol. Toxicol.* 2016, *118* (2), 160.

(75) Ruiz, L. M.; Libedinsky, A.; Elorza, A. A. Role of Copper on Mitochondrial Function and Metabolism . *Frontiers in Molecular Biosciences* . 2021.

(76) Nassir, F.; Ibdah, J. A. Role of Mitochondria in Nonalcoholic Fatty Liver Disease. *International Journal of Molecular Sciences*. MDPI AG May 15, 2015, pp 8713–8742.

(77) Ahmed, U.; Latham, P. S.; Oates, P. S. Interactions between Hepatic Iron and Lipid Metabolism with Possible Relevance to Steatohepatitis. *World J. Gastroenterol.* 2012, *18* (34), 4651–4658.

(78) Buzzetti, E.; Pinzani, M.; Tsochatzis, E. A. The Multiple-Hit Pathogenesis of Non-Alcoholic Fatty Liver Disease (NAFLD). *Metabolism* 2016, *65* (8), 1038–1048.

(79) Benedict, M.; Zhang, X. Non-Alcoholic Fatty Liver Disease: An Expanded Review. *World Journal of Hepatology*. Baishideng Publishing Group Co June 1, 2017, pp 715–732.

(80) Einer, C.; Leitzinger, C.; Lichtmannegger, J.; Eberhagen, C.; Rieder, T.; Borchard, S.; Wimmer, R.; Denk, G.; Popper, B.; Neff, F.; et al. A High-Calorie Diet Aggravates Mitochondrial Dysfunction and Triggers Severe Liver Damage in Wilson Disease Rats. *CMGH* 2019, *7* (3), 571–596.

(81) Arnal, N.; De Alaniz, M. J. T.; Marra, C. A. Cytotoxic Effects of Copper Overload on Human-Derived Lung and Liver Cells in Culture. *Biochim. Biophys. Acta - Gen. Subj.* 2012, *1820* (7), 931–939.

(82) Tchounwou, P. B.; Newsome, C.; Williams, J.; Glass, K. Copper-Induced Cytotoxicity and Transcriptional Activation of Stress Genes in Human Liver Carcinoma (HepG2) Cells. *Met. ions Biol. Med. Proc. ... Int. Symp. Met. Ions Biol. Med. held ... = Les ions Met. en Biol. en Med. ... Symp. Int. sur les ions Met. .* 2008, *10*, 285.

(83) Morrell, A.; Tallino, S.; Yu, L.; Burkhead, J. L. The Role of Insufficient Copper in Lipid Synthesis and

Fatty-Liver Disease. *IUBMB Life* 2017, *69* (4), 263–270.